FINAL REPORT
UNIFIED CONTROL/STRUCTURE DESIGN AND MODELING RESEARCH
Report No. 957114-6
Oct. 31, 1986

Volume II

Appendix II

A Modified Loop Transfer Recovery Approach for Robust Control of Flexible Structures

NAS7-918

P. A. Blelloch

Mechanical, Aerospace and Nuclear Engineering Department
University of California
Los Angeles, CA 90024

FINAL REPORT
UNIFIED CONTROL/STRUCTURE DESIGN AND MODELING RESEARCH
Report No. 957114-6
Oct. 31, 1986

Volume II

Appendix II

A Modified Loop Transfer Recovery Approach for Robust Control of Flexible Structures

P. A. Blelloch

Mechanical, Aerospace and Nuclear Engineering Department
University of California
Los Angeles, CA 90024

Appendix II

(Volume II of Report)

A Modified Loop Transfer Recovery Approach for Robust Control of Flexible Structures

P. A. Blelloch

TABLE OF CONTENTS

LIST OF FIGURES

LIST OF TABLES

LIST OF NOTATION

Abbreviations		Page
l.h.p. -	left half plane	58
r.h.p. -	right half plane	58
KBF (KB filter) -	Kalman-Bucy Filter	3
LQR (LQ regulator)-	Linear Quadratic Regulator	4
LQG -	Linear Quadratic Gaussian	2
LTR -	Loop Transfer Recovery	1

Mathematical Notation		
j -	$\sqrt{-1}$	19
iff -	if and only if	20
$\forall$ -	for all	20
$\Longrightarrow$ -	implies	156
ε -	element of	19
$\lvert\bullet\rvert$ -	magnitude of a complex scalar	23
$\det[\bullet]$ -	determinant of a complex matrix	33
$\sigma_i[\bullet]$ -	ith singular value of a complex matrix	19
$\lambda_i[\bullet]$ -	ith eigenvalue of a complex matrix	156
adj[•] -	adjoint of a complex matrix	60
sup -	supremum	34
deg{•} -	the degree of a polynomial function	62

Page

Chapter II

s -	complex frequency (Laplace transform variable)	15
$R(s)$ -	command signal vector	15
$K(s)$ -	compensator transfer function matrix	15
$U(s)$ -	plant input signal vector	15
$G'(s)$ -	true plant transfer function matrix	15
$Y(s)$ -	plant output signal vector	15
$S(s)$ -	sensitivity function matrix	17
$T(s)$ -	complementary sensitivity function matrix	17
$G(s)$ -	nominal plant transfer function matrix	17
$L_o(s)$ -	output relative plant error	17
$L_i(s)$ -	input relative plant error	17
$\Delta_m(s)$ -	multiplicative unstructured uncertainty	19
$\Delta_d(s)$ -	divided unstructured uncertainty	19
$\ell_m(s)$ -	bound on $\overline{\sigma}[\Delta_m(s)]$	19
$\ell_d(s)$ -	bound on $\overline{\sigma}[\Delta_d(s)]$	19
$\overline{\sigma}[\cdot]$ -	maximum singular value of a complex matrix	19
$\underline{\sigma}[\cdot]$ -	minimum singular value of a complex matrix	19
Ω_R -	Nyquist D-contour	19
ω_o -	nominal plant frequency	23
ω' -	true plant frequency	23

		Page
$\Delta\omega$ -	normalized variation in plant frequency	23
ζ -	modal damping ratio	23
ω -	imaginary part of s	23
$W_{ij}(s)$ -	multi-dimensional, frequency dependent weightings	30
Δ -	matrix of plant uncertainties	30
M(s) -	system interconnection structure	30
$M_{cl}(s)$ -	closed-loop system interconnection structure	30
μ -	structured singular value	34
x(t) -	state vector	36
y(t) -	output vector	36
u(t) -	input vector	36
A,B,C,D -	state-space representation of the plant	36
c_i, A_i, B_i, C_i, D_i -	representation of parameter errors	36
α_{ij}, β_{ij} -	factorization of parameter error representation	36
I_k -	kxk identity matrix	38
λ_i -	ith damping ratio	39
ω_i -	ith nominal natural frequency	39
Δ_i -	relative uncertainty in ω_i	40
R -	control weighting in LQR problem	45
w -	process noise in KBF formulation	45
n -	measurement noise in KBF formulation	45

		Page
Q_r -	state weighting in LQR problem	47
$\hat{Q}_r$ -	process noise covariance in KBF formulation	47

Chapter III

E(s) -	output error vector	52
D(s) -	disturbance input vector	52
K -	LQR feedback gain matrix	54
$\hat{x}(t)$ -	estimate of the state vector	54
G -	KBF Kalman gain matrix	55
q -	large scalar parameter increased to achieve loop recovery in the asymptotic (KBF) method	55
$\Phi(s)$ -	$(sI-A)^{-1}$	55
$\bar{\Phi}(s)$ -	$(sI-A+BK)^{-1}$	55
$\hat{y}(s)$ -	estimate of ouput vector	55
M -	process noise covariance matrix in the KBF problem	57
M_o -	nominal process noise covariance matrix in the KBF problem	57
P -	solution to either the LQR or KBF Riccati Equation	57
N -	measurement noise covariance matrix in the KBF problem	57
T -	arbitrary unitary matrix	57
N(s) -	SISO plant numerator polynomial	58
D(s) -	SISO plant denominator polynomial	58

		Page
$n(s)$ -	SISO compensator numerator polynomial	58
$d(s)$ -	SISO compensator denominator polynomial	58
$\gamma(s)$ -	desired loop numerator polynomial	58
$d_\ell(s)$ -	uncancelled portion of d(s)	58
m -	number of plant outputs (measurements)	61
n -	plant order	61
$g_i(s)$ -	ith channel of 1-input, m-output plant	61
$N_i(s)$ -	numerator polynomial of $g_i(s)$	61
$k_i(s)$ -	ith channel of m-input, 1-output compensator	61
$n_i(s)$ -	numerator polynomial of $k_i(s)$	61
$d_c(s)$ -	portion of d(s) corresponding to pole/zero cancellations	62
n_γ -	degree of $\gamma(s)$	62
n_c -	number of pole/zero cancellations (degree of $d_c(s)$)	62
n_ℓ -	number of uncancelled compensator poles (degree of $d_\ell(s)$)	62
n_N -	maximum degree of $N_i(s)$'s	62
n_n -	degree of $n_i(s)$'s	62
$n_{i,j}$ -	jth coefficient of $n_i(s)$	64
$N_{i,j}$ -	jth coefficient of $N_i(s)$	64

		Page
S -	matrix of $N_{i,j}$'s	64
n -	vector of $n_{i,j}$'s	64
d -	vector of coefficients of $\gamma(s)$	64
$a_k(s)$, $b_k(s)$ -	arbitrary polynomials	65
ε -	error in measurement location for 2 disk example	71

Chapter IV

ϕ -	modal coordinates for the antenna model	78
D -	damping matrix for the antenna model	78
Ω^2 -	diagonal matrix of ω_i^2 for the antenna model	78
σ_i -	ith approximate balanced singular value	83
δ -	maximum variation in natural frequencies	91
q_c -	parameter multiplying Q in LQR problem	91
Q_{RMS} -	Q matrix weighting RMS surface error in LQR problem	91

ACKNOWLEDGEMENTS

I would like to acknowledge the help and support of a number of people who have been especially influential in the preparation of this work. First and foremost is my advisor, Dr. Tino Mingori, who has not only provided direction for my studies and this dissertation, but also a great deal of appreciated advice. I would also like to thank my commitee members, Dr. Steve Gibson, Dr. Peretz Friedmann, Dr. Richard Nelson and Dr. Kenneth Bube, for their time and support. My officemates, Allen Compito, Faryar Jabbari and Armen Adamian deserve special recognition for the number of illuminating conversations that we have shared. Armen Adamian developed the structural model for the antenna and has contributed a great deal of work and insight into the problem. I would like to thank Dr. John Doyle for allowing me to attend his advanced control class at the California Institute of Technology and for the insights that he has given me into this problem. Finally, I would like to thank my wife again, both for her overall support and also for producing all the hand-drawn illustrations in this dissertation.

This work was performed for the Jet Propulsion Laboratory, California Institute of Technology, sponsored by the National Aeronautics and Space Administration under contract NAS 7-918.

VITA

December 9th, 1959	Born: Milan, Italy
1981	B.S. Massachusetts Institute of Technology
1984	M.S. University of California, Los Angeles
1981-1986	Teaching and Research Assistant in the Department of Mechanical, Aerospace and Nuclear Engineering, University of California, Los Angeles

ABSTRACT OF THE DISSERTATION

A Modified Loop Transfer Recovery Approach

for Robust Control of Flexible Structures

by

Paul Andrew Blelloch

Doctor of Philosophy in Mechanical Engineering

University of California, Los Angeles, 1986

Professor D.L. Mingori, Chair

A procedure is developed for dealing with performance and robustness issues in the design of multi-input multi-output compensators for lightly damped flexible structures. The procedure is based upon representing errors in the plant design model as structured uncertainties, and applying a modified version of the Loop Transfer Recovery (LTR) design method. Real parameters errors such as frequency errors, damping errors or modal displacement errors can be treated. The modified method may be implemented in either of two slightly different forms, both of which permit a controlled tradeoff between performance and robustness.

The first approach is the main focus of the dissertation. It involves adjusting the cost function in the regulator problem and the process noise model in the estimator problem in a particular manner which reflects the assumed structure of the modeling errors. Numerical examples dealing with the control of a large flexible space antenna with uncertain frequencies demonstrate that this approach represents a considerable improvement over standard LTR methods. Convenient design parameters can be varied until a satisfactory compromise is achieved between performance and robustness.

The second approach is a variation on the first in that it uses a similar procedure for adjusting the cost function in the (full-state feedback) regulator problem. Instead of implementing the controller with an estimator, however, an algebraic procedure is used to achieve loop recovery with a compensator whose poles can be placed at arbitrary locations. This works for a single-input, multiple-output plant, and results in a reduced order compensator. This approach is also applied to the space antenna problem, and the results indicate that while a satisfactory combination of performance and robustness is possible, the robustness of the compensator is quite sensitive to the pole locations selected.

Chapter I

INTRODUCTION

As control theory develops, both the perfomance demanded and the size and complexity of the systems that must be controlled is increasing rapidly. An application in which this is especially evident is the control of flexible structures, particularily large space structures. These structures can be extremely complex and highly flexible. Furthermore, performance demands may require that a large number of lightly damped, possibly poorly modeled modes must be actively controlled. The problem is far from trivial, and though it has fascinated a large segment of the control system community for a number of years, no universally acceptable solution has emerged. This dissertation presents a modified LTR approach for achieving robust control. This approach is based on analysis of the problem from the point of view of structured uncertainties. It is shown to produce produce considerable improvement in robustness over the standard LTR approach.

Difficulties in the control of flexible structures arise at a number of different points. The first is in the structural modeling of the system, and the selection of an appropriate reduced order model for control design. This does not appear, however, to be a limiting problem. Finite element methods, among others, have facilitated the development of complex structural models, though these are difficult to validate for structures which can be deployed only in a zero gravity environment. An essential ingredient in these models is that they must include some estimate of the model uncertainties. Model reduc-

tion has received a great deal of attention, and a number of competing methods are available. Most of these work with a state-space description of the system and many offer the advantage of working in a "modal representation," enabling the selection of "important" modes. The structural modeling and mode selection processes for a specific flexible antenna model will be discussed in the context of an example. For the purposes of this dissertation it is assumed that the design model has been extracted from a larger analytical model on the basis of some modal selection scheme, and that some estimate of uncertainties (particularily in the modal frequencies of the reduced order model) is available.

Once an appropriate (reduced order) model is chosen for control design, a number of further difficulties arise. Most large space structures are inherently multiple-input multiple-output (MIMO), indicating that classical control methods are, in general, not applicable. The control designer is then faced with an array of modern control design methods. Two approaches that have become especially popular are the optimal LQG approach which is a time domain method based on a state-space description of the system, and the various polynomial, or transfer function approaches, which deal in the frequency domain, more in the spirit of classical control.

The LQG approach is very appealing. It allows the designer to specify a control objective in terms of a quadratic cost functional, and then step back while the computer provides the "optimal" solution. Any number of inputs and outputs are handled naturally and the solu-

tion to the full-state feedback regulator is shown to have excellent gain and phase margins [SA-4,LE-2]. On the other hand, the addition of a state estimator (Kalman Filter) can produce arbitrarily poor gain and phase margins. Furthermore, the entire LQG approach fails to deal directly with one of the major issues of feedback control, the ability to achieve perfomance specifications in the face of plant uncertainties.

Polynomial approaches have become increasingly popular, especially with regard to designing robust systems. This is because many constraints on the performance and robustness of the feedback system can be stated directly in the frequency domain. Performance is usually assured by maintaining high loop gains in frequency ranges where disturbance rejection is important, while robustness with respect to a special form of uncertainty is also a function of loop gain as indicated in Chapter II. Furthermore, the entire approach is similar in spirit to that of classical control, and provides a good "intuitive" feel for feedback system properties. Classical control concepts such as sensitivity, bandwidth, gain and phase margins, etc. are more apparent in the polynomial or transfer function approach.

One approach which combines both LQG and transfer function methods is Loop Transfer Recovery (LTR), originally suggested by Kwakernaak [KW-1] and later extended by Doyle and Stein [DO-1,2]. Kwakernaak derives a method to asymptotically recover the loop shape of a given Kalman-Bucy Filter (KBF) at the plant output, by allowing the control weighting in a specific LQR problem to approach zero. This offers the

advantage of recovering the minimal sensitivity properties of the Kalman Filter. Doyle and Stein indicate that the dual to Kwakernaak's approach, allowing the noise covariance in a KBF problem to approach zero, asymptotically recovers the LQR loop shape at the plant input. Both procedures will be referred to as Loop Transfer Recovery (LTR), where Kwakernaak's approach [KW-1] recovers a loop shape at the plant output, and is only valid when the plant has at least as many inputs as outputs, while the approach of Doyle and Stein [DO-1,2] recovers a loop shape at the plant input, and is only valid when the plant has at least as many outputs as inputs. Both approaches require that the plant be non-minimum phase and it is only in the case of square plants that the designer has a choice of recovering the loop shape at either the input or output[1]. Ref. [FR-1] discusses more fully some aspects of examining the feedback loop at various points.

A number of papers on various applications of LTR have appeared in the literature. The first to deal specifically with the problem of flexible structures was Ref. [SU-1]. In this work the design model is reduced to the three rigid body modes of the antenna, while all the flexible modes are treated as uncertainties. This is a valid application of LTR, but results in a very low performance control law, (This point is discussed further in Chapter III). In fact, the resulting control law indicates an open-loop bandwidth below 10^{-3} rad./sec.,

---

[1] Margins at both the input and the output can be guaranteed simultaneously only when the inequalities $\sigma[I+K(s)G(s)]\geq 1$ and $\sigma[I+G(s)K(s)]\geq 1$ both hold [LE-1].

where the first flexible mode is not encountered until approximately .75 rad./sec.. This is a severe limitation since it is often necessary for compensators to actively control frequencies which lie within the control bandwidth. More recently, a compensator design for the TRW experimental truss structure was presented in Ref. [OP-1]. In this case a standard LTR design procedure with frequency dependent weighting functions and colored noise was used. The results indicate a robust design with reasonable performance characteristics. However, robustness with respect to frequency errors was not specifically dealt with. A number of other applications have also been reported in the literature. A very recent one applies LTR to the control of turbo-fan jet engines [KA-2,AT-1].

There are two primary motivations for the LTR method. The first is performance, since disturbance rejection specifications can be met by maintaining sufficiently high loop gains over a frequency band of importance. The term performance will be associated with high loop gains through out this dissertation The second is robustness. The idea that loop recovery leads to robustness appears to be based on the belief that an appropriate loop shape along with large gain and phase margins is a guarantee of good robustness. Examples presented in this dissertation demonstrate clearly that this is not the case. On the other hand, loop revovery does appear to be an effective way to achieve a level of nominal performance that is comparable to full-state feedback. A primary goal of the present work is to develop a controller design method which retains the desirable features of loop

recovery and also improves robustness. To meet this goal, a modified LTR approach is developed. The modified approach contains a small number of design parameters which permit the designer to trade off performance and robustness in a controlled way. By this means it is possible to generate a substantially more robust LTR controller with very little reduction in performance. The major difference between this dissertation and previous work is the emphasis on robustness with respect to parameter variations, in particular frequency errors. Previous applications of the LTR method either assumed uncertainties, such a unmodeled dynamics, that are well represented by the unstructured uncertainty approach, or simply defined robustness in terms of some general criteria such as gain and phase margins.

The properties of the modified LTR design method are demonstrated by using the approach to design a high perfromance controller for a flexible space antenna with uncertain modal frequencies. These are poorly characterized by an unstructured uncertainty model. The system is lightly damped and has more outputs than inputs. Since this is a relatively common situation for flexible space structures, the case of an excess of outputs over inputs will be emphasized. In particular, the special case of 1-input and m-outputs, which, by reducing the loop gain at the plant input to a scalar function, both simplifies the analysis and clarifies conceptual ideas, will be used extensively.

The first implication of the excess of outputs over inputs is that the loop shape can be recovered only at the plant input, while a second implication is that a number of extra degrees of freedom are avai-

lable. This motivates an alternate, algebraic design approach which provides Loop Transfer Recovery with arbitrary compensator pole placement and a reduced order compensator. It is shown than this approach offers some advantages over standard LTR methods, but it is quite sensitive to compensator pole location.

The organization of the dissertation is as follows. First the question of robustness is discussed, paying particular attention to some of the important modern robustness theorems that have appeared in the last 10 years. The most important results relative to this discussion are representations of two types of plant uncertainty. These are the unstructured uncertainties of Doyle and Stein [DO-1] and Lehtomaki [LE-1,2,3,4], and the corresponding structured uncertainties of Doyle [DO-3,4,5,6,7]. When modeling errors are well characterized by a single unstructured uncertainty robustness can be guaranteed by making the minimum singular value of either the return difference or inverse return difference transfer function matrix, large enough. This leads to the idea of defining robustness in terms of loop shape, and provides the motivation for loop shaping as a control design method, and LTR as a particular approach to achieving some desired loop shape. Using a simple one mode example however, it is found that the unstructured uncertainty is far too conservative to treat poorly modeled frequencies. It is concluded that in the case of a strict parameter uncertainty such as a frequency error, robustness is not necessarily determined by loop shape alone, since the system component uncertainties cannot be accurately described in terms of unstructured

uncertainties.

The next step in Chapter II is to discuss the structured uncertainty, which promises to reduce the conservativeness of the unstructured approach [DO-3,4,5,6,7]. It does this by treating perturbation matrices which are block diagonal, where each block corresponds to either an unstructured uncertainty, or a real parameter variation. The robustness of systems with structured uncertainties is defined in terms of a parameter μ. μ defines how large an uncertainty of a given structure must become before it can destabilize the plant. In particular, if μ is less than one, the system is robustly stable, while the distance of μ from one indicates a stability margin with respect to the structure of the uncertainty. Methods that choose a controller so as to minimize μ are known as μ-synthesis. These methods, however, are closer in spirit to H^{∞}-optimization than the LTR methods considered in this dissertation. First the general case of a structured uncertainty is discussed briefly and then the representation of the problem for real parameter variations is discussed in greater detail. This case has only appeared recently in the literature [MO-1,2]. It is essential to take into account the constraint that parameter variations remain real whenever uncertain modes are close to the imaginary axis. The reason for this is illustrated by the single mode example discussed in Section 2.1, where it is indicated that a complex representation of frequency uncertainty is conservative even in the case of a single flexible mode. Therefore, even though the transfer function for a flexible system can be separated into its modal components, any

method which allows complex parameter variations in the individual modes will still be conservative. Unfortunately, the real parameter variation version of the structured uncertainty approach for a flexible system with uncertain parameters, does not lead to simple requirements on either the plant input or output loop gain, and therefore does not directly provide useful information for an LTR design. However, the analysis of this problem from a structured uncertainty point of view does result in a transfer function for which μ is minimized to achieve robustness. While μ-synthesis problem is not the subject of this dissertation, the method suggests that minimizing the 2-norm of the same transfer function might improve robustness. This observation is the key to developing the modified LTR approach which is the primary subject and contribution of this dissertation. When the required modifications are implemented, one discovers that the LQG problem one must solve to improve robustness is not necessarily the same one which must be solved to achieve satisfactory performance. In general a trade-off is required. This trade-off is explored in detail later in the dissertation.

In Chapter III a description of the standard LTR method is given, along with a discussion of some of its properties. Again, particular attention is paid to implications for lightly damped, flexible structures. As expected, it is concluded that the LTR method does not always guarantee a robust system, even if the corresponding full-state feedback design is extremely robust. Thus, great care is required in the design of robust compensators for lightly damped, flexible sys-

tems. This is a result of the previously noted conclusion that robustness is not necessarily a function of loop shape alone. In Section 3.3 an alternative algebraic approach to achieving loop recovery is presented and the issue of existence of solutions is discussed. Section 3.4 gives an overview of robustness problems associated with the standard Loop Transfer Recovery approach and discusses some specific issues raised in Ref. [SH-1].

In Chapter IV the methods developed in Chapters II and III are applied to a wrap-rib antenna model. The design goals are to achieve robustness with respect to frequency uncertainty, and also maintain a loop shape which represents a satisfactory level of performance. The antenna model is chosen because it is much more sensitive to frequency errors than other models we have tried. Particular emphasis is placed on finding scalar parameters which allow the designer to control trade-offs between performance and robustness. The results demonstrate the effectiveness of the modified LTR approach for achieving a satisfactory balance between performance and robustness.

The final chapter draws some important conclusions from the simulation results and proposes a general approach to using LTR for the design of robust control systems for non-square, lightly damped, flexible structures.

Background information may be found in the appendices, including a review of singular values, proofs of theorems, a discussion of numerical considerations in the application of the two LTR methods and a

listing of model data for the wrap-rib antenna.

Chapter II

ROBUSTNESS MEASURES FOR MIMO FLEXIBLE SYSTEMS

One of the major reasons for the application of feedback control, is to minimize the effect of variations in plant dynamics (or equivalently, plant frequency response) on the system performance. In this context, two relevant notions of robustness with respect to plant uncertainty are "robust performance" and "robust stability." Robust performance refers to the ability of a plant to meet performance objectives in the face of uncertainty, while robust stability simply requires that the plant remain stable for all allowable plant variations. Only nominal performance and robust stability are considered in detail in this dissertation. If the system is SISO, or if both performance and robust stability are measured at the same point in the feedback loop, then satisfying both nominal performance and robust stability implies robust performance. In a more general case this is not strictly true. Methods required to deal with the general situation are presented in Section 2.2. A detailed applicationof these methods, however, falls beyond the scope of this dissertation. For the remainder of the dissertation, the term robustness refers to robust stability.

The basic work in single-input-single-output (SISO) feedback systems was done more than forty years ago by Nyquist, Bode [BO-1] and their colleagues. The most important robustness result is the Nyquist Stability Criterion, and the related concepts of gain margin and phase margin. These margins specify, in an exact sense, how much the gain

and phase of the plant frequency response can vary separately before the closed-loop system will go unstable. In particular the gain margin measures the amount by which the open-loop gain can be increased without causing instability, while the phase margin measures the amount by which the open-loop phase lag can be increased without causing instability. These provide an approximate measure of the closeness of the Nyquist plot to the -1 point, thereby generalizing the Nyquist Stability Criterion from a measure of absolute stability to one of relative stability.

The purpose of this dissertation is to develop robust, high performance control laws for large, flexible, lightly damped structures. There are two aspects of these systems that cause some difficulty in analyzing robustness properties. The first is their lightly damped, flexible nature, which implies a highly oscillatory frequency response, making concepts such as gain and phase margin much more difficult to interpret. This difficulty, however, can still be handled within the context of classical control methods, provided sufficient care is taken. The second difficulty proves to be more fundamental, and stems from the existence of a number of interconnected inputs and outputs. Since there is no longer one loop gain to be analyzed, classical methods cannot be applied directly. Furthermore, it has been shown that analyzing each loop of a multiple loop system separately, does not always give results that are valid for the interconnected system [DO-1]. Fortunately the robustness of multivariable systems has been studied extensively in the last ten years. It is the purpose

of this chapter, to give a quick overview of the state-of-the-art in the robustness of multiple-input-multiple-output (MIMO) feedback control systems.

An extremely general approach to MIMO robustness can be found in the work of Zames [ZA-1,2] on cone bounded perturbations and Safonov [SA-1,2] on even more general perturbations. These results rely heavily on the mathematical field of functional analysis and are applicable to both non-linear and time-varying plants. The special case of linear, time-invariant plants, however, can be dealt with much more simply, and a number of more practical robustness theorems have been developed. These theorems can be divided into two groups, paralleling the two modern approaches to control theory mentioned in the last chapter, i.e., frequency domain and time domain. The most popular approaches to describing the robustness of linear, time-invariant MIMO feedback control systems deal with a transfer function description of the plant uncertainty. A particular representation is the unstructured uncertainty, which leads to conditions on various loop transfer functions. This immediately implies that loop shape is the fundamental issue in robustness, and therefore provides a simple and clean-cut case for the application of Loop Transfer Recovery.

The unstructured representation of plant uncertainty leads to conditions on loop gain that will ensure robust stability. In this approach the phase is ignored, sometimes leading to conservative requirements on the loop gain. Some work on the "phase" of MIMO systems has appeared the in recent literature. [OW-1,PO-1,2,KO-1]. How-

ever, the concept of phase is not easily extended from SISO to MIMO systems and consequently these results have not proved to be especially useful in characterizing robustness. Therefore, just the structured and unstructured representations of plant uncertainty will be presented in detail.

2.1 Unstructured Uncertainty

Consider the simple feedback system illustrated in Fig. 2.1,

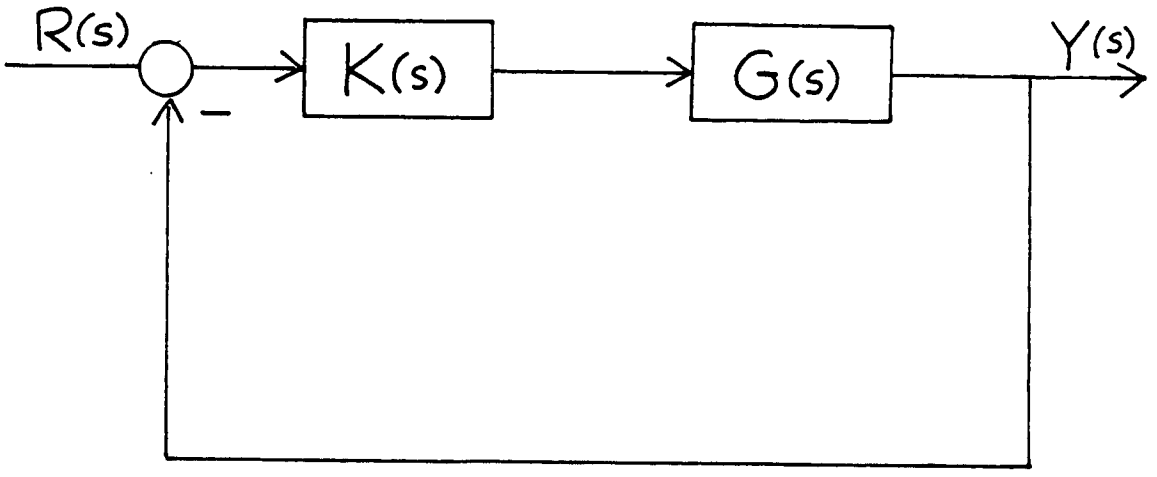

Figure 2.1.1 MIMO Feedback System Configuration

where:

R(s) - Command Signal
K(s) - Compensator
U(s) - Control signal to the plant
G'(s)- True, possibly unknown plant, described by a nominal plant, G(s), and some characterization of errors
Y(s) - Output variables (Measurements)

Dropping the dependence on s, some transfer functions describing the system can then be evaluated as follows:

$$Y = [(I+GK)^{-1}GK]R = [GK(I+GK)^{-1}]R \tag{2.1}$$

$$E = R - Y = (I+GK)^{-1}R \tag{2.2}$$

$$U = [(I+KG)^{-1}K]R = [K(I+KG)^{-1}]R \tag{2.3}$$

Also define the following functions:

GK - Output Loop Transfer Function

KG - Input Loop Transfer Function

[I+GK] - Output Return Difference

[I+KG] - Input Return Difference

$[I+(GK)^{-1}]$ - Output Inverse Return Difference

$[I+(KG)^{-1}]$ - Input Inverse Return Difference

And make note of the following identities:

$$[I+(GK)^{-1}]^{-1} = GK[I+GK]^{-1} = [I+GK]^{-1}GK \tag{2.4a}$$

$$[I+(KG)^{-1}]^{-1} = KG[I+KG]^{-1} = [I+KG]^{-1}KG \tag{2.4b}$$

$$[I+(GK)^{-1}]^{-1} + [I+GK]^{-1} = I \tag{2.5a}$$

$$[I+(KG)^{-1}]^{-1} + [I+KG]^{-1} = I \tag{2.5b}$$

The first two identities show that the inverse return difference is simply the inverse of the closed loop transfer function. The inverse of the return difference is often called the sensitivity function

S(s), while the closed loop transfer function is often called the complementary sensitivity T(s). The second two identities show that the sum of the sensitivity and complementary sensitivity functions is equal to the identity. The implications of this fact, in terms of fundamental limitations on design, are discussed in Ref. [SA-3].

Note that the output loop and input loop transfer functions and related return differences are not in general the same for MIMO systems, though they are for SISO systems. In fact, if the number of inputs is not equal to the number of outputs, they will not even have the same dimensions. This property affects the way in which an uncertainty is described. In particular the true plant G'(s) might be described in terms of a nominal plant G(s) in one of the following two ways:

$$G'(s) = L_o(s)G(s) \tag{2.6a}$$

or $$G'(s) = G(s)L_i(s) \tag{2.6b}$$

$L_o(s)$ will have the dimension of the plant output, and can be considered an uncertainty acting at the output, while $L_i(s)$ will have the dimension of the plant input, and can be considered an uncertainty acting at the input. In some cases a physical interpretation can be attached to the use of either $L_i(s)$ or $L_o(s)$. For example if the errors are due to imperfect actuators $L_i(s)$ would give the appropriate description, while sensor errors would be better described by $L_o(s)$.

On the other hand, when errors are due to uncertainties in the internal plant model the choice of $L_i(s)$ or $L_o(s)$ is more arbitrary. In this case $L_o(s)$ would provide the most convenient error description when the output loop shape is analyzed, since $G'(s)K(s)=L_o(s)G(s)K(s)$, while $L_i(s)$ would provide the most convenient error description when the input loop is analyzed, since $K(s)G'(s)=K(s)G(s)L_i(s)$. The point at which the loop is "opened" to examine robustness will therefore depend on the way in which the error is described, and vice-versa. For simplicity, only errors acting at the plant input will be considered here, but the results for errors acting at the output can be easily found by replacing $K(s)G(s)$ by $G(s)K(s)$ in the theorems of the following sections.

The unstructured uncertainty was introduced by Doyle and Stein [DO-1] and by Lehtomaki [LE-1,2,3,4]. It is simply a single uncertainty which can be given no more structure than a bound on its size. For matrices, size is measured by singular values, which are discussed in Appendix A. It is assumed that the reader is familiar with the concept of maximum and minimum singular values as well as some of their properties.

Consider the following two[1] possibilities for $L(s) = L_i(s)$:

---

[1] Two other unstructured uncertainty representations are the additive and subtracted representations, which are discussed in Ref. [LE-1]. These are, however, equivalent to the multiplicative and divided disturbances respectively and will not be discussed here.

$$L(s) = [I+\Delta_m(s)] \text{ (multiplicative uncertainty)} \tag{2.7a}$$

$$\text{or } L(s) = [I+\Delta_d(s)]^{-1} \text{ (divided uncertainty)} \tag{2.7b}$$

In each case the perturbation can be bounded by a positive, frequency dependent function:[2]

$$\bar{\sigma}[\Delta_m(s)] \leq \ell_m(s), \qquad \bar{\sigma}[\Delta_d(s)] \leq \ell_d(s) \tag{2.8}$$

The closed loop stability of the true system ($KG'[I+KG']^{-1}$) can be determined by the multivariable generalization of the Nyquist Criterion [RO-1]. This requires that the det[I+KG'], evaluated on the standard Nyquist D-contour (denoted by $s\varepsilon\Omega_R$), encircle the origin in a counter-clockwise direction, as many times as there are unstable open-loop poles of KG'. For most practical problems involving flexible structures, the only poles of G on the imaginary axis will be at the origin, and there will be an excess of poles over zeros, implying that $\lim_{s\to\infty} K(s)G(s)=0$. In this case the Nyquist D-contour reduces to the imaginary axis, with the possibility of an identation about the origin, and $s\varepsilon\Omega_R$ can be replaced by $j\omega$. Under the assumptions that G and G' have the same number of open-loop unstable poles, and that KG' and

---

[2] Another method for bounding the uncertainties is the cone-bounded perturbation [DO-4]. This essentially corresponds to a multi-dimensional frequency dependent scaling of the problem. In the case of structured uncertainties (Section 2.2), this scaling is important, but for the unstructured representation it provides no further information.

KG have identical open-loop poles on the jω-axis we have the following two results:

Theorem 2.1: (Multiplicative Disturbance) The closed loop system will remain stable for all allowable perturbations iff:

$$\bar{\sigma}[KG(s)(I+KG(s))^{-1}] < 1/\ell_m(s) \quad \forall s\varepsilon\Omega_R \tag{2.9a}$$

or equivalently if KG is invertible:

$$\underline{\sigma}[I+(KG(s))^{-1}] > \ell_m(s) \quad \forall s\varepsilon\Omega_R \tag{2.9b}$$

Theorem 2.2: (divided disturbance) The closed loop system will remain stable for all allowable perturbations iff both a) and b) are true:

a) L(s) has no zero or strictly negative real eigenvalues for any $s\varepsilon\Omega_R$

b) $$\bar{\sigma}[(I+KG)^{-1}] < 1/\ell_d(s) \quad \forall s\varepsilon\Omega_R \tag{2.10a}$$

or equivalently:

$$\underline{\sigma}[I+KG] > \ell_d(s) \quad \forall s\varepsilon\Omega_R \tag{2.10b}$$

A proof of the above results is given in Appendix B.

It should be noted that these are not conservative results, given the error characterization of Eq. (2.8). In fact, if the above conditions are not met, there exists a perturbation, $\Delta_m(s)$ or $\Delta_d(s)$, whose maximum singular value lies below $\ell_m(s)$ or $\ell_d(s)$ respectively, which will destabilize the system. The unstructured uncertainty, however,

can be unduly conservative in its characterization of error. If the error is known to have some structure it is quite possible that the particular $\Delta_m(s)$ or $\Delta_d(s)$ required to cause instability cannot occur. A number of "structured uncertainty" approaches have attempted to take advantage of some form of error structure, and these will be discussed later, but first the results of the multiplicative and divided uncertainties will be compared, and then a simple example which illustrates the application of the unstructured uncertainty approach to a SISO, lightly damped, flexible system will be presented.

One major difference between the above two results is the additional requirement for divided uncertainties, that L(s) have no zero or strictly negative real eigenvalues for $s\varepsilon\Omega_R$. This is needed to insure that the function $[I+\varepsilon\Delta_d]^{-1}$ remains continuous as ε varies from zero to one, and indicates that Theorem 2.2 cannot guarantee robustness in the case where phase is completely arbitrary. See Appendix B and Ref. [LE-1] for further details. This places a limit on the situations in which a divided disturbance can be used to study robustness. For most practical problems, however, the phase will be known to within $\pm 180^\circ$ for some range of frequency, and both Theorems 2.1 and 2.2 are applicable in that range. When the error in phase is less than 180°, the system can therefore be made robust to multiplicative uncertainties by maintaining a large inverse return difference, or equivalently a small loop gain, while the same system can be made robust to divided uncertainties by maintaining a large return differ-

ence, or equivalently a large loop gain. The two representations therefore imply opposite requirements for achieving robustness, and together imply that a system can be made robust either by maintaining very high loop gains, or by maintaining very low loop gains, while it will be most sensitive to errors in the region of gain cross-over. This is a familiar result from classical control, corresponding to the fact that perturbations of the Nyquist plot far away from the -1 point will not affect stability. Unstructured uncertainties provide the MIMO generalization of this idea. One final note is that Eq. (2.5b) indicates that the return difference and inverse return difference are not independent, implying that a system cannot be made robust to both multiplicative and divided uncertainties acting simultaneously at a single given frequency.

The multiplicative uncertainty is most appropriate when dealing with high freqeuncy errors where phase is completely unknown, while the divided disturbance is most appropriate when dealing with low frequency errors when some information on phase is available. Consequently, the divided disturbance motivates high loop gains, typically used at low frequencies, while the multiplicative disturbance motivates low loop gains, typically used at high frequencies. It should be emphasized that both disturbance models are unstructured, with the only difference being that the phase cannot be completely arbitrary for the divided disturbance.

A flexible structure with uncertain modal frequencies within the system bandwidth must also have uncertain modal frequencies near

cross-over. This implies that high loop gain cannot be maintained for all frequencies and the divided uncertainty is not particularily useful in this case. The unstructured uncertainty, when applied to lightly damped flexible structures therefore implies that the loop gain must be kept below some level, whenever poorly modeled frequencies are present. To gain an appreciation for this limit, consider a very simple SISO flexible model.

2.1.1 Example of a Multiplicative Unstructured Uncertainty Approach -

Since the unstructured uncertainty approaches are generalizations of classical SISO theory, they will work for more complicated systems only if they work for a simple SISO system. With this in mind consider a system with a single, underdamped, flexible mode whose gain and damping ratio are known, but whose frequency is known only within given bounds. Such a system might be described as follows:

$$G'(s) = \frac{\omega'^2}{s^2+2\zeta\omega' s+\omega'^2} \qquad G(s) = \frac{\omega_0^2}{s^2+2\zeta\omega_0 s+\omega_0^2} \tag{2.11}$$

let $$\Delta\omega = (\omega' - \omega_0)/\omega_0$$

then $$\Delta_m(s) = \frac{\Delta\omega s[(2 + \Delta\omega)s + 2\zeta\omega']}{s^2 + 2\zeta\omega' s + \omega'^2} \tag{2.12}$$

and $$|\Delta_m(j\omega)| = |\Delta\omega|\omega \frac{(2+\Delta\omega)^2 + (2\zeta\omega')^2}{(\omega'^2-\omega^2)^2 + (2\zeta\omega')^2\omega^2} \leq \ell_m(\omega) \tag{2.13}$$

This $\ell_m(\omega)$ is for one particular error in frequency ($\Delta\omega$), but $\Delta\omega$ is

actually only known to be within certain bounds. The correct $\ell_m(\omega)$ would then take the worst case of the above bound for every possible $\Delta\omega$. A simple though naive algorithm to find $\ell_m(\omega)$ for a set of bounds on $\Delta\omega$ would, for every ω, calculate Eq. (2.12) for a sufficient number of $\Delta\omega$'s between the bounds, and then plot the worst case.

Fig. 2.2a illustrates the result of such an algorithm. In this case $\omega_0 = 1$ rad/sec, $\zeta = .01$ and $\Delta\omega$ is allowed to vary between -.10 and +.10. $20\log_{10}(1/\ell_m(\omega))$ is plotted, taking the worst case of 200 different $\Delta\omega$'s between -.10 and +.10 at 400 frequency points between .75 rad/sec and 1.25 rad/sec.

A computationally simpler approximation would be to consider only the two worst cases of $\Delta\omega$, ($\Delta\omega = -.10$ and $\Delta\omega = +.10$). The result of an algorithm that did this for the same number of frequency points is plotted in Fig. 2.2b. The plots are similar, though the shapes vary slightly between the limits on $\Delta\omega$. The second approach, might provide guidelines for a first cut design, though it would not strictly guarantee stability by Theorem 2.1.

The function $(1/\ell_m(\omega))$ places strict limitations on the bandwidth of the system, since the closed-loop gain must fall below it. This implies that the bandwidth is limited by the first time that $(1/\ell_m(\omega))$ falls below 0 db. This occurs when $\ell_m(\omega)$ first becomes larger than 1, or when the errors in frequency response first rise above the nominal

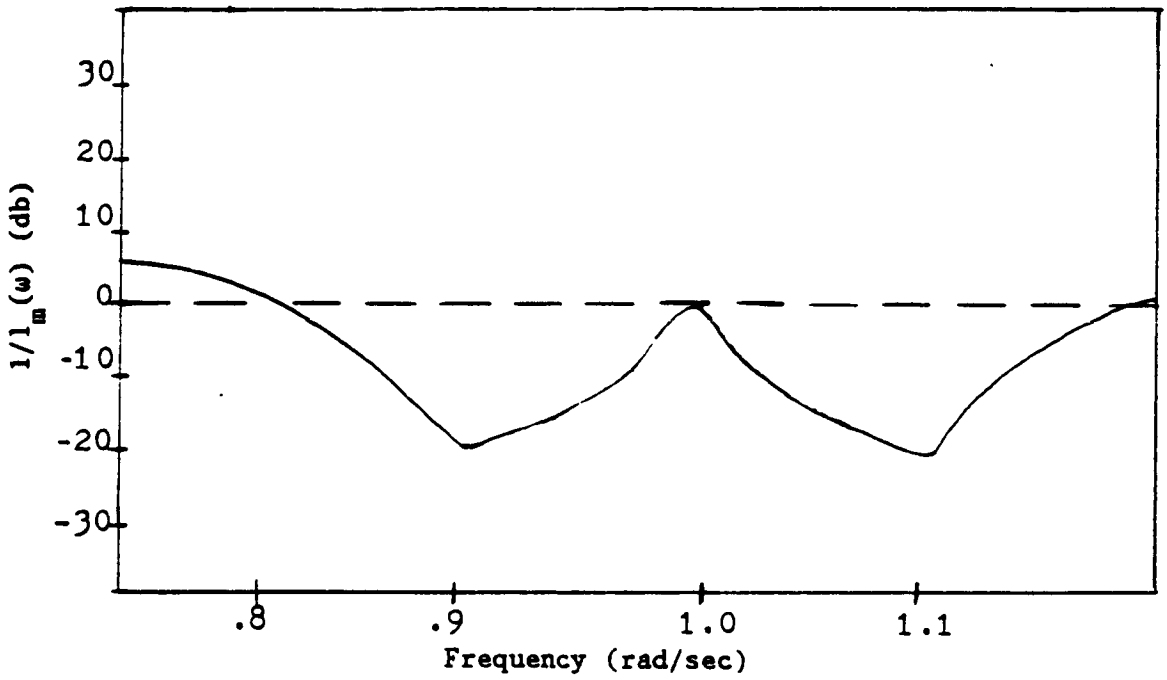

Figure 2.1.2a $1/\ell_m(\omega)$ for $-0.1 \leq \Delta\omega \leq +0.1$

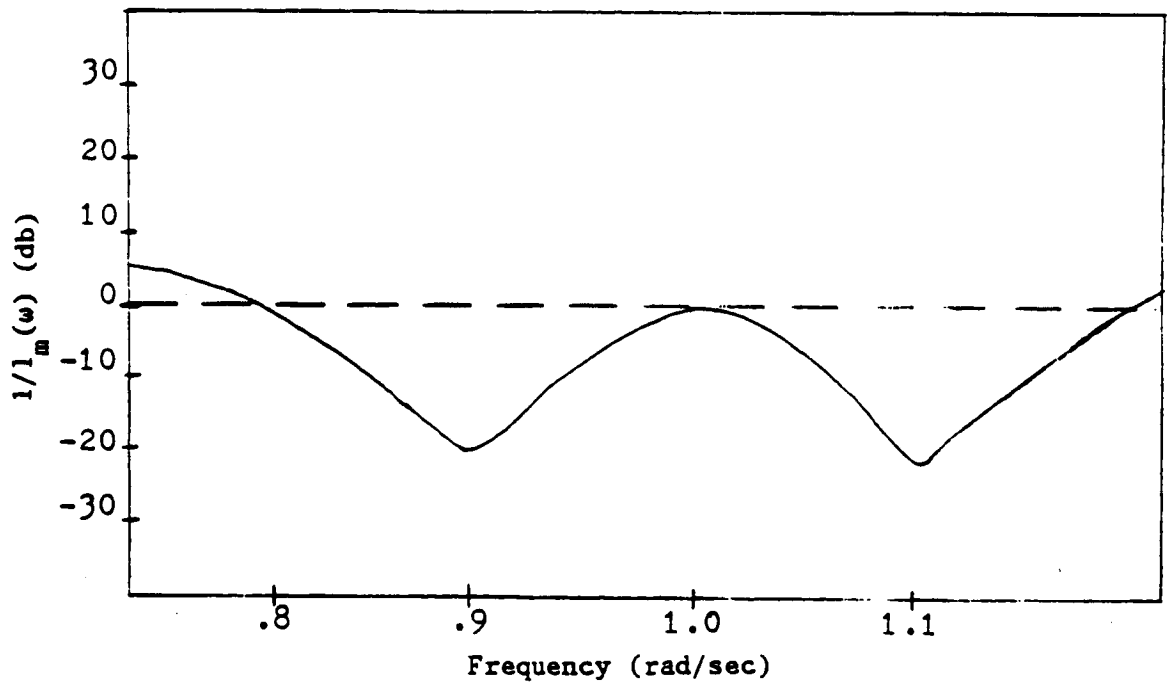

Figure 2.1.2b $1/\ell_m(\omega)$ for $\Delta\omega = -0.1$ and $+0.1$

frequency response. For any real plant $\ell_m(\omega)$ will eventually rise above 1, since no model will be accurate over all frequencies. The question in this case is whether $\ell_m(\omega) > 1$ for ω near the uncertain natural frequency. In the cases plotted in Figs. 2.1.2a and b $\max_{\omega}\{\ell_m(\omega)\} \simeq 10$ at $\omega \simeq .9$ and $\omega \simeq 1.1$. Theorem 2.1 would therefore imply that a SISO feedback system with a 1% damping ratio and 10% frequency error would be required to have a loop gain that fell below -20 db near the uncertain frequency, sharply limiting bandwidth and therefore performance.

To get a rough idea of the extent of the limits imposed by Theorem 2.1, consider an approximation of Eq. (2.13). Assume that ζ and $\Delta\omega$ are both small as compared to 1, and that the function reaches a maximum at $\omega = \omega'$. Then:

$$|\Delta(j\omega)|_{max} \simeq \Delta\omega/\zeta = \ell_m(\omega)_{max} \tag{2.14}$$

This indicates that relative frequency errors on the order of the damping ratio will limit the system closed-loop bandwidth to the lowest uncertain modal frequency. This is a relatively severe limitation, since if the damping ratio in a particular mode is 1%, a reasonable value for flexible space structures, a 1% frequency error might destabilize a system whose bandwidth included that mode. To state this differently, the only way to guarantee robustness would be to require that the nominal loop gain cross the zero db line below the first uncertain frequency.

This limit seems somewhat overly restrictive, but to gain a more concrete appreciation of the conservativeness of the unstructured uncertainty for this particular example consider a simple constant gain controller in the feedback loop. The closed-loop characteristic equation of the system is:

$$s^2 + 2\zeta\omega' s + (1+k)\omega'^2 = 0 \qquad (2.15)$$

This is clearly stable for all $k > -1$, for all $\zeta > 0$ and for all ω'. The bandwidth of the closed-loop system can therefore be increased without bound, for arbitrary error in frequency and arbitrary non-zero damping ratios, in conflict with the requirements implied by Theorem 2.1. The reason that the unstructured uncertainty is so conservative, even for this very simple, SISO system, is that it doesn't take into account any information concerning the phase of the system. Essentially it defines limits on the gain error, while allowing completely arbitrary phase error. For the example just considered, the phase error is uniquely determined by the gain error, so that the exact phase shifts that would be necessary to destabilize the system for a given gain shift can never occur. The unstructured uncertainty of Ref. [DO-1] is therefore not a good characterization of error due to uncertain frequencies in the modeled modes of a lightly damped, flexible structure. Next apply Theorem 2.2 to the same problem.

2.1.2 Application of Theorem 2.2 to the Example Problem -

In applying Theorem 2.2, the first step is to determine whether L(s) is ever zero, or strictly negative on $s\varepsilon\Omega_R$, or equivalently whether the phase of $L(j\omega)$ ever reaches $\pm 180^0$. For the example:

$$L(j\omega) = \frac{\omega'^2[(\omega_o^2-\omega^2)(\omega'^2-\omega^2)+4\zeta^2\omega_o\omega'\omega^2+2\zeta\omega[\omega_o(\omega'^2-\omega^2)-\omega'(\omega_o^2-\omega^2)]j]}{\omega^2[(\omega'^2-\omega^2)^2+4\zeta^2\omega'^2\omega^2]} \tag{2.16}$$

Clearly, this expression is zero iff $\zeta=0$ and is strictly negative and real iff $\zeta\leq 0$. Thus, Theorem 2.2 is applicable.[4] For the example the divided disturbance is given as follows:

$$\Delta_d(s) = \frac{\Delta\omega s[(2+\Delta\omega)s+2\zeta\omega_o]}{s^2+2\zeta\omega_o s+\omega_o^2}, \quad \text{where } \Delta\omega=(\omega_o-\omega')/\omega' \tag{2.17}$$

$|\Delta_d(j\omega)|$ will reach a maximum near $\omega=\omega_o$, so:

$$|\Delta_d(j\omega)|_{max} \simeq \Delta\omega/\zeta \tag{2.18}$$

Theorem 2.2 therefore implies that whenever the frequency error is on the order of the damping ratio, loop gain at that frequency must lie above 0db, or equivalently, that sufficiently high gain will stabilize the system. Theorem 2.1 indicates that the system can also be robustly stabilized with sufficiently low gain. However, in the case where $\Delta\omega>\zeta$, Theorem 2.1 requires that loop gain remain below $\zeta/\Delta\omega$,

---

[4] Actually the phase of $L(j\omega)$ asymptotically reaches $\pm 180^0$, but it is never exactly equal to $\pm 180^0$.

while Theorem 2.2 requires that loop gain remain above $\Delta\omega/\zeta$ to guarantee robust stability. Therefore the theorems indicate that there exists an intermediate range of gains for which the system is not guaranteed to be robustly stable. This is a conservative result since it has been ascertained that the above example is robustly stable for arbitrary frequency errors and for any positive feedback gain.

In conclusion, errors in the frequency of a lightly damped oscillator provide a highly structured parameter variation and the unstructured uncertainties of Doyle and Lehtomaki provide an overly conservative characterization of these errors. This implies that direct application of unstructured uncertainties is not an appropriate approach for determining the robustness of lightly damped, flexible systems with poorly modeled frequencies.

2.2 Structured Uncertainties

As noted in the previous section, the unstructured uncertainty is often conservative in the sense that it allows the plant perturbations more freedom to destabilize the system than might be realistically possible. For flexible structures with uncertain frequencies, this is certainly the case. One attempt at correcting this deficiency is the "structured uncertainty" approach also due to Doyle [DO-3,4,5,6,7]. The structured uncertainty leads to stability requirements that are not a function of loop shape alone, and therefore LTR may not be an entirely appropriate design technique for robustness enhancement.

However, analysis of the structured uncertainty for a flexible structure with uncertain frequencies does suggest a modified LQG/LTR approach that results in improved robustness. To motivate this approach, some aspects of the structured uncertainty error representation will be discussed briefly. For more details, the most readable references are [DO-4,6,7].

2.2.1 Robust Stability with Arbitrary Structured Uncertainty -

For analysis of the closed loop system, the feedback loop (K) can be absorbed into the nominal system. The uncertainties can then be represented as an external loop. This is illustrated in Figure 2.2.1.

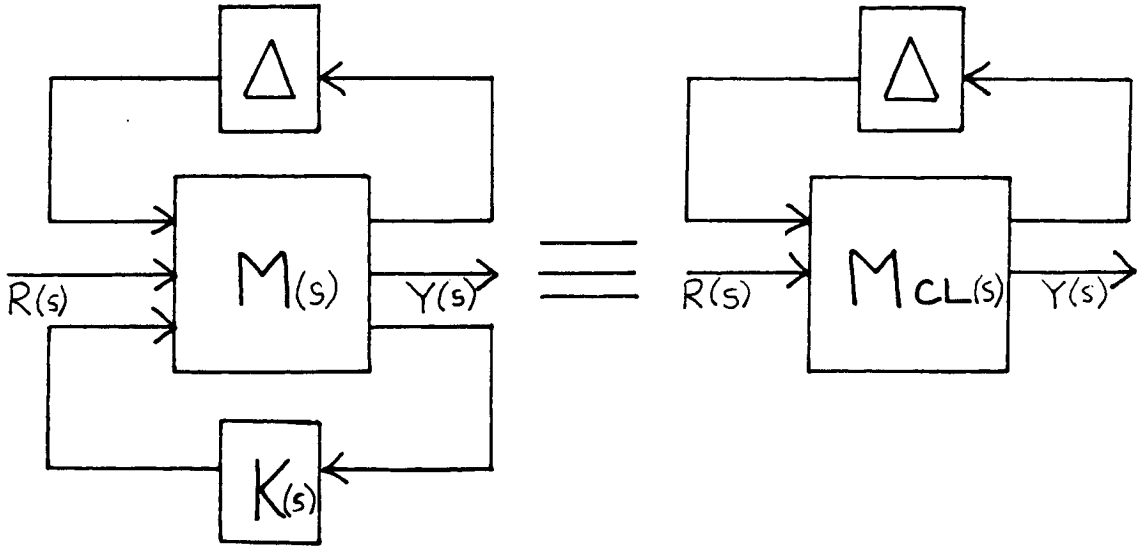

Figure 2.2.1 Linear System with Model Uncertainty

Any linear interconnection of systems can be represented as shown in this figure, though the required manipulations may not be obvious.

Fortunately computer software exists to perform this task. As a simple example, consider a multiplicative unstructured uncertainty acting at a plant output, along with a divided unstructured uncertainty acting at the plant input, as illustrated in Figure 2.2.2.

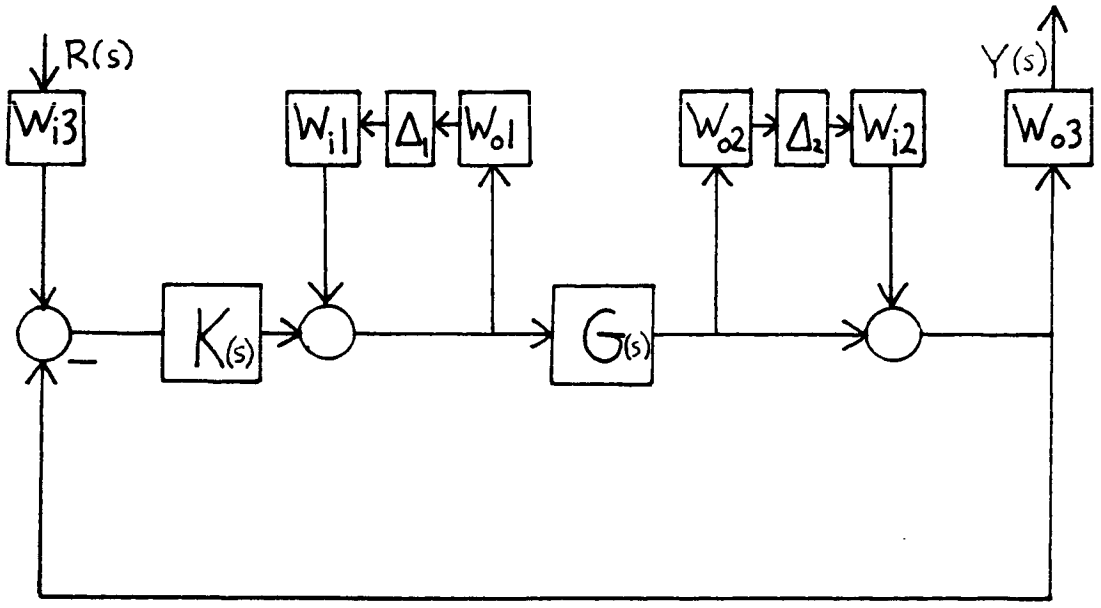

Figure 2.2.2 Example Leading to Structured Uncertainty Representation

The matrices W_{i1}, W_{o1}, W_{i2} and W_{o2} are simply multi-dimensional, frequency dependent weightings, such that $\sigma[\Delta_1]=\sigma[\Delta_2]=1$. While these weightings were not incorporated in the case of an single unstructured uncertainty (Theorems 2.1 and 2.2), they are necessary when considering the effect of a number of uncertainties acting simultaneously, (also see Section 2.1, footnote 2). The weightings W_{i3} and W_{o3} are selected such that the performance requirement is $\|Y(s)\|_2 \leq 1$ for all $\|R(s)\|_2$. Again, this is simply a frequency dependent scaling which

allows the designer to compare performance requirements with the effect of perturbations. The interconnection structure M_{CL} can, in general, be represented by an (n+1)x(n+1) matrix of transfer functions[1], where n is the number of perturbations. The i,jth element of the matrix M_{CL} is given by the transfer function from an input at the location of the ith perturbation (or plant input) to an output at the location of the jth perturbation (or plant output). For the example illustrated in Figure 2.2.2 this is:

$$M_{CL} = \begin{bmatrix} -W_{o1}(I+KG)^{-1}KGW_{i1} & -W_{o1}(I+KG)^{-1}KW_{i2} & W_{o1}(I+KG)^{-1}W_{i3} \\ W_{o2}(I+GK)^{-1}GW_{i1} & W_{o2}(I+GK)^{-1}W_{i2} & W_{o2}(I+GK)^{-1}GW_{i3} \\ W_{o3}(I+GK)^{-1}GW_{i1} & W_{o3}(I+GK)^{-1}W_{i2} & W_{o3}(I+GK)^{-1}GW_{i3} \end{bmatrix} \qquad (2.19)$$

The matrix Δ (Figure 2.3) for this case is block diag.$\{\Delta_1, \Delta_2\}$ with norm bounded blocks. The "structure" in this perturbation is therefore that Δ must remain block diagonal, with norm bounded blocks (unstructured uncertainties). This is a very specific structure, arising when uncertainties in various components of a feedback system are described by unstructured uncertainties. Real parameter variations, however, cannot be represented by this structure since they

---

[1] Here each element of M_{CL} is itself a MIMO transfer function since each perturbation and each performance requirement may be represented by a MIMO transfer function, so M_{CL} can be thought of as a matrix of matrices.

require the more restrictive structure that Δ be diagonal (rather than block diagonal) with real entries. Therefore, to deal with real parameter uncertainty, Δ must be allowed a more general structure. Conceptually every linear-time-invariant plant uncertainty can be represented by a Δ of appropriate structure. Furthermore, nonlinear and time-varying uncertainties can often be be bounded by appropriate structures on Δ. Consequently, the following theorem considers the general case where Δ can have any arbitrary structure[2].

Theorem 2.3: (Structured Uncertainty)
The system described in terms of Figure 2.3 will remain stable for all pertubations Δ ($\bar{\sigma}[\Delta]<1$) D of a given structure iff $\det[I-M_{CL}(j\omega)\Delta]\neq 0$ for all allowable Δ ($\bar{\sigma}[\Delta]<1$) with the given structure and for all ω. (Note that in the case where Δ represents a single unstructured uncertainty, Theorem 2.3 reduces to the results of Theorems 2.1 and 2.2).

The $\det [I-M_{CL}(j\omega)\Delta]$ is essentially a multivariable Nyquist plot for each allowable Δ. Since $M_{CL}(j\omega)$ is stable by assumption (stability of the nominal closed-loop system), the multivariable Nyquist criteria is requires that $\det[I-M_{CL}(j\omega)\Delta]$ not encircle the origin for any allowable Δ. In particular, if there exists an allowable Δ such that $\det[I-M_{CL}(j\omega)\Delta]=0$, then the system will go unstable for a set of

---

[2] Currently, computational methods can deal with a number of different structures on Δ, but the case of arbitrary structure is purely conceptual.

perturbations of slightly larger than Δ. On the other hand, if no such Δ exists, then the system is stable for all allowable Δ's. Note, that the above result does not imply that a Nyquist plot should be checked for every allowable Δ, since there will, in general, be an infinity of allowable Δ's. The only promise of Theorem 2.3 is that given a structure for Δ, requirements on $M_{CL}(j\omega)$ can be found that will ensure $\det[I-M_{CL}(j\omega)\Delta]\neq 0$. In particular, in the unstructured case, where Δ is simply norm bounded by one (i.e. $\sigma(\Delta)<1$), the requirement is that $\bar{\sigma}[M_{CL}(j\omega)]\leq 1$ for all ω. However, the more structure enforced on Δ, the larger $\bar{\sigma}[M_{CL}(j\omega)]$ can become before robust stability is violated.

The next step in the formulation of the structured uncertainty is to define a function $\mu(\omega)$ on the complex matrix $M_{CL}(j\omega)$, such that $\mu(\omega)$ is the inverse of the size of the smallest Δ of the correct structure such that $\det[I-M_{CL}(j\omega)\Delta]=0$ for some ω.[3] This is usually written in a norm notation (i.e., $\|M_{CL}\|_\mu$), though $\mu(\omega)$ is not a norm, and furthermore depends not only on M_{CL}, but on the structure of Δ. For stability though, it is required that $\|M_{CL}\|_\mu<1$ for all ω, or that $\sup_\omega \|M_{CL}\|_\mu<1$. In a further abuse of notation this is often written as $\|M_{CL}\|_\mu$ again. So μ is both a measure on $M_{CL}(j\omega)$ at each frequency ω,

---

[3] Size is again measured by singular values, see Appendix A.

and also a measure on $M_{CL}(j\omega)$ as an overall function of frequency.

It should be emphasized that μ simply defines the problem of finding the smallest perturbation of a defined structure which destabilizes the system. Fortunately methods for computing μ in some important cases have been developed. In particular, the case where Δ is block diagonal with non-repeated complex, norm-bounded blocks is well understood. In this case an upper bound which is exact for three or fewer blocks, and reasonably accurate for four or more, exists [DO-3]. This bound can be found by a gradient search on a convex function, or it can be approximated by balancing the matrix M in the sense of Osborne[4]. Furthermore a lower bound which is exact for an arbitrary number of blocks also exists. This bound, however, depends on maximizing a function that is not necessarily concave, and a global solution is not guaranteed. Some important results concerning the efficient calculation of the lower bound have appeared in Ref. [FA-1].

The case where a number of blocks depend on a single scalar δ arises in the case of parameter variations. If the scalar is allowed to be a complex number, this is a minor generalization of the above results. If, however, the parameter is constrained to remain real, as in the case of frequency variations, the corresponding scalar is also constrained to remain real, and the problem becomes much more diffi-

---

[4] This is a standard and computationally efficient technique used to reduce the Frobenius norm of a matrix, typically used before solving an eigenvalue problem.

cult. Since, for the case of a flexible structure with uncertain frequencies the real nature of parameter variations is essential, it will be discussed in greater detail.

2.2.2 Structured Uncertainty for Real Parameter Variations -

The following results can be found in Refs. [MO-1,2]. First consider the interconnection structure M_{CL}, and corresponding perturbation structure Δ arising from a real parameter variation. The state-space description of the nominal plant is as follows:

$$\begin{Bmatrix} \dot{x} \\ y \end{Bmatrix} = \begin{bmatrix} A & B \\ C & D \end{bmatrix} \begin{Bmatrix} x \\ u \end{Bmatrix} \tag{2.20}$$

Now consider m real parameter variations, such that the true plant is:

$$\begin{Bmatrix} \dot{x} \\ y \end{Bmatrix} = \left[\begin{bmatrix} A & B \\ C & D \end{bmatrix} + \sum_{i=1}^{m} c_i \begin{bmatrix} A_i & B_i \\ C_i & D_i \end{bmatrix} \right] \begin{Bmatrix} x \\ u \end{Bmatrix} \tag{2.21}$$

Assume that the problem is normalized so that the allowable range of each c_i is $|c_i| \leq 1$, and furthermore, that the ith state-space quadruple $[A_i, B_i, C_i, D_i]$ is of rank k_i. It can then be rewritten as follows:

$$\begin{bmatrix} A_i & B_i \\ C_i & D_i \end{bmatrix} = \begin{bmatrix} \alpha_{i1} \\ \alpha_{i2} \end{bmatrix} \begin{bmatrix} \beta_{i1} & \beta_{i2} \end{bmatrix} \tag{2.22}$$

where α_{i1}, α_{i2} have k_i columns and β_{i1}, β_{i2} have k_i rows. Though α and β are not unique the effect of making various choices has not been examined in this dissertation. Eq. (2.22) then becomes:

$$\begin{Bmatrix} \dot{x} \\ y \end{Bmatrix} = \left[\begin{bmatrix} A & B \\ C & D \end{bmatrix} + \sum_{i=1}^{m} c_i \begin{bmatrix} \alpha_{i1} \\ \alpha_{i2} \end{bmatrix} \begin{bmatrix} \beta_{i1} & \beta_{i2} \end{bmatrix} \right] \begin{Bmatrix} x \\ u \end{Bmatrix} \tag{2.23}$$

The desired interconnection structure has the form

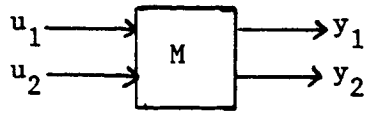

where y_1 is fed back through the perturbation structure to u_1, while u_2 and y_2 are the nominal plant inputs and outputs for performance specification. It then follows that the state space realization of M is:

$$\begin{Bmatrix} \dot{x} \\ y_1 \\ y_2 \end{Bmatrix} = \begin{bmatrix} A & \alpha_{11} & \cdots & \alpha_{m1} & B \\ \beta_{11} & 0 & \cdots & 0 & \beta_{12} \\ \vdots & \vdots & & \vdots & \vdots \\ \beta_{m1} & 0 & \cdots & 0 & \beta_{m2} \\ C & \alpha_{12} & \cdots & \alpha_{m2} & D \end{bmatrix} \begin{Bmatrix} x \\ u_1 \\ u_2 \end{Bmatrix} \tag{2.24}$$

The algebra can be verified by feeding the y_{1i}'s through the c_i's to the u_{1i}'s to get:

$$y_1 = \begin{bmatrix} \beta_{11} \\ \beta_{m1} \end{bmatrix} x + \begin{bmatrix} \beta_{12} \\ \beta_{m2} \end{bmatrix} u_2 \tag{2.25a}$$

$$\dot{x} = Ax + Bu_2 + \sum_{i=1}^{m} c_i [\alpha_{i1}][[\beta_{i1}]x + [\beta_{i2}]u_2] \tag{2.25b}$$

$$y_2 = Cx + Du_2 + \sum_{i=1}^{m} c_i[\alpha_{i2}][[\beta_{i1}]x + [\beta_{i2}]u_2] \qquad (2.25c)$$

which in turn is equivalent to Eq. (2.22). The corresponding perturbation structure is:

$$\Delta = \begin{bmatrix} c_1 I_{k_1} & 0 & \cdots & 0 \\ 0 & c_2 I_{k_2} & & \vdots \\ \vdots & & \ddots & \vdots \\ 0 & \cdots & 0 & c_m I_{k_m} \end{bmatrix} \qquad (2.26)$$

where I_{k_i} is the $k_i x k_i$ identity matrix, and c_i is a real parameter allowed to vary between ± 1. This sets up the structured uncertainty problem for real parameter variations, but does not solve it. Lower and upper bounds on μ for the above case do exist, and in the case where these are close, they constitute a good approximation. The development of a better test for μ in the real parameter variation case is a current topic of research in the control community. One promising method is described in Ref. [GA-1], though this is computationally difficult for a large number of varying parameters. When an accurate and numerically efficient solution is found the problem can be approached directly in terms of μ, and μ-synthesis can be used to generate an "optimal," robust controller. For the purposes of this dissertation, the problem statement for a flexible structure with uncertain frequencies will be set up, and some conclusions will be drawn. The exact solution of this problem, however, remains an area for

future research.

It is recognized that the preceding discussion of "structured uncertainties" is far too brief to properly cover the subject. Again the reader is referred to Refs. [DO-4,6,7]. However, the information given is sufficient to construct the perturbation model of a flexible structure with uncertain frequencies. This, in turn, suggests an approach to the LQG/LTR design procedure that improves robustness with respect to frequency errors. The perturbation model is constructed in the following section.

2.2.3 Application of Structured Uncertainty to Flexible Structures -

Consider a flexible structure with p-inputs and m-outputs, described in a "modal" state-space representation as follows:

$$A = \begin{bmatrix} 0 & 1 & 0 & \cdots & 0 \\ -\omega_1^2 & -2\zeta_1\omega_1 & 0 & \cdots & 0 \\ 0 & 0 & 1 & 0 \cdots & 0 \\ 0 & 0 & -\omega_2^2 & -2\zeta_2\omega_2 \; 0 \cdots & 0 \\ \vdots & \vdots & & & \vdots \\ & & & & 0 \\ 0 & 0 & & & 0 \quad 1 \\ 0 & 0 & \cdots & 0 & -\omega_n^2 \; -2\zeta_n\omega_n \end{bmatrix} \qquad (2.27a)$$

$$B = \begin{bmatrix} 0 & \cdots & 0 \\ b_{11} & & b_{12} \\ 0 & & 0 \\ b_{21} & \cdots & b_{22} \\ \vdots & & \vdots \\ 0 & \cdots & 0 \\ b_{n1} & \cdots & b_{np} \end{bmatrix} \tag{2.27b}$$

$$C = \begin{bmatrix} c_{11} & 0 & c_{12} & 0 & \cdots & c_{1n} & 0 \\ \vdots & \vdots & \vdots & \vdots & \cdots & \vdots & \vdots \\ c_{m1} & 0 & c_{m2} & 0 & \cdots & c_{mn} & 0 \end{bmatrix} \tag{2.27c}$$

Now consider the problem of designing a controller which maximizes robustness with respect to variations in the imaginary parts of the plant poles (variations in plant frequencies). The first step involves using the methods outlined in the previous section to find a state-space representation of the interconnection structure M for this problem. Consider a perturbation corresponding to uncertainty in the ith plant frequency (ω_i^2) of amount Δ_i. Δ_i is the size of the maximum variation in ω_i^2 (i.e., Δ_i=.21 for a 10% allowable variation in ω_i). The corresponding α_{i1}, α_{i2}, β_{i1} and β_{i2} from Eq. (2.22) are not unique since the quantity $\omega_i^2 D_i$ can be arbitrarily factored between the α's and the β's, but one possibility is:

$$\alpha_{i1}^T = (\overbrace{0 \quad \cdots \quad 0}^{2(i-1)} \mid 0 \quad \omega_i \mid 0 \quad \cdots \quad 0) \qquad \alpha_{i2} = 0 \tag{2.28a}$$

$$\beta_{i1} = (0 \quad \cdots \quad 0 \mid -\omega_i\Delta_i \quad 0 \mid 0 \quad \cdots \quad 0) \qquad \beta_{i2} = 0 \tag{2.28b}$$

To illustrate this procedure, consider the simple one mode example presented in Section 2.1 (Eq. 2.11). In this case the plant is described by the following state-space representation:

$$\begin{Bmatrix} \dot{x} \\ y \end{Bmatrix} = \left[\begin{array}{cc|c} 0 & 1 & 0 \\ -\omega_0^2 & -2\zeta\omega_0 & \omega_0 \\ \hline \omega_0 & 0 & 0 \end{array}\right] \begin{Bmatrix} x \\ u \end{Bmatrix} \tag{2.29}$$

If the ω_0^2 term is allowed to vary by an amount Δ, then a state-space representation of the interconnection structure M is given by Eq. (2.24):

$$\begin{Bmatrix} \dot{x} \\ y_1 \\ y_2 \end{Bmatrix} = \begin{bmatrix} 0 & 1 & 0 & 0 \\ -\omega_0^2 & -2\zeta\omega_0 & \omega_0 & \omega_0 \\ -\Delta\omega_0 & 0 & 0 & 0 \\ \omega_0 & 0 & 0 & 0 \end{bmatrix} \begin{Bmatrix} x \\ u_1 \\ u_2 \end{Bmatrix} \tag{2.30}$$

u_1 and y_1 are the inputs and outputs respectively for the uncertainty model. U_2 and y_2 are the control inputs and measured outputs respectively. Note that in this example α_1 is proprotional to B and β_1 is proportional to C. This is a very special situation which will not be true in the general case of n modes. The transfer function representation of M is:

$$\begin{Bmatrix} Y_1(s) \\ Y_2(s) \end{Bmatrix} = \begin{bmatrix} -\Delta\omega_0^2 & -\Delta\omega_0^2 \\ \omega_0^2 & \omega_0^2 \end{bmatrix} / s^2+2\zeta\omega_0 s+\omega_0^2 \begin{Bmatrix} U_1(s) \\ U_2(s) \end{Bmatrix} \tag{2.31}$$

By feeding Y_1 through a constant c_1 ($-1 \leq c_1 \leq 1$) and back into U_1, we ascertain that the perturbed plant transfer function is

$$G'(s) = \frac{\omega_0^2}{s^2 + 2\zeta\omega_0 s + (1+c_1\Delta)\omega_0^2} \tag{2.32}$$

as expected. In this case only the ω_0^2 term in the denominator of the transfer function varies, while in Eq. (2.11) of Section 2.1 all terms involving ω_0 vary. However for the case of light damping and small $\Delta\omega$ the two problems are almost identical, so the same robustly stable proportional feedback scheme suggested in Section 2.1 will be considered. The closed-loop transfer function for μ-analysis is:

$$M_{CL}(s) = \frac{-\Delta\omega_0^2}{s^2 + 2\zeta\omega_0 s + (1+k)\omega_0^2} \tag{2.33}$$

μ is the inverse of the smallest size c_1 such that $[1-M_{CL}(j\omega)c_1]=0$. In this case it reduces to the smallest size c_1 such that:

$$[2\zeta\omega_0]j\omega + [(1+k+c_1\Delta)\omega_0^2 - \omega^2]=0 \tag{2.34}$$

Since a real c_1 cannot affect phase, $\mu=0$ for $\omega>0$ and $\mu=\Delta/(1+k)$ for $\omega=0$. Since $\Delta<1$ and $k>0$, this indicates that the closed-loop system is robustly stable for all frequency variations as expected. This should not come as a surprise, since given the correct structure for the uncertainty, μ is never conservative. The only problem with using μ is that of defining the correct structure and calculating μ for that structure. Now consider the case where c_1 is allowed to be complex. In this case c_1 can introduce arbitrary phase shift, and there exists

a c_1 that satisfies Eq. (2.34) at every frequency ω. In fact μ can be found by solving Eq. (2.34) for c_1 and inverting the result:

$$[M_{CL}(j\omega)]_\mu = \frac{\Delta\omega_0^2}{(j\omega)^2 + 2\zeta\omega_0(j\omega) + (1+k)\omega_0^2} \tag{2.35}$$

$[M_{CL}(j\omega)]_\mu$ will reach a peak near $\omega=\sqrt{(1+k)}\omega_0$, so:

$$[M_{CL}]_\mu \simeq \frac{\Delta}{2\zeta(1+k)} \tag{2.36}$$

This indicates that the system will not be robustly stable whenever $\Delta>2\zeta(1+k)$. This result is equivalent to Eqs. (2.14) and (2.18), except that Δ is a variation in ω_0^2, resulting in the factor of 2, and the closed-loop, rather than the open-loop system is analyzed, resulting in the appearance of k. In general the structured uncertainty approach analyzes the closed-loop system, while Theorems 2.1 and 2.2 give robustness results in terms of open-loop system parameters. Eq. (2.36) is still conservative, and indicates that the conservativeness of the unstructured uncertainty approach for lightly damped flexible structures is due to allowing the frequency variations to be complex rather than real.

Now return to the original problem of synthesizing a robust controller for a plant with m uncertain frequencies. The problem is to find a compensator K(s), for the system illustrated in Fig. 2.2.1, such that the resulting closed-loop system will have $\|M_{11}\|_\mu<1$. The

system has no external inputs or outputs since these are not defined in the problem statement. This is because no performance specifications have been defined. In a realistic problem, performance is generally traded off against robustness, but the point of this example is to suggest a control problem that will improve robustness. The state-space representation of M is:

$$\begin{Bmatrix} \dot{x} \\ y_{11} \\ \cdot \\ \cdot \\ y_{m1} \\ y_2 \end{Bmatrix} = \begin{bmatrix} A & \alpha_{11} & \cdots & \alpha_{m1} & B \\ \beta_{11} & 0 & \cdots & 0 & 0 \\ \cdot & \cdot & & \cdot & \cdot \\ \cdot & \cdot & & \cdot & \cdot \\ \beta_{m1} & 0 & \cdots & 0 & 0 \\ C & 0 & \cdots & 0 & 0 \end{bmatrix} \begin{Bmatrix} x \\ u_{11} \\ \cdot \\ \cdot \\ u_{m1} \\ u_2 \end{Bmatrix} \qquad (2.37)$$

where A, B and C are given by Eq. (2.27) and the α_i's and β_i's for m uncertain frequencies are given in Eq. (2.28). Note that M_{11}, M_{12}, M_{21} and M_{22} all share the same state-space system matrix A. This is generally true of the interconnection structures arising from the structured uncertainty approach. Computationally this means that the entire interconnection structure can be described by one state-space representation.

The structured uncertainty controller synthesis problem suggested by the interconnection structure illustrated in Fig. 2.2.1 would be to find a compensator K(s) which minimizes μ on the resulting closed loop transfer function. In the notation used in Refs. [DO-3,4,5,6,7], the closed loop transfer function is denoted by $F_\ell(M,K)$, where

$F_\ell(M,K)=[M_{11}+M_{12}K(I-M_{22}K)^{-1}M_{21}]$. A direct application of this approach would require the use of untested numerical methods. However, within the context of LQG control design, a possible related approach is to minimize $\|F_\ell(M,K)\|_2$. To accomplish this, formulate the LQG probelm which consists of designing a full-state feedback control law and KB-filter for the system with the following state space description:

$$\dot{x} = Ax + Bu + [\alpha_{11}, \alpha_{21}, \ldots \alpha_{m1}]w \qquad E[ww^T] = I \tag{2.38a}$$

$$y = Cx + n \qquad E[nn^T] \to 0 \tag{2.38b}$$

so as to minimize the cost functional

$$J = E\left[\int_0^{\infty} (x^T\beta^T\beta x + u^TRu)dt\right], \qquad R \to 0. \tag{2.39}$$

where $\beta^T = [\beta_{11}^T | \beta_{21}^T | \ldots | \beta_{m1}^T]$.

The control and estimator gains in this case approach infinity. This R and $E[nn^T]$ are approaching zero because no constraints on input actuator magnitude or measurement noise have been taken into account. For a practical design, some penalty must be placed on control effort and some finite measurement noise covariance must be assumed. Then the problem then reduces to a standard LQG formulation.

The power in the above observation, is that while the LQG method

cannot directly take into account plant variations, Eqs. (2.38) and (2.39) give some indication of how the state cost functional in the LQR problem and the state noise covariance matrix in the KBF problem might be chosen so as to minimize sensitivity of the closed-loop dynamics to frequency variations. The result is somewhat counter-intuitive, since it indicates that a high penalty should be placed on the displacement of uncertain modes, while a natural inclination might be to minimize the effect of control efforts on those modes, indicating a low penalty. It also indicates that the modal penalties in the LQR state-cost matrix Q, should be proportional to the frequencies squared. This suggests that a cost based on elastic strain energy will improve robustness. Numerical simulation results on the antenna model to be described in Chapter IV, support this notion. It was found that LQR designs which weight elastic energy, result in considerably more robust compensators.

It should be emphasized that formulating an LQG prolbem along the lines just discussed is not the same as directly minimizing $\|M_{11}\|_\mu$, a problem which is very difficult to solve. Instead, the difficult problem is replaced by the by the alternate problem of minimizing $\|M_{11}\|_2$. While reducing the 2-norm of a transfer function will usually reduce the ∞-norm, it may not reduce μ. However, since the ∞-norm is always an upper bound on μ, forcing it down will eventually force μ below one, and therefore ensure robust stability. Experience gained by applying the LQG approach will be described in in Chapter IV, and this experience suggests that solving the LQG problem defined by

Eqs. (2.38) and (2.39) will improve the robustness of flexible structures with respect to variations in frequencies.

To reiterate, the suggested LQG problem incorporates the following state cost matrix Q_r, and state noise covariance matrix $\hat{Q}_r$:

$$Q_r = \begin{bmatrix} \Delta_1^2\omega_1^2 & 0 & \cdots & 0 \\ 0 & 0 & \cdots & 0 \\ 0 & \Delta_2^2\omega_2^2 & & 0 \\ 0 & 0 & & 0 \\ \vdots & \vdots & & \vdots \\ 0 & \cdots & \Delta_n^2\omega_n^2 & 0 \\ 0 & \cdots & 0 & 0 \end{bmatrix} \qquad \hat{Q}_r = \begin{bmatrix} 0 & 0 & 0 & \cdots & 0 \\ 0 & \omega_1^2 & 0 & \cdots & 0 \\ 0 & 0 & 0 & 0 & 0 \\ 0 & 0 & 0 & \omega_2^2 & 0 \\ \vdots & \vdots & \vdots & & \vdots \\ & & & 0 & 0 \\ 0 & \cdots & \cdots & 0 & \omega_n^2 \end{bmatrix} \tag{2.40}$$

A realistic LQG design might balance robustness against performance by weighting the sum of two terms in the LQR cost functional. The first would weight the elastic strain energy, Eq. (2.40), while the second would weight a performance objective such as RMS surface error or pointing accuracy. This allows the designer to make a controlled trade-off between robustness and performance.

An estimator design can be achieved by a number of methods. One possibility would be to choose the process noise covariance defined by Eq. (2.40), or perhaps balance this against a physically motivated disturbance. Another approach would be to use an LTR design where the columns of the B-matrix are used to weight the square of the modal frequency. This would result in a process noise covariance of the form $q_1(BB^T+q_2WW^T)$, where:

$$W^T = [\ 0\ \ \omega_1\ \ 0\ \ \omega_2\ \ \ldots\ \ 0\ \ \omega_n\ ].$$

The results of the modified LTR compensator designs based on this principle will be presented in Chapter IV. The rest of this chapter is devoted to a very brief discussion of robustness results based on a time-domain viewpoint.

2.3 Time Domain Approaches to Robustness

Some work has been done in characterizing the robustness of feedback systems directly in the time domain. Typically these results are defined in terms of interval matrices. An interval matrix is one in which each element is known to lie in a specified interval. One early result on the stability of interval matrices was published in Ref. [BI-1]. This defined conditions for stability based on the coefficients of the corresponding characteristic equation, which is an interval polynomial. Unfortunately, though the results concerning interval polynomials were correct, the extension of those results to interval matrices were not, as evidenced by the counter-example of Ref. [BA-1]. The original reference, however, led to a flurry of results concerning the stability of interval polynomials [KA-4,SO-1,BA-2] and at least one result on sufficient conditions for the stability of interval matrices [HE-1]. Design methods based on these results have appeared in Refs. [SO-2,3,EV-1]. While the results are promising, and may be useful for simple problems, the corresponding design methods are too cumbersome for practical implementation in

realistic problems. Some related results have also appeared [PE-1,YE-1,KH-1,HO-1]. Again, in the opinion of the author, the results are either not general enough, or too cumbersome. The advantage of the "structured/unstructured uncertainty" approach is that it is both very general, and results in a single scalar measure of robustness which is amenable to global minimization.

In conclusion, it is the opinion of the author that the current robustness results based on a time domain representation of the system are not sufficiently developed for application to the complex problem considered in this dissertation. They will not be considered further.

Chapter III

LOOP TRANSFER RECOVERY (LTR) CONTROL DESIGN

LTR is an appealing approach to control design for two basic reasons. The first is that it can be used to recover the gain and phase margins of a Linear Quadratric Regulator (LQR) at the plant input, or of a Kalman Bucy Filter (KBF) at the plant output. This is sometimes called robustness recovery [DO-2] or sensitivity minimization [KW-1]. These are, however, somewhat misleading terms since they suggest that the loop recovered system will have the same robustness properties as the full state feedback LQ regulator or the KB filter. This is not generally true as will be indicated more specifically later. The second appeal of the LTR approach is its applicability to loop shaping as a more general control design method. The idea of loop shaping is most clearly spelled out in Ref. [DO-1], where it is pointed out that a number of system properties, including performance, sensitivity, noise rejection, "robustness" and control effort, depend on the system loop shape (maximum and minimum singular values of the system transfer function matrix). The LTR loop shaping approach involves first designing an LQR loop or a KBF loop with desired characteristics, and then recovering that loop shape by LTR methods. Again there is a dangerous implication in the loop shaping approach, that all systems with the same loop shape will behave identically. This is true for the nominal plant, but when the plant parameters are perturbed, the two loops may no longer be identical and the system response (and stability) may vary considerably. In Chapter IV, a number of examples of

systems with identical loop shape, but different robustness characteristics will be given.

For simplicity, the input loop recovery procedure of Doyle and Stein [DO-1,2] will be considered, noting that output loop recovery [KW-1] is simply its dual. After describing the procedure it will be interpreted for SISO systems, and for 1-input, m-output systems. This interpretation will lead to a polynomial (pole/zero cancellation) approach to loop recovery. Finally methods for using the extra degrees of freedom available in the loop recovery procedure to find an "optimal" loop recovered system will be considered.

3.1 Input Loop Recovery

The LQR loop has excellent robustness properties. In particular an LQ regulator with diagonal input weighting matrix R is guaranteed to have atleast an infinite gain margin, a gain reduction margin of 1/2 and a phase margin of $\pm 60^{0}$, simultaneously in all the feedback loops [LE-1,2]. The idea of input loop recovery is to design an LQ regulator with some loop shape and then use an asymptotic procedure to design a KB filter that recovers that loop shape. Since gain and phase margins are a function of loop shape, the output feedback system, using a KB filter to estimate the plant states, will have the identical gain and phase margins as the LQR loop. For this reason, input loop recovery is sometimes called robustness recovery. This is the point of view taken in Ref. [DO-2]. Another advantage of the loop

recovery approach is that it is relatively simple to specify the LQR loop shape at low frequencies, by carefully choosing the weightings in the LQR cost functional [HA-1]. Loop Transfer Recovery (LTR) can then be used to achieve the identical loop shape for an output feedback system. This is the loop shaping control approach, and is the point of view taken in Ref. [DO-1].

Performance specifications are usually defined in terms of errors in the plant outputs for some set of disturbance inputs. In general, the disturbance inputs may enter at points other than the plant input or the plant output. The configuration presented in Ref. [DO-1], however, indicates disturbances acting at the plant outputs, as illustrated in Fig. 3.1.1. In this case the transfer function between D(s) and E(s) is:

$$E(s) = [I + G(s)K(s)]^{-1}D(s) \tag{3.1}$$

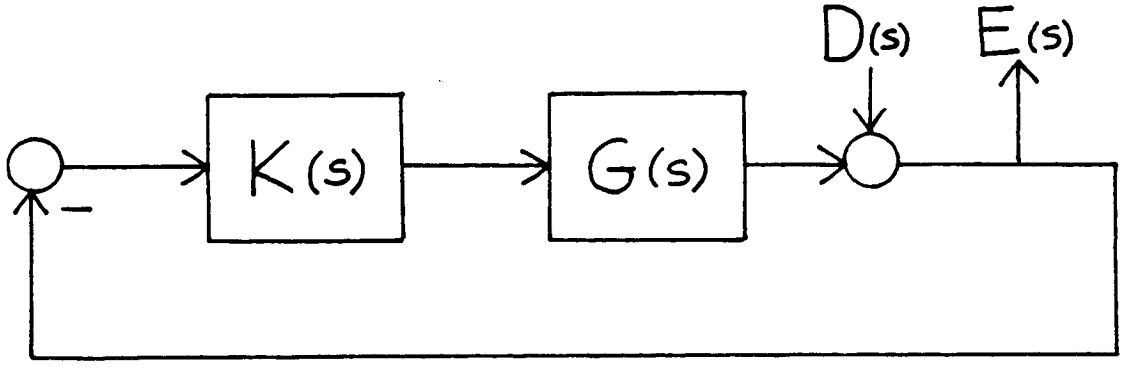

Figure 3.1.1 Output Errors for Disturbance Acting at Output

This implies that the system has good disturbance rejection whenever the output return difference is large, or equivalently whenever the output loop gain is large. This is the motivation for defining performance in terms of output loop gain. A motivation for considering input loop gain to be an important performance specification can be constructed by considering the transfer function from disturbance inputs acting at the plant inputs to errors in the plant inputs. This is illustrated in Fig. 3.1.2. In this case the transfer function between D(s) and E(s) is:

$$E(s) = [I + K(s)G(s)]^{-1}D(s) \tag{3.2}$$

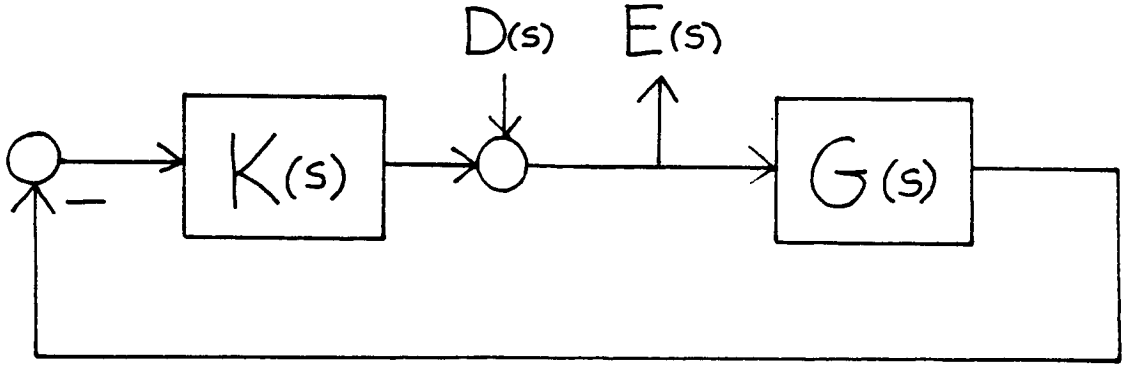

Figure 3.1.2 Input Errors for Disturbance Acting at Input

This is a somewhat artificial performance specification, but it does lead to requirements on the input loop gain. A third configuration would have disturbances acting at the plant input and errors measured at the plant output. This is a good model for a number of systems and results in the following relationship between E(s) and D(s):

$$E(s) = G(s)[I + K(s)G(s)]^{-1}D(s) \tag{3.3}$$

Since G(s)is fixed, this again indicates that disturbance rejection is good whenever K(s)G(s) is large, suggesting high input loop gain. Therefore, for the remainder of this dissertation, performance is measured by input loop gain. In particular, high input loop gain at a frequency ω indicates good disturbance rejection at that frequency, while low input loop gain indicates poor disturbance rejection.

To see how loop transfer recovery works, consider a full-state feedback control law, u=-Kx. The input loop transfer function for this system will be $K(sI-A)^{-1}B$. Now consider a state estimator of the form,

$$\dot{\hat{x}} = A\hat{x} + Bu + G(y - C\hat{x}) \tag{3.4}$$

and a control law based on the state estimate $\hat{x}$, $u=-K\hat{x}$. In this case the compensator transfer function is,

$$K(s) = K(sI - A + BK + GC)^{-1}G \tag{3.5}$$

and the input loop transfer function for the output feedback system is:

$$K(s)G(s) = K(sI - A + BK + GC)^{-1}GC(sI - A)^{-1}B \tag{3.6}$$

To get loop recovery choose an estimator gain matrix G, such that,

$$K(sI-A+BK+GC)^{-1}GC(sI-A)^{-1}B \rightarrow K(sI-A)^{-1}B \tag{3.7}$$

In Refs. [DO-1,2] it is stated that any Kalman gain matrix G which asymptotically satisfies $G \to qBW$ as $q \to \infty$ will recover the LQR loop shape. W is an arbitrary, symmetric, positive definite matrix, while q is a large scalar parameter which is increased to achieve asymptotic loop recovery. To demonstrate this result, note that the transfer function between y and $\hat{y}$ in the state estimator can be written as follows,

$$\hat{y} = (I + C\bar{\Phi}G)^{-1}C\bar{\Phi}Gy \tag{3.8}$$

where $\bar{\Phi}$ denotes $(sI - A + BK)^{-1}$. This leads to the following alternate representation of K(s):

$$K(s) = K[\bar{\Phi} - \bar{\Phi}(I + C\bar{\Phi}G)^{-1}C\Phi]G \tag{3.9}$$

which after some further manipulations can be rewritten as:

$$K(s) = K\bar{\Phi}G(I + C\bar{\Phi}G)^{-1} \tag{3.10}$$

Now if $G \to qBW$ as $q \to \infty$, then

$$K(s) \to K\bar{\Phi}B(C\bar{\Phi}B)^{-1}. \tag{3.11}$$

Using the identity, $\bar{\Phi}B = \Phi B(I+K\Phi B)^{-1}$, where $\Phi = (sI-A)^{-1}$, Eq. (3.11) becomes,

$$K(s) \to K\Phi B(C\Phi B)^{-1} \tag{3.12}$$

and,

$$K(s)G(s) \rightarrow K\Phi B(C\Phi B)^{-1}C\Phi B = K\Phi B \qquad (3.13)$$

This shows explicitly how loop recovery inverts the plant dynamics from the left and replaces them by the full-state feedback dynamics.

So far there has been no requirement that K be derived from an LQR problem, nor that the estimator be a KB filter. In fact any appropriate method (e.g., pole placement) could be used to select the control gains K, and any estimator (e.g., an observer) which asymptotically satisfies $G \rightarrow qBW$ and simultaneously stabilizes the plant can be used to calculate the estimator gains G. However, the choice of an LQR approach for finding K has the advantage that the resulting loop will have desirable properties, and the use of a KB filter to recover that loop shape guarantees a stable plant at every stage in the asymptotic loop recovery procedure.

In using a KB filter for LTR, the designer is allowed to append additional columns to the B matrix until the plant is square. In the original formulation [DO-1,2] a square plant was required, but it has since been shown [MA-1] that this is not necessary to achieve loop recovery. The freedom to append columns however, will be retained in this study for the purpose of examining variations in robustness resulting from different choices in the appended columns. The only requirement on these columns is that the resulting plant be minimum phase. Once the system is "squared up," a KB filter is found, where the measurement noise covariance N is an arbitrary positive definite matrix, and the state noise covariance has the following special form,

$$M = M_o + q^2 BWB^T \tag{3.14}$$

where M_o is some nominal noise covariance, q is the parameter which will be increased to achieve recovery and W is an arbitrary positive definite matrix. Note that the B matrix in Eq. (3.14) includes the appended columns, so the rank of BWB^T can be as high as the number of plant outputs.

To show that this KB filter will asymptotically recover the loop shape consider the Riccati equation:

$$AP + PA^T - PC^T N^{-1} CP + M_o + q^2 BWB^T = 0 \tag{3.15}$$

and divide by q^2:

$$A(P/q^2) + (P/q^2)A^T - (G/q)N(G/q)^T + (M_o/q^2) + BWB^T = 0 \tag{3.16}$$

Since $\lim_{q\to\infty}(P/q^2)=0$ iff $C(sI-A)^{-1}B$ has no r.h.p. transmission zeros [KW-1, p.307], the assumption of a minimum phase plant is required to conclude that

$$-(G/q)N(G/q)^T + BWB^T \to 0 \tag{3.17}$$

The KBF estimator gains G will therefore have the following asymptotic property:

$$G \to qBW^{\frac{1}{2}}TN^{-\frac{1}{2}} \tag{3.18}$$

Where T is an orthonormal matrix (i.e., $TT^T = T^TT = I$). The KB filter asymptotically recovers the loop shape as q approaches infinity.

Next the SISO case will be examimed to gain a more intuitive understanding of the LTR procedure. One quick note, however, is that the estimator gain matrix G may become very large before loop recovery is achieved. This may cause some computational problems and may not provide the best solution for a robust compensator, as will be discussed further in Section 3.4.

3.2 SISO Interpretation of Loop Recovery

The SISO loop recovery problem is as follows. Given a SISO $G(s) = N(s)/D(s)$, find a proper (or strictly proper) $K(s) = n(s)/d(s)$ such that $K(s)G(s) = G(s)K(s) \simeq \gamma(s)/D(s)$ for some specified $\gamma(s)$. The obvious solution is to let $n(s) = \gamma(s)$ and $d(s) = N(s)d_\ell(s)$, where $d_\ell(s)$ consists of enough poles to make K(s) proper (or strictly proper), and these poles are placed far enough into the l.h.p. that they do not significantly affect the loop shape in the design region. This interpretation also clarifies the minimum phase condition, since if G(s) is non-minimum phase, this procedure will result in a pole/zero cancellation in the r.h.p., that will destabilize the closed loop system.

The asymptotic LTR procedure does not calculate an exact pole/zero cancellation, but achieves this cancellation asymptotically. It is

clear, however, that it is possible to achieve loop recovery by specifying a compensator that does achieve exact cancellation, without going through an asymptotic process. In both cases the cancellation will be close to exact before loop recovery is achieved, so it will be assumed that it is exact.

This interpretation indicates the essential difference between the true LQR loop and the LTR loop. While both loops may look identical over any given frequency range, the LTR loop will contain a number of hidden pole/zero cancellations. These cancellations do not show up for the nominal plant, but as soon as the plant changes, they will no longer be exact and the LQR and LTR loop shapes may be considerably different. This is especially evident for lightly damped systems, since the plant zeros in this case will lie close to the imaginary axis. Very small errors in the plant zeros will therefore produce very large errors in the LTR loop shape. It is because of this property that an LTR design will in general <u>not</u> have the same robustness characteristics as the corresponding LQR design.

3.2.1 Some Comments on the MIMO Case -

LTR is a more interesting and less obvious design procedure in the MIMO case, but the same basic properties carry through. In this case the designer would choose the following compensator,

$$K(s) = K\Phi B(C\Phi B)^{-1}/d_{\ell}(s) \tag{3.19}$$

where $d_\ell(s)$ would have the same interpretation as the SISO case. Eq. (3.19) can be rewritten by dividing out the common factor det[sI - A] to get,

$$K(s) = [Kadj(sI-A)B][Cadj(sI-A)B]^{-1}/d_\ell(s) \tag{3.20}$$

where Kadj(sI-A)B is the MIMO generalization of $\gamma(s)$ and Cadj(sI-A)B is the MIMO generalization of N(s).

One method for realizing LTR for square MIMO plants, involves exploiting the eigenstructure of the plant. In Ref. [KA-3] it is shown that an observer design which not only cancels the plant transmission zeros, but matches specified eigenvectors, will recover loop shape. The cancelling approach taken in this dissertation is somewhat different.

For the special case of 1-input and m-outputs [Cadj(sI-A)B] will be a square matrix where only the first column is fixed and the next m-1 columns are at the designer's discretion (within the constraint of a non-minimum phase plant). Thinking again in terms of the SISO problem, this is somewhat like having an N(s) at the designer's discretion, corresponding to some freedom in the placement of compensator poles. Once the poles are picked, however, loop recovery will specify the compensator zeros. Keeping this in mind an algebraic, direct pole/zero cancellation, design of a LTR compensator for a 1-input, m-output plant will be considered.

3.3 Algebraic Loop Recovery

As indicated in the previous section, loop recovery can be achieved for a SISO system by defining a compensator that exactly cancels the plant zeros and replaces them by a set of "optimal" zeros corresponding to the LQR loop. For the case of a 1-input, m-output plant, a similar procedure can be carried out, but now the designer has a set of free design variables. This freedom can be used in a variety of ways. Some possibilities include choosing a minimum order loop recovery compensator or specifying the location of the compensator poles. Here a minimal order compensator for which the compensator poles can be chosen arbitrarily will be considered. In this case a simple set of linear equations is solved to find the coefficients of the compensator numerator polynomials, such that loop recovery is achieved.

A 1-input, m-output plant and compensator will have the following special form:

$$G(s) = \begin{Bmatrix} g_1(s) \\ g_2(s) \\ . \\ . \\ g_m(s) \end{Bmatrix} = \begin{Bmatrix} N_1(s) \\ N_2(s) \\ . \\ . \\ N_m(s) \end{Bmatrix} /D(s) \qquad (3.21a)$$

$$K(s)=[k_1(s)\ k_2(s)\ \ldots\ k_m(s)]=[n_1(s)\ n_2(s)\ \ldots\ n_m(s)]/d(s) \qquad (3.21b)$$

The input loop transfer function will be:

$$K(s)G(s) = \sum_{i=1}^{m} N_i(s)n_i(s)/D(s)d(s) \tag{3.22}$$

To achieve loop recovery it is necessary and sufficient that:

$$K(s)G(s)= \sum_{i=1}^{m} N_i(s)n_i(s)/D(s)d(s)=\gamma(s)/D(s)d_\ell(s)\simeq\gamma(s)/D(s) \tag{3.23}$$

where $\gamma(s)$ is the numerator polynomial for the LQR input loop. $d_\ell(s)$ is again a set of poles required to maintain a proper (or strictly proper) compensator, where those poles are kept sufficiently far out in the l.h.p. so that they don't significantly affect the loop shape in the design region. Then $d(s)=d_c(s)d_\ell(s)$, where $d_c(s)$ must be cancelled out by the input loop numerator. Once the compensator poles are selected, the following equation must be solved to find the compensator numerator polynomials:

$$\sum_{i=1}^{m} N_i(s)n_i(s) = \gamma(s)d_c(s) \tag{3.24}$$

To find the minimal order compensator satisfying Eq. (3.24), let $n_\gamma = \deg\{\gamma(s)\}$, $n_c = \deg\{d_c(s)\}$, $n_\ell = \deg\{d_\ell(s)\}$, $n_N = \max[\deg\{N_i(s)\}]$ and $n_n = \deg\{n_i(s)\}$. The degree of the left side of (3.24) will be $n_N + n_n$, while the degree of the right side of (3.24) will be $n_\gamma + n_c$, so the first requirement on n_n is that:

$$n_N + n_n = n_\gamma + n_c \tag{3.25}$$

The second requirement on n_n is that there must exist enough degrees of freedom to satisfy Eq. (3.24) for arbitrary $\gamma(s)D_c(s)$. The number of free parameters is $m(n_n+1)$, while the number of polynomial coefficients that must be satisfied is $n_\gamma+n_c+1$, this implies that:

$$m(n_n+1) = n_\gamma + n_c + 1 \tag{3.26}$$

Combining Eqs. (3.22) and (3.23) gives the following result for n_n:

$$n_n = (n_N/(m-1)) - 1 \tag{3.27}$$

For a strictly proper compensator, the order of the compensator is $n_c + n_\ell = n_N/(m-1)$. So a 1-input, 2-output plant has a strictly proper loop recovery compensator of the same order as the maximum degree of the plant numerator polynomials, while a 1-input, 3-output plant has a loop recovery compensator of half that order, etc.. This approach therefore leads to lower order compensators than the asymptotic, observer based approach described in the previous section. In fact, as m increases, the order of the compensator can become very small, while still achieving loop recovery.

Once the order of the compensator and the location of the compensator poles are chosen, the compensator numerator polynomials are found by the solution of a set of $m(n_n+1)$ linear equations. Let the ith compensator numerator polynomial be written as follows:

$$n_i(s) = n_{i,n_n} s^{n_n} + \ldots + n_{i,1} s + n_{i,0} \tag{3.28a}$$

and similarily let the ith plant numerator polynomial be:

$$N_i(s) = N_{i,n_N} s^{n_N} + \ldots + N_{i,1} s + N_{i,0} \tag{3.28b}$$

Then the equations can be written in the following matrix form:

$$Sn=d \tag{3.29}$$

where,

$$S = \begin{bmatrix} N_{1,0} & 0 & \cdots & 0 & \cdots & N_{m,0} & 0 & \cdots & 0 \\ N_{1,1} & N_{1,0} & \cdots & 0 & \cdots & N_{m,1} & N_{m,0} & \cdots & 0 \\ \vdots & \vdots & & \vdots & & \vdots & \vdots & & \vdots \\ N_{1,n_N} & N_{1,n_N-1} & \cdots & \cdots & \cdots & N_{m,n_N} & N_{m,n_N-1} & \cdots & \cdots \\ 0 & N_{1,n_N} & \cdots & \cdots & \cdots & 0 & N_{m,n_N} & \cdots & \cdots \\ \vdots & \vdots & \cdots & \cdots & \cdots & \vdots & \vdots & \cdots & \cdots \\ \vdots & \vdots & \cdots & \cdots & \cdots & \vdots & \vdots & \cdots & \cdots \\ 0 & 0 & \cdots & N_{1,n_N} & \cdots & 0 & 0 & \cdots & N_{m,n_N} \end{bmatrix} \tag{3.30a}$$

$$n = [n_{1,0} \cdots n_{1,n_n} \; n_{2,0} \cdots n_{2,n_n} \; \cdots\cdots \; n_{m,0} \cdots n_{m,n_n}]^T, \tag{3.30b}$$

$$d = [\, d_0 \; \cdots\cdots \; d_{n_\gamma+n_c}]^T, \tag{3.30c}$$

and d_i is the ith coefficient of $\gamma(s)D_c(s)$. The above algorithm is

easily implemented on digital computer whenever a unique solution to Eq. (3.24) exists, or equivalently whenever the matrix S is non-singular. The following two paragraphs describe in greater detail the conditions under which S is non-singular.

The matrix S is similar in structure to a Sylvester matrix used to determine the coprimeness of two polynomials [KA-1,CH-1], so it is reasonable to expect that the conditions for S to be non-singular would be related to the coprimeness of the N_i's. In fact a necessary condition for a unique solution to exist is that there exist no $a_k(s)$ and $b_k(s)$, such that $\deg\{a_k(s)\}$, $\deg\{b_k(s)\} \leq n_n$ and,

$$\frac{N_i(s)}{N_j(s)} = \frac{a_k(s)}{b_k(s)}, \quad 1 \leq i \neq j \leq m, \quad k=1,\ldots, \sum_{i=1}^{m-1} (m-i) \qquad (3.31)$$

The index k simply counts the number of possible combinations of n_i and n_j taken 2 at a time from a collection of m. To show this result, assume that there exist a_k and b_k satisfying the above properties. Then the equation $\sum_{i=1}^{m} N_i(s)n_i(s) = 0$ has the nontrivial solution given by $n_i(s)=N_j(s)$ and $n_j(s)=-N_i(s)$ with all other n_i's=0. This implies that Eq. (3.24) has no unique solution. There are two cases in which the necessary conditions would not be satisfied. The first would be if there exists a pair, $N_i(s)$ and $N_j(s)$ both with degree less than or equal to n_n. In this case let $a_1(s)=N_i(s)$ and $b_1(s)=N_j(s)$ and the

necessary conditions are violated. Note that $n_N \geq n_n$, but that n_N is the maximum degree of the N_i's, and some N_i might have a degree considerably less than n_N, so this case is a real possibility whenever the degrees of the plant numerator polynomials vary considerably. The first necessary condition is therefore that no two plant numerator polynomials may have degree less than or equal to n_n. The second case would be where an N_i failed to have a factor of degree n_n which was coprime with every other N_i. Incidentally, if the condition on the degree of a_k and b_k were changed to $\deg\{a_k(s)\} < \deg\{n_i(s)\}$, then (3.31) would be identical to the requirement that all N_i's be coprime. Therefore, coprimeness of all the N_i's is not a necessary condition, though the result is similar.

For the case of m=2 these conditions are also sufficient since the existence of a non-unique solution to Eq. (3.24) immediately implies that there exist a_k and b_k with the correct properties. For the case of m>2 the sufficient conditions do not depend only on properties of the N_i's taken two at a time, but are simply that Eq. (3.24) have a unique solution. To show that the necessary conditions are not also sufficient in this case consider the following simple counter-example, where m=3, $n_N=2$ and $n_n=0$. Eq. (3.24) has a unique solution iff

$$(s+a_1)(s+b_1)n_1 + (s+a_2)(s+b_2)n_2 + (s+a_3)(s+b_3)n_3 = 0 \qquad (3.32)$$

has only the trivial solution, $n_1=n_2=n_3=0$. Consider the case where $a_i=-b_i$ for i=1,2,3 in which case the following solution exists:

$$n_2 = (a_1^2-a_3^2)/(a_3^2-a_2^2)n_1, \text{ and } n_3 = (a_2^2-a_1^2)/(a_3^2-a_2^2)n_1$$

for abitrary n_1. In this case none of the N_i's are necessarily coprime, nor do any have degree less than n_n, but a unique solution to Eq. (3.24) does not exist. The only reliable test for sufficiency in the case of m>2 is to check the non-singularity of the matrix S.

3.4 Robustness of LTR Designs

Perhaps the primary conclusion concerning the robustness of LTR designs to plant parameter variations depends upon the relationship between loop shape and robust stability implied by Theorems 2.1 and 2.2. Specifically, if model errors are accurately described by unstructured uncertainties, then LTR methods can be used to ensure that the conditions of Theorems 2.1 and 2.2 are met, thereby guaranteeing robust stability. This constitutes the ideal case for applying Loop Transfer Recovery, since specifying constraints on the loop shape is a necessary and sufficient condition for robustness. On the other hand, some model errors are not well described by unstructured uncertainties. In particular frequency errors in the model of a lightly damped flexible structure fall into this category (see Section 2.1), as do most cases of strict parameter variations. In this case Theo-

rems 2.1 and 2.2 give sufficient but not necessary conditions for robust stability, and a design based upon constraining loop shape on the basis of unstructured uncertainties will be conservative, resulting in low performance. In the case of lightly damped structures the implied constraints on loop shape would require that uncertain flexible modes not be actively controlled (again see Section 2.1). Therefore, the robustness of designs which actively control flexible modes cannot be analyzed by examining loop shape alone. In fact, for a given loop shape, a whole family of LTR designs may exist, where the robustness of these designs varies. In conclusion, the application of LTR methods to lightly damped structures with uncertain frequencies cannot be blindly approached in terms of conditions implied on the loop shape. A major emphasis of the current study has been to identify conditions which are important. These results will be illustrated by the examples presented in Chapter IV.

The next observation concerns the fact that LTR designs rely on a series of pole/zero cancellations, as noted in Section 3.2. Whenever these cancellations occur near the imaginary axis a small perturbation in the plant, resulting in a small shift of the plant zero, will cause a very large variation in the open-loop frequency response. It would therefore be reasonable to expect that an LTR design which achieves fewer pole/zero cancellations near the imaginary axis will be more robust than one that achieves more. One way to reduce the number of plant zeros, and therefore the number of cancellations, is to add measurements. A second order flexible system, with m-inputs and m-dis-

placement outputs, can have at most (n-2m) transmission zeros [ED-1][1]. Remembering that in the asymptotic LTR approach, each additional measurement entails an additional artificial input, this implies that every measurement removes a pair of transmission zeros. In the algebraic approach, additional measurements are used to reduce the compensator order, so it is unclear whether any robustness improvement might result.

A method for shifting the cancellations away from the imaginary axis in the asymptotic approach would be to use the extra degrees of freedom available in the choice of artificial inputs to shift the plant transmission zeros to the left. One option for doing this is to use a non-linear programming approach as described in the previous section. The results of this approach will be presented in Chapter IV. It shoud be noted that this idea is also the motivation behind the algebraic LTR approach, which allows the designer to place the pole/zero cancellations as far into the left half plane as desired.

Another comment on the robustness of LTR designs refers to issues raised in Ref. [SH-1], dealing specifically with the robustness problems associated with any compensator design that incorporates very high estimator gains. Asymptotic LTR designs can result in extremely high (on the order of 10^6 or higher) gains in the estimator Kalman

---

[1] For velocity outputs the maximum number of finite transmission zeros is (n-2m+1)

gain matrix G. Two difficulties are pointed out. The first involves the case where a plant perturbation changes the structure of the plant transmission zeros at infinity. This is a perturbation that affects the excess of poles over finite transmission zeros[2]. An example in which this occurs for a realistic flexible system is as follows: Consider the system illutrated in Fig. 3.4.1, consisting of two disks (of inertia 1), stacked one on top of the other, connected by a rod (of length 1) which acts as a rotational spring (of spring constant 1/2). The input is a torque about the lower disk. The nominal output is the rotation of the top of the rod (equal to the rotation of the upper disk). The nominal transfer function is:

$$G(s) = \frac{1/2}{s^2(s^2+1)} \tag{3.33}$$

An LQR design which minimizes the mechanical energy, plus the rotation of the lower disk squared, plus the control input squared, results in the following control gain vector (in modal coordinates):

$$K = [\ 1.0000 \quad 2.0555 \quad 1.6124 \quad 0.6325\ ] \tag{3.34}$$

An asymptotic LTR design can be achieved by setting the process noise covariance equal to $(1x10^{12})BB^T$, resulting in the following Kalman Filter gains:

---

[2] Note that this is not the same as the finite transmission zeros added when neglected dynamics are appended to the design plant. In this case the number of poles increases along with the number of transmission zeros, indicating that the excess does not change, and the structure of the zeros at infinity therefore does not change.

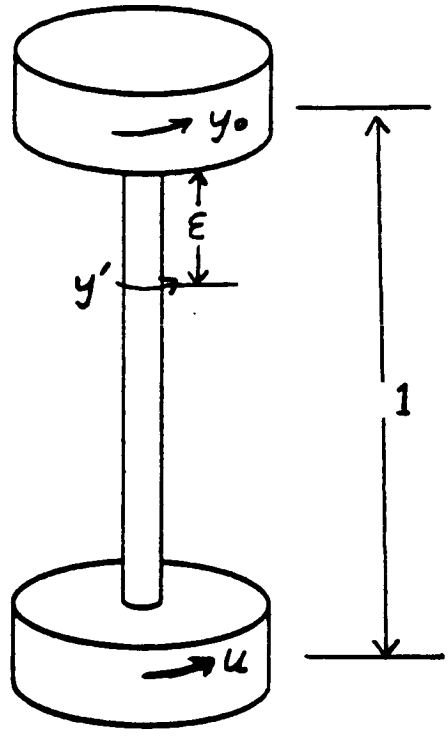

Figure 3.4.1 Two Disk System

$$G = \begin{bmatrix} 98255.0 \\ 1000000.0 \\ 98116.0 \\ 995170.0 \end{bmatrix} \tag{3.35}$$

This design is relatively robust with respect to frequency variations (withstands ±30% errors in the flexible frequency), but consider an error corresponding to a manufacturing defect which places the rotation sensor at a point ε below the top disk. The true transfer function would then become:

$$G'(s) = \frac{\varepsilon s^2+1/2}{s^2(s^2+1)} \tag{3.36}$$

Therefore, while the nominal plant has no finite zeros, the true plant

has a pair at $\pm\sqrt{-1/2\varepsilon}$, satisfying the conditions referred to in Ref. [SH-1]. The asymptotic LTR design defined by Eqs. (3.34) and (3.35) will be unstable for $\varepsilon>0.04$,[3] corresponding to finite zeros at $\pm 3.54j$ or lower on the imaginary axis. This might be a realistic robustness problem in some applications, but it can occur only under very special circumstances. In particular, for any square flexible structure with displacement outputs, the maximum number of finite transmission zeros is (n-2m) [ED-1]. Therefore, if the nominal plant has this maximum number of transmission zeros, no perturbation in plant parameters can result in the conditions required by Ref. [SH-1] for robustness problems.

In conclusion the robustness problems associated with LTR control exposed in Ref. [SH-1] depend on a nominal plant which is chosen such that there exists a perturbation in plant parameters which will increase the number of finite transmission zeros by atleast 2. This possibility can always be ruled out by ensuring that the nominal plant has the maximum possible number of finite transmission zeros, which will be the case in most practical problems. In particular the antenna model studied in this report satisfies the condition of always having the maximum number of transmission zeros, and the designs presented in Chapter IV are therefore not affected by the robustness problems exposed in Ref. [SH-1].

---

[3] It will also be unstable for $\varepsilon<-0.01$, but this corresponds to a measurement location above the disk and is not physically realistic.

The second observation in [SH-1] is that, due to the very high gains involved, a small error in the realization of the compensator could destabilize the system. The authors suggest that a compensator be realized directly from the transfer function $K(sI-A+GC+BK)^{-1}G$. This, however falls outside the realm of robustness dealt with in this dissertation and will not be discussed further.

Chapter IV

EXAMPLES AND RESULTS

Rather than continue an abstract discussion of the application of LTR to the control of flexible structures, the concepts will be illustrated via a specific example. This is the control of a large flexible antenna, which will be presented in detail.

This chapter is organized as follows. First the antenna and related control problem are described (model data is listed in Appendix D). Next the structural modeling problem is presented, resulting in a modal description of the antenna. The sequence in which modes are retained for a reduced order model is motivated by approximate balanced singular values [BL-1,GR-1]. These provide an approximate measure of a mode's importance in the input-ouput map (transfer function) of the system. After selecting a sequence of modes, the question of compensator order is addressed. The compensator order is increased until the open loop frequency response of the reduced order compensator in series with the full-order plant model converges. This indicates that the reduced-order compensator approximates the "optimal" ∞-dimensional compensator. Next, the robustness of various LQR designs (with a nominal LTR estimator design) are compared. It is indicated that a tradeoff between robustness and performance can be controlled by the choice of an appropriate Q-matrix in the LQR design method. After an LQR design which offers both satisfactory robustness and satisfactory performance (with a nominal LTR estimator design) is found, variations on the estimator design are made to further improve

robustness, without sacrificing performance. It is shown that adding appropriate process noise to the KB-filter problem can result in improved robustness. Again a tradeoff is involved between robustness and performance, where in this case performance is related to the recovery of high loop gain at low frequency. The final section presents results of the algebraic LTR procedure.

4.1 Antenna Model

The antenna is a wrap-rib design, approximately 180 feet in diameter, consisting of a central hub containing two orthogonal torque inputs, surrounded by eight equally spaced ribs connected by a flexible mesh. The term wrap-rib means that the ribs are initially wrapped around the hub, and then released during deployment to achieve the full antenna shape. The antenna configuration is illustrated in Fig. 4.1.1. A complete list of the model data can be found in Appendix D.

Though the antenna has two control inputs, symmetry can be used to divide the problem first into a semi-circle with one control input, and then, finally into a 90° sector with one control input. The 90° sector is illustrated in Fig. 4.1.2, and all results will be based on this model.

The system is modeled by a component mode method, i.e., mode shapes of the beams and the mesh sections are found separately, and the "modal" representations are then connected to form the 90° sector. Modal data, including frequencies, modal input influence coefficients,

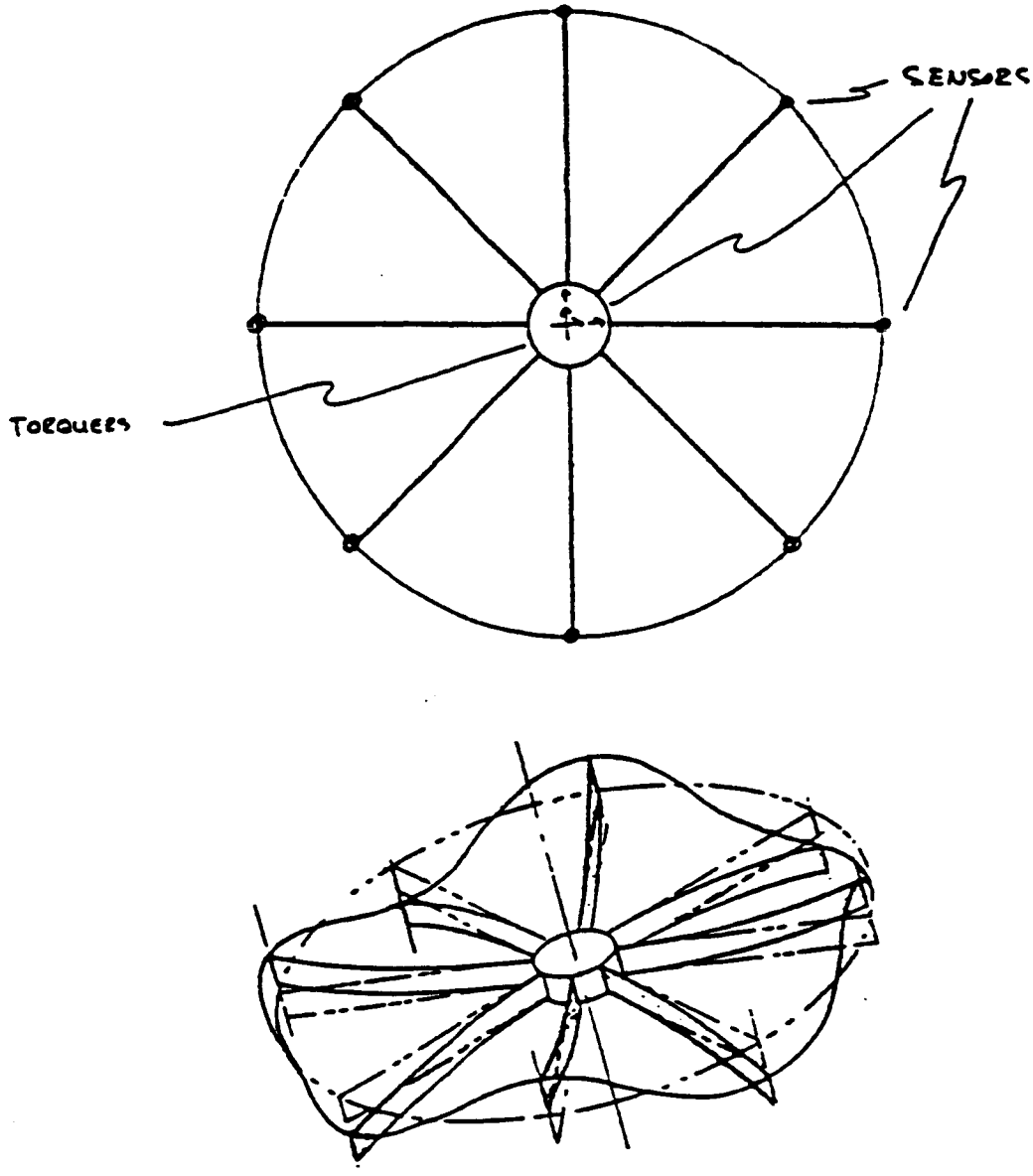

Figure 4.1.1 Wrap-Rib Antenna Model

and modal output influence coefficients are listed in Appendix D.

Damping is assumed to be visco-elastic (i.e., the damping matrix is proportional to the stiffness matrix)[1], but the model allows different damping coefficients[2] for the beam and the mesh portions of the sector

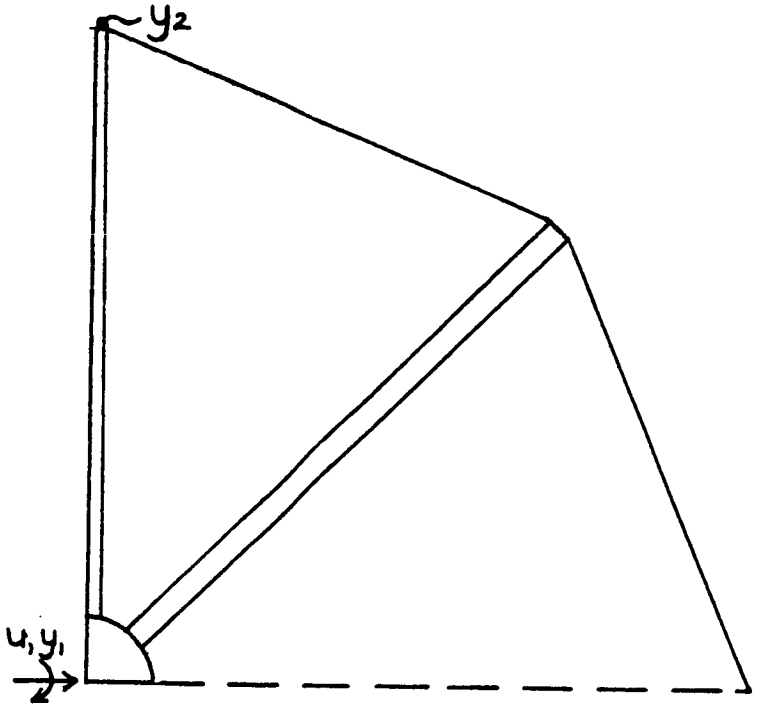

Figure 4.1.2 Antenna Quadrant Model

model. This implies that damping is added at the component mode stage, and furthermore that the damping matrix, after combining the beam and mesh component mode models and calculating the overall modal representation, will include off-diagonal terms. The final antenna model, in a second-order modal reprensentation, will have the following form:

---

[1] Visco-elastic damping implies that the damping ratio of a mode increases in proportion to the frequency of that mode. Higher frequency modes will therefore be more highly damped. This is a realistic situation for most materials, particularily in the higher modes.

[2] The damping coefficient is a scalar number which multiplies the stiffness matrix, resulting in the damping matrix.

$$\ddot{\phi} + D\dot{\phi} + \Omega^2\phi = Bu, \quad y = C\phi \tag{4.1}$$

where Ω^2 is the diagonal matrix of the natural frequencies squared, while D is symmetric, positive-semidefinite, but is diagonal only in the case when the damping coefficients in both the beams and the mesh are identical. The particular model studied in this dissertation has higher damping in the mesh, and the damping matrix is therefore not diagonal, though the off-diagonal terms are in general an order of magnitude smaller than the diagonal terms. The entire damping matrix is listed in Appendix D.

The control problem involves maintaining antenna shape and pointing accuracy in the face of external disturbances. These disturbances might arise from environmental effects such as solar winds or gravity gradients, or they might arise from induced motion on the antenna, such slew maneuvers or moving parts. Since only a subset of the antenna modes are controllable from the torque inputs, a rigorous way of viewing the problem is to consider disturbances acting only at the plant inputs. This guarantees that all modes which are excited by disturbances are also controllable, and therefore stabilizable. Motion in the uncontrollable modes is allowed to decay as a result of damping in those modes. It should be noted that this is the best that can be done without the addition of further actuators. The antenna model is not meant to illustrate every problem in the control of a large, flexible structure, but it does include many of the fundamental aspects, with a model of sufficient complexity to provide some realism.

The wrap-rib antenna has been a primary focus of this research. Simpler models, including series of connected masses and springs, as well as a beam/hub model have also been studied, but the difficulty in achieving robust control designs has been much greater for the antenna sector model. From the point of view of control design, the important aspect of this particular model is that it is difficult to control robustly, and therefore poses a challenging problem.

The number of available measurements (or plant outputs) is not necessarily fixed. However, there must be at least one measurement relative to inertial space to ensure that the rigid body mode is observable. This measurement is provided by a rotation sensor colocated with the hub torque input. To effectively control the shape of the antenna, measurements on the antenna surface must also be taken. The present work assumes that these measurements are at the tips of the two beams as illustrated in Fig. 4.1.2, and are relative to the central hub position. The C-matrix for these measurements is listed in Appendix D. For the examples presented in this dissertation, only the measurement at the tip of the vertical beam will be used. The reason for this is that for the reduced order model used in the control design, the two tip measurements are not independent, and a measurement of the second tip displacement therefore provides no further information to the compensator. To see this fact consider the following argument. The complete mathematical model of the antenna sector includes symmetric beam modes (the two beams move together in the same direction) and asymmetric beam modes (the motion of one beam exactly

opposes the motion of the other). With no mesh, the asymmetric modes are uncontrollable, and even with the mesh they are only very slightly controllable. These modes were therefore neglected in the mathematical design model, since they do not have much affect on the control problem. This, however, implies that in terms of the mathematical design model, the two beams will always move together, and the measurements at two tips will be linearly dependent upon each other. This points to an important consideration in determining the independence of measurements. The fact that measurements are independent for a physical system or even for some mathematical model does not imply that they are independent for every possible reduced order mathematical model. The two tip measurements are clearly independent for the overall mathematical (and the physical) antenna model, but due to the exclusion of asymmetric modes, they are not independent for the reduced order mathematical design model studied in this dissertation. The independence of measurements is especially important in the algebraic design method, since linearly dependent measurements will usually result in a singular matrix S in Eq. (3.30) (see Section 3.3). This means that no solution to the minimal order algebraic loop transfer recovery compensator exists, unless one of the measurements is neglected, or the compensator order is increased until the matrix S is of sufficient rank.

The result that the two beam tip measurements are not independent also indicates that if a third measurement is taken it should be at a location other than the tip of the second beam. Possibilities include

a point near the center of the beam or a point on the mesh. Though the symmetry of these locations is not as appealing, the corresponding measurement will provide the controller with additional information on the state of the reduced order antenna model, whereas the second beam tip measurement does not.

While using a second tip measurement provides no useful information to the controller, this does not mean that all further measurements are useless. It does indicate that a third measurement should be taken at an alternate location, such as an intermediate point on the beam or a point on the mesh. The effect of alternate measurement locations has not been studied in this dissertation.

4.2 Selection of Reduced Order Model

It is relatively simple to produce a mathematical model of any desired dimension for a given flexible structure. Using the component mode method, the dimension can be increased both in the finite element mesh used to generate the component modes, and also in the number of component modes used to construct the full structural model. Large order models of flexible structures are therefore available, but there are a number of reasons why reduced order models are desired. The first is that the computational complexity of both the control law and the manipulations required to synthesize that control law are dependent on the model order. This implies that the use of large order design models will both complicate the design process and result in exces-

sively high order implementations of the control law. The second and perhaps more fundamental limitation is that linear models based on simplifying structural approximations, such as the Bernoulli-Euler assumption, cantilevered joints, etc., decrease in accuracy with the number of modes. This means that large mathematical models may not accurately reflect the actual physical system beyond the first few modes.

On the other hand, a model which is too simple can result in poor performance or even instability when the resulting compensator is applied to the "true" full-order plant. An example of this effect is spillover, where control effort spills over to unmodeled flexible modes, so as to drive them unstable. It is clear therefore that a good design model for a flexible structure must contain the minimal amount of information necessary to describe the "important" dynamics of that structure. Furthermore, the model order is a function of performance demands. If performance requirements are modest, a simple model may suffice. However, if high performance is a required, a more complex model will be needed. Therefore, a model reduction scheme must take into account both the sequence in which dynamics are added to the model and also the relationship between perfomance and model order.

One traditional approach to model reduction for flexible structures is modal truncation. The most basic version of this method retains all modes below a prescribed frequency (dependent on system bandwidth) and neglects all modes above this frequency. This works well for sim-

ple structures, but in a more realistic situation a number of low frequency modes may be almost uncontrollable or unobservable. In this case the lower frequency modes may be less important than some higher frequency modes which are highly controllable and observable. This naive modal truncation approach might therefore result in the retention of many more modes than necessary. An alternate approach is the method of balanced realizations [MO-3], which neglects states on the basis of their importance in the input/output map (transfer function) of the system. However, the state-space reqpresentation implied by the balanced realization method may not be physically meaningful, sometimes resulting in a loss of insight into the problem. Fortunately, in the case of a lightly damped flexible structure, the modal realization is almost identical to the balanced realization [GR-1,BL-1]. In this case an approximate balanced singular value can be associated with each mode. For the modal representation given by Eq. (4.1), with p-inputs and m-outputs, this is:

$$\sigma_i = \frac{\sqrt{(b_{i1}^2+b_{i2}^2+\ldots+b_{ip}^2)(c_{1i}^2+c_{2i}^2+\ldots+c_{mi}^2)}}{4D_{ii}} \qquad (4.2)$$

where b_{ij} is the i,jth element of B, c_{ij} is the i,jth element of C and D_{ii} is the ith diagonal element of D. The importance of a mode is therefore proportional to its input and output coupling, while it is inversely proportional to damping and frequency. This provides an intuitively pleasing measure of modal importance which is indicative of the effect of that mode on the plant transfer function.

The approximate balanced singular values for a 32-mode model are listed in Appendix D. These are derived from a model which originally had 63-modes, of which 31 were approximately uncontrollable, corresponding to assymmetric motion of the beams as discussed in the previous section. The 32-mode model constitutes the evaluation or "truth" model of the system. One argument that this is a large enough model for evaluation is that it is significantly larger than the model used for control design (8-modes).

The next step in determining the reduced order design model is to choose the model order. Two different approaches can be taken. One is to ensure that addition of the neglected modes will not destabilize the system. This can be done by treating neglected modes as an unstructured uncertainty and then applying Theorem 2.1. This is the approach taken in Ref. [SU-1]. However it does not address the issue of performance. The approach taken in this dissertation is to continue adding modes until little further change in the compensator design is observed. One measure for this is to examine the functional gains. This method treats the convergence of the LQR and KBF problems separately. A variation on this method which fits well into the context of loop transfer recovery is to examine the loop gain as the model order is increased. This gives a measure on the performance of the overall compensator, and provides a simple but accurate test of the relationship between desired performance and required model order.

Consider a series of compensators applied to the full-order (32-mode) plant. The control design objective is identical for each

compensator in the series, but the number of modes in the design model (corresponding to the order of the LQR and KBF problems) is increased until the resulting loop gain stops changing significantly. This process is illustrated in Figs. 4.2.1 - 4.2.4, where 4, 6, 8 and 10 mode versions of compensator design # 4.3.3e are applied to the 32-mode plant model. There is a relatively large change from 4 to 6 and from 6 to 8 modes, but little change from 8 to 10 modes. This indicates that a compensator based on an 8-mode model will approximate the ∞-dimensional compensator for design # 4.3.3e. Since the other compensator designs presented in Sections 4.3 and 4.4 place less emphasis on the higher modes that # 4.3.3e, they will also converge before 8-modes.

It was found that robustness of a compensator based on 8-modes applied to a 32-mode plant is essentially the same as that of an 8-mode compensator applied to an 8-mode plant. In particular, design #4.3.3e has the same robustness properties when applied to the 32-mode model as it does when applied to the 8-mode model. This is because the convergence of the compensator implies that the addition of further modes has little effect on the control problem. All robustness tests will therefore be based on an 8-mode compensator applied to an 8-mode plant, thereby reducing computational cost.

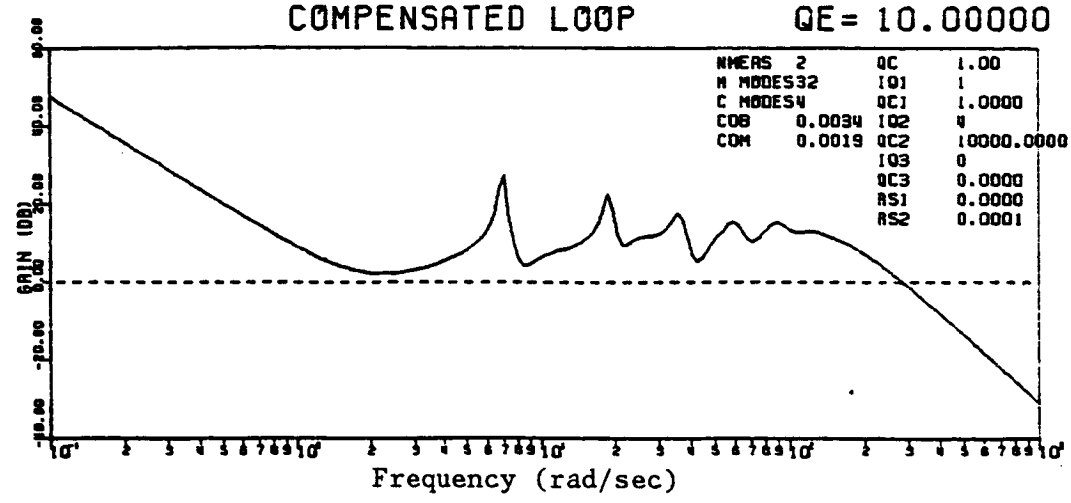

Figure 4.2.1 Compensator Convergence for 4-mode Design Model

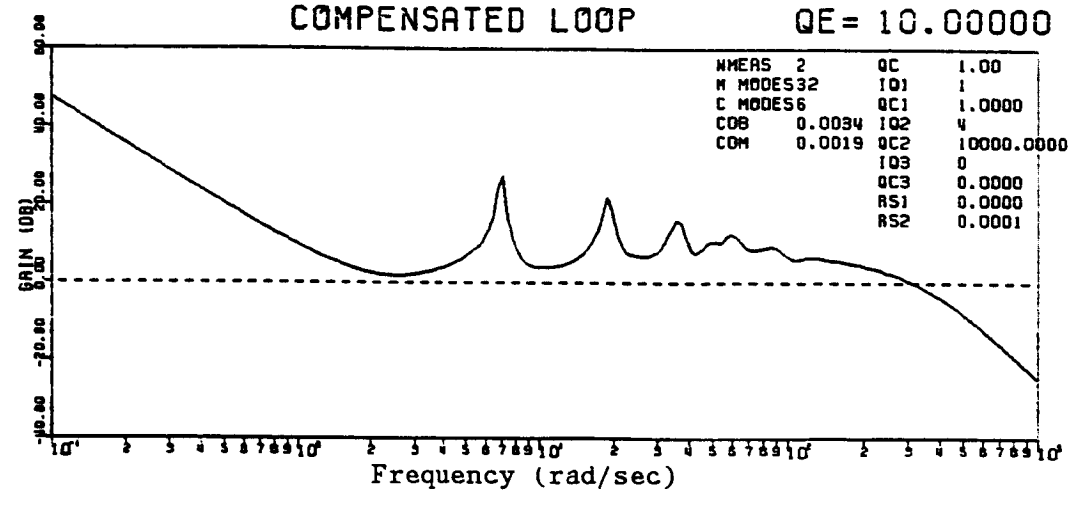

Figure 4.2.2 Compensator Convergence for 6-mode Design Model

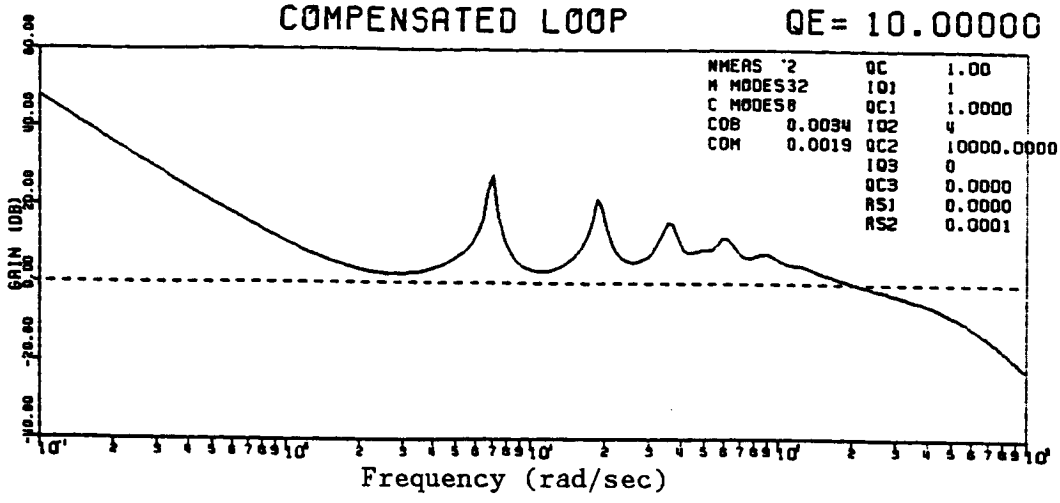

Figure 4.2.3 Compensator Convergence for 8-mode Design Model

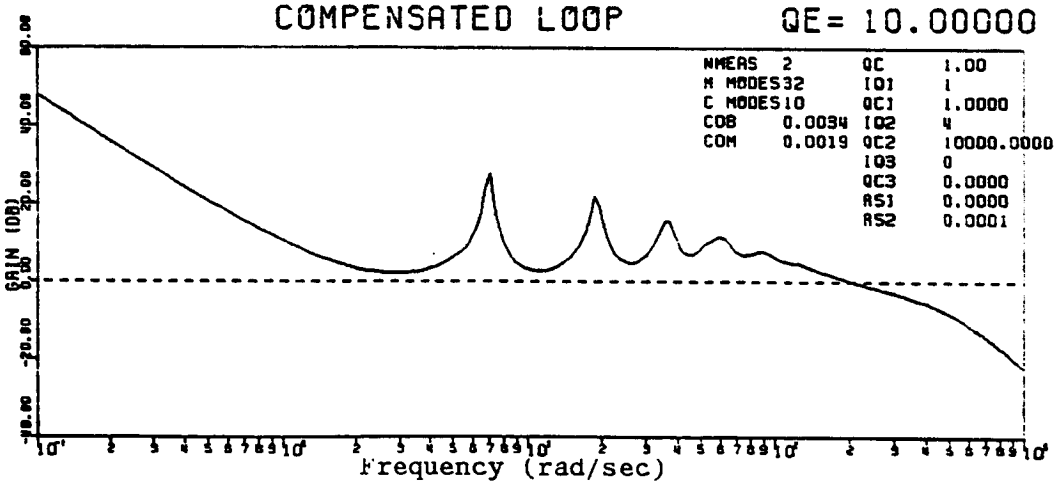

Figure 4.2.4 Compensator Convergence for 10-mode Design Model

4.3 LQR Design Problem

The first step in a Loop Transfer Recovery (LTR) control design is the choice of a full-state feedback control law, or equivalently the matrix K of control gains. The matrix K can be found by a number of methods, including pole placement, but, perhaps the most common is by solving a Linear Quadratic Regulator (LQR) problem. The statement of the LQR problem is as follows:

Given
$$\dot{x} = Ax + Bu \tag{4.3}$$

Minimize the following cost functional:

$$J = \int_0^\infty (x^T Q x + u^T R u) dt \tag{4.4}$$

where Q is symmetric, positive semi-definite and R is symmetric, positive definite. The solution to the problem, for full-state feedback is:

$$u = -Kx \tag{4.5}$$

where $K = R^{-1}B^T P$ and P satisfies the following Riccati equation:

$$PA + A^T P - PBR^{-1}B^T P + Q = 0 \tag{4.6}$$

There are a number of appealing aspects of the LQR approach, including guaranteed gain and phase margins[3], the ability to shape the loop gain at low frequencies [HA-1] and the computational simplicity

of the approach. The designer simply has to choose the Q and R matrices and let the computer do the rest.

For the antenna problem, the input is a scalar, so without loss of generality R can be replaced by 1. The problem then reduces to finding a Q matrix of the following form:

$$Q = q_c Q_o \tag{4.7}$$

where q_c is a scalar parameter which is increased to increase system performance (and loop gain), and Q_o is a matrix which specifies the form of the cost weighting on the states. There are a number of bases for choosing Q_o. One might wish to achieve a particular loop shape, or a particular closed loop pole configuration. Ideally, however, there exists a physically meaningful objective function which can be expressed in the form of Eq. (4.4). Examples of such functions include the mechanical energy of the system, the pointing error, or the RMS error of a surface or signal. Another basis for selecting Q_o might be to achieve satisfactory robustness. In particular, an analysis of the flexible structure control problem with uncertain frequencies presented in Section 2.2.3 suggests that a Q_o matrix which weights strain energy will improve robustness.

---

[3] This constitutes a large part of the appeal of the LTR control design approach

For any realistic design, a number of factors will have to be traded off. For the purposes of this dissertation two factors will be considered. The first will be performance, represented by either RMS error or hub pointing error. The second will be robustness with respect to frequency errors. The examples will illustrate this trade-off between robustness and performance.

Full-state feedback designs are inherently robust, not only in terms of gain and phase margins, but also with respect to frequency errors. This is because full-state feedback provides the exact displacement and velocity of every mode in the control problem, independent of frequency errors. Given this information, practically any matrix of control gains will provide a robustly stable feedback system. In particular, the full-state feedback versions of every LQR design presented in this dissertation is stable for -99% to +100% frequency variations[4]. Therefore, to examine the effect of varying LQR designs it is necessary to choose a fixed estimator design. The estimator design which is chosen is the solution to the KB-filter problem with a measurement noise covariance of one, and a process noise covariance given by:

$$Q = 1x10^{9}(B*B^{T}) + 1x10^{4}(\hat{Q}_{r}) \qquad (4.8)$$

---

[4] However, this does not imply that the LQR design has little effect on robustness. In fact, the way estimates of the modal displacements and velocities are used, has a large effect on the robustness of the resulting compensator. This will be clearly illustrated by the examples presented later in this section.

where $\hat{Q}_r = \begin{bmatrix} 0 & 0 & \cdots & 0 \\ 0 & \omega_1^2 & & \\ \vdots & & 0 & 0 \\ 0 & \cdots & 0 & \omega_n^2 \end{bmatrix}$

The form of $\hat{Q}_r$ is suggested by Section 2.2.3 to improve robustness with respect to frequency errors. This is also estimator design # 4.4.4b presented in Section 4.4, where the details of a number of varying estimator designs will be discussed. This choice results in relatively robust compensators, while achieving reasonable loop recovery.

In order to balance the effect of performance vs. robustness consider an LQR cost functional of the following form:

$$J = \int_0^\infty [qc(qc1[Q_{RMS}] + qc2[Q_r]) + u^2]dt \qquad (4.9)$$

The parameters in the LQR design are qc, qc1 and qc2. qc is an overall weighting, while qc1 can be thought of as a weighting on performance, and qc2 can be thought of as a weighting on robustness. The form of Q_r is motivated by the structured uncertainty problem presented in Section 2.2.3. Again it should be emphasized that the robustness results are not for full-state feedback, but are for a fixed estimator design.

The control designs are presented in groups. Each group corresponds to increasing one parameter while keeping all others fixed.

Each group is given a design number and the individual elements are labeled a,b,c etc.. Loop gains, as a rough indication of performance, are presented. As indicated in Chapter III, disturbance rejection is related to high loop gain. In particular, high loop gain at a frequency ω reflects good disturbance rejection of signals at that frequency. The locus of closed loop poles is also presented to indicate the relative control effort applied to the various modes.

The issue of verifying stability robustness is not a trivial one. The basic question is under what types of modeling errors will the closed-loop system first go unstable. In the notation of Section 2.3, this can be represented by μ, the inverse of the smallest size Δ of a given structure which destabilizes the system. Methods for addressing this problem are beginning to appear in the literature. One approach determines upper bounds on μ by representing errors as circles in the complex plane [MO-1,2]. Another finds lower bounds based on a gradient search method which constructs destabilizing perturbations [FA-1]. A third seeks to find exact non-conservative bounds, but at present the method is computationally inefficient [GA-1].

Application of these methods to the problem considered in this dissertation is non-trivial, due to the large number of varying parameters and the large number of designs to be checked. As an approximation, two tests of stability robustness are presented. In both cases the open-loop plant frequencies are varied while other parameters are held fixed. While only frequency variations are considered, we have found that feedback control systems for lightly damped flexible struc-

tures are more sensitive to frequency errors than other parameter variations.

The first robustness test involves determining the maximum increase and decrease in frequencies for which the system remains stable when all flexible frequencies are shifted uniformly in the same direction by the indicated percentage. Some low bandwidth designs are stable for arbitrary increases in frequency. In this case stability is checked for up to a 100% increase. This rough check offers a simple and computationally efficient measure of the effect of stiffening and softening the structure, but does not consider the situation where frequencies can shift in different directions. The second test mixes the direction of frequency shift by looking at the vertices of the parameter space for a maximum variation in the frequencies δ. For m uncorrelated varying frequencies the parameter space is an m-dimensional hypercube, so for each frequency variation δ, 2^m vertices must be checked. For seven varying frequencies this is 128 stability checks. To simplify the computation only the first four frequencies are varied. Variations of the last three are found to have little effect and are all set to $-\delta$. Furthermore the cases where all frequencies decrease and where all frequencies increase has already been checked, so only fourteen corners are needed. The results are indicated by a percentage, corresponding to the largest δ for which the system remains stable at all its corners, and also the direction in which the system first goes unstable. The direction is presented as a string of four +'s and -'s where a + indicates increase of the corres-

ponding frequency while - indicates a decrease. While the first robustness check ensures that natural frequencies do not cross, the second allows this possibility. In particular, a 46% increase in the lowest natual frequency (6.951 rad/sec) combined with a 46% decrease in the second natural frequency (18.940 rad/sec) will result in two open-loop poles with identical imaginary parts. Since the real parts of the poles are not varied the poles will never lie on top of each other. A 32% increase in the second natural frequency along with a 32% decrease in the third will result in the same phenomenon as will a 24% increase in the third and a 24% decrease in the fourth. The case where natural frequencies actually shift relative position may be unrealistic and this should be kept in mind when interpreting the mixed frequency variations. These two checks do not guarantee that the system will remain stable for all frequency variations less than or equal to δ, but they do provide a good measure of robustness.

Gain and phase margins for the designs are also presented. The gain margin is the negative of the gain at -180^0 phase cross-over. Since the phase of the following designs only crosses -180^0 at one point, the gain margin is unambiguous. The phase margin is the distance of the phase from -180^0 at 0db gain cross-over. For some of the designs, gain crosses 0db at a number of points. In this case the phase margin is taken as the smallest of the phase margins at the various gain cross-overs. The purpose of listing gain and phase margins is to examine the relationship, if any, between these margins and robustness with respect to frequency errors.

4.3.1 Weighting on RMS Surface Error -

For an initial test simply weight the RMS surface error, while placing no emphasis on robustness. In this case qc1 = 1.0, qc2 = 0.0 and qc is varied from .01 to 100.0. Loop gains for qc = .01, 1.0 and 100.0 are illustrated in Figs. 4.3.1 - 4.3.3.

Table 4.3.1 Design Sequence 4.3.1 (qc1=1.0, qc2=0.0, increase qc)

Design #	qc	Uniform Frequency Shifts	Mixed Frequency Shifts	GM	PM
4.3.1a)	.01	-13% to +100%	13% ----	56db	65°
4.3.1b)	.1	-12% to +100%	12% ----	51db	64°
4.3.1c)	1.	-14% to +48%	14% ----	44db	66°
4.3.1d)	10.	-17% to +35%	16% -+--	36db	65°
4.3.1e)	100.	-20% to +26%	18% -+--	26db	68°

As indicated by the figures, performance, as measured by low frequency loop gain, increases as qc is increased. For qc =.01, gain at .1 rad/sec is approximately 33db and practically no control effort is applied to the flexible modes. For qc=100.0, gain at .1 rad/sec is approximately 72db and significant control effort is applied to four flexible modes. Unfortunately none of the designs is robust, and increasing RMS weighting seems to increase sensitivity to frequency errors. Again this is not surprising since no weighting on the robustness term is included. It is interesting to note that this design is sensitive to decreases in frequency, even for very low performance. This is because a 50% decrease in frequency brings the first flexible mode into the region of gain cross-over where the sys-

tem is very sensitive to errors in frequency response.

The locus of closed loop pole locations for design sequence # 4.3.1 is illustrated in Fig. 4.3.4. The plot scale includes only frequencies below 70 rad/sec, corresponding to the rigid body mode and the first four flexible modes. This scale provides a good illustration of the relative control effort applied to the modes. In particular, Fig. 4.3.4 indicates that weighting RMS surface error emphasizes controlling the rigid body mode. The real part of the closed loop poles for the rigid body modes lies to the left of the first two or three flexible modes. This relationship will become more clear as more robust designs are examined.

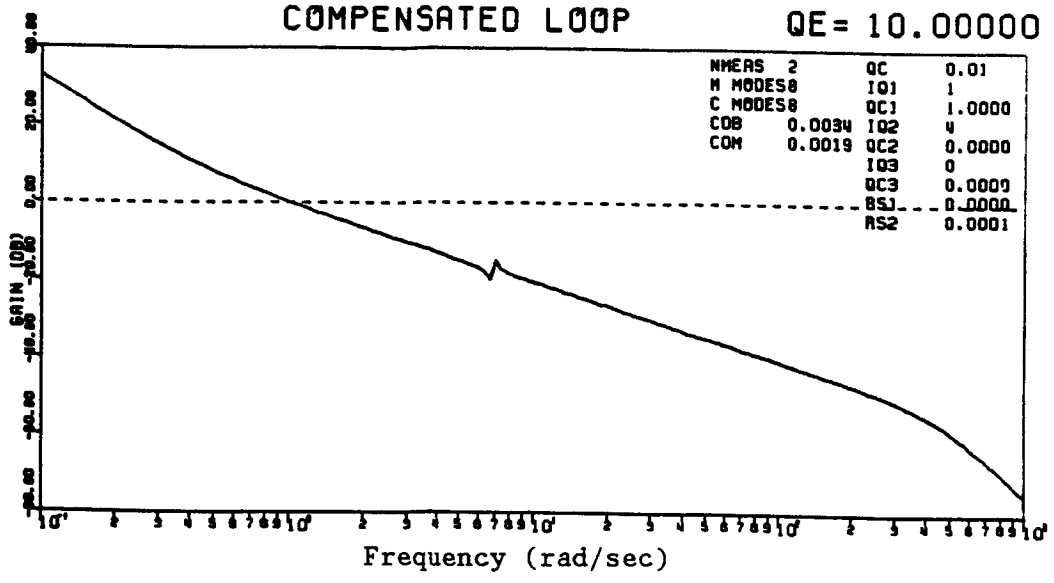

Figure 4.3.1 Loop Gain for Design # 4.3.1a

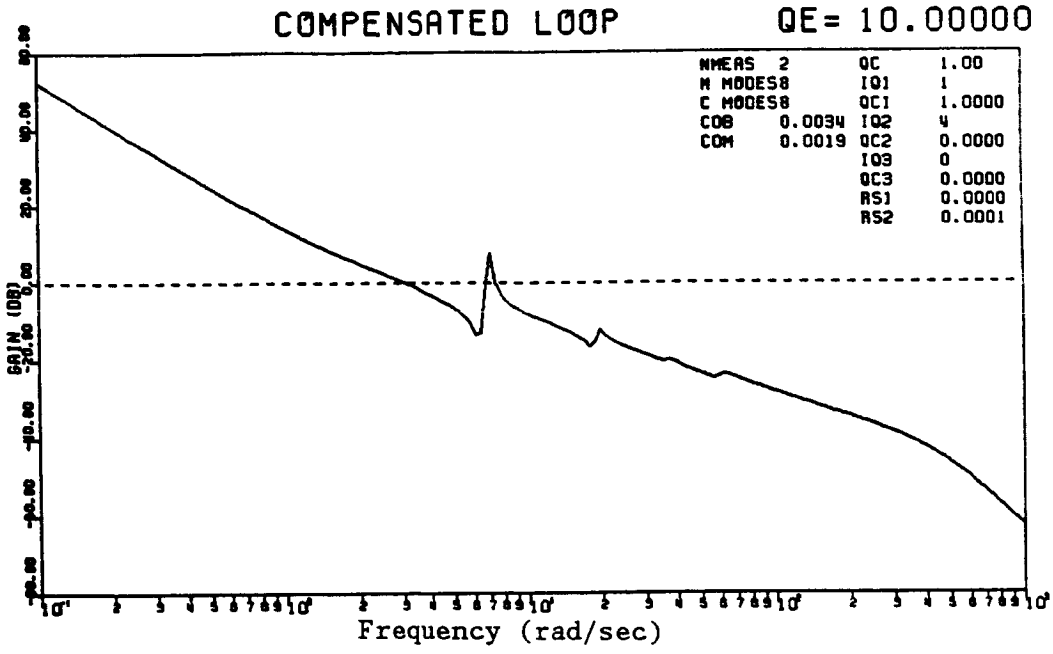

Figure 4.3.2 Loop Gain for Design # 4.3.1c

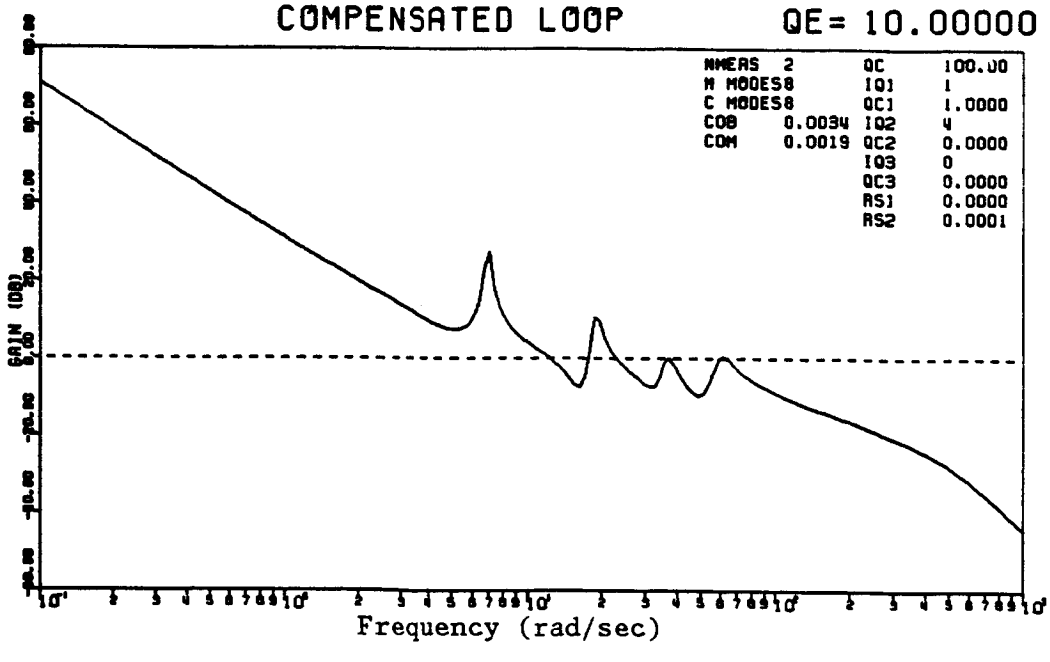

Figure 4.3.3 Loop Gain for Design # 4.3.1e

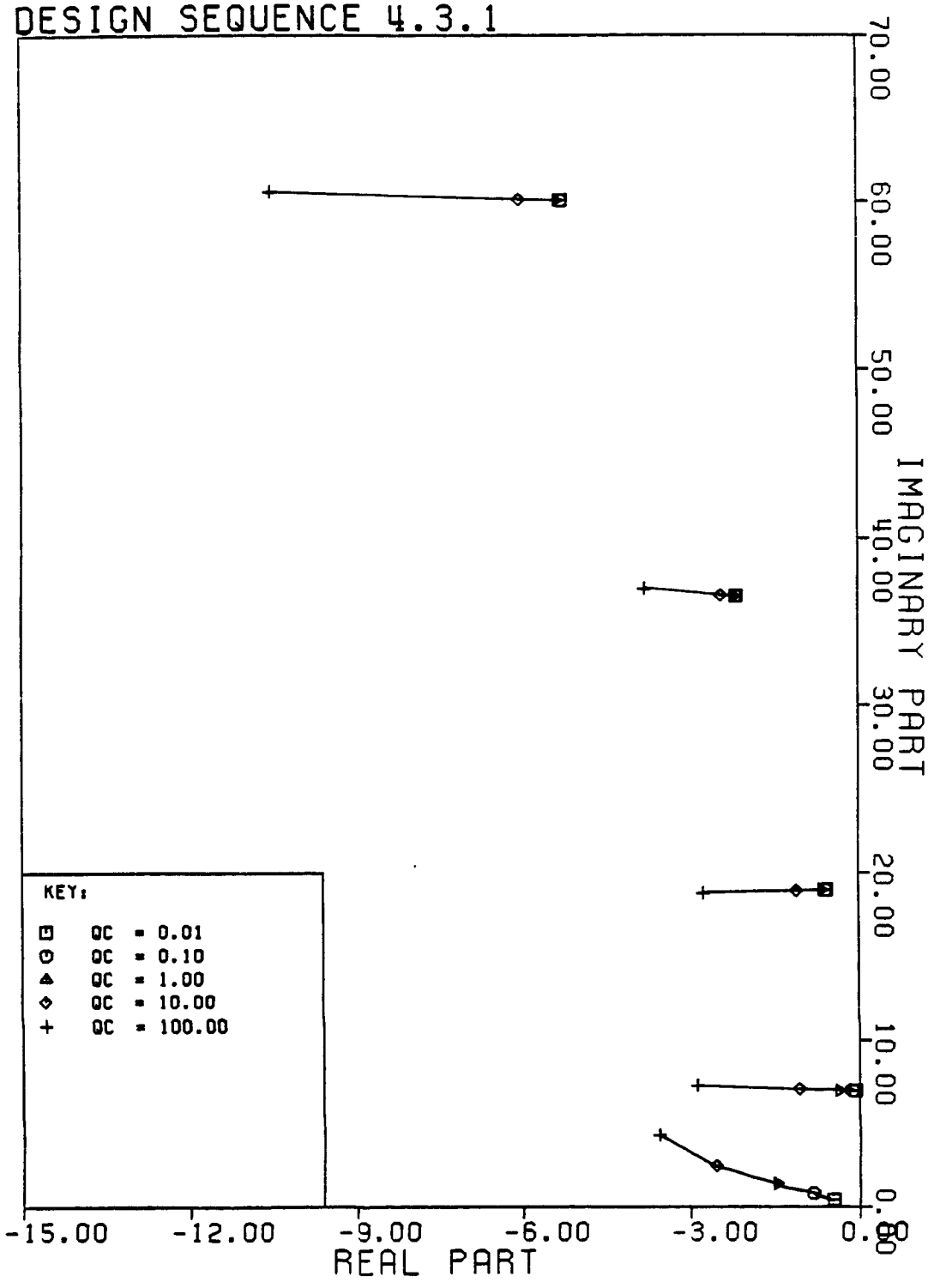

Figure 4.3.4 Closed Loop Regulator Poles for Design Sequence # 4.3.1

4.3.2 Weighting on Pointing Error -

Another possible control objective is to minimize pointing error. Therefore consider the case where qc1 weights the hub pointing error. Pointing error is measured directly by the hub rotation sensor, so the appropriate weighting matrix is $C_1^T C_1$, where C_1 is the first row of the C matrix. Again qc1 = 1.0, qc2 = 0.0 and qc is increased, this time from 100.0 to 1,000,000.0.

Table 4.3.2 Design Sequence 4.3.2 (qc1=1.0, qc2=0.0, increase qc)

Design #	qc	Uniform Frequency Shifts	Mixed Frequency Shifts	GM	PM
4.3.2a)	100.	-22% to +100%	22% ----	63db	65°
4.3.2b)	1000.	-16% to +100%	16% ----	58db	65°
4.3.2c)	10000.	-15% to +100%	14% --+-	52db	63°
4.3.2d)	100000.	-20% to +66%	19% ---+	43db	5?°
4.3.2e)	1000000.	-35% to +53%	32% -+++	31db	55°

Note that the elements of $C_1^T C_1$ are approximately four orders of magnitude lower than those of the weighting matrix Q_{RMS} This results in lower control gains for the same qc, as indicated in Figs. 4.3.5 - 4.3.7. The results of parameter variations, however, are still similar. In particular the designs are not very robust. The locus of closed loop pole positions, illustrated in Fig. 4.3.8 also indicates that this control applies relatively less control effort to the flexi-

ble modes than to the rigid body mode. Also note that this sequence indicates increasing robustness with decreasing gain and phase margin, illustrating the lack of correlation between actual robustness and the margins. For the rest of the dissertation it will be assumed the control objective is to minimize RMS error, so qc1 will weight RMS error in all remaining cases.

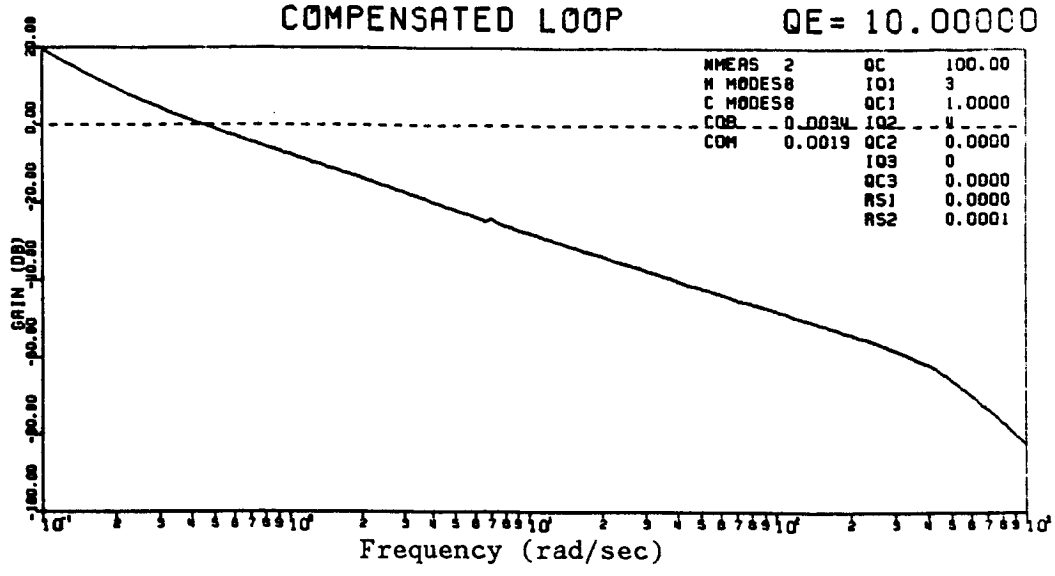

Figure 4.3.5 Loop Gain for Design # 4.3.2a

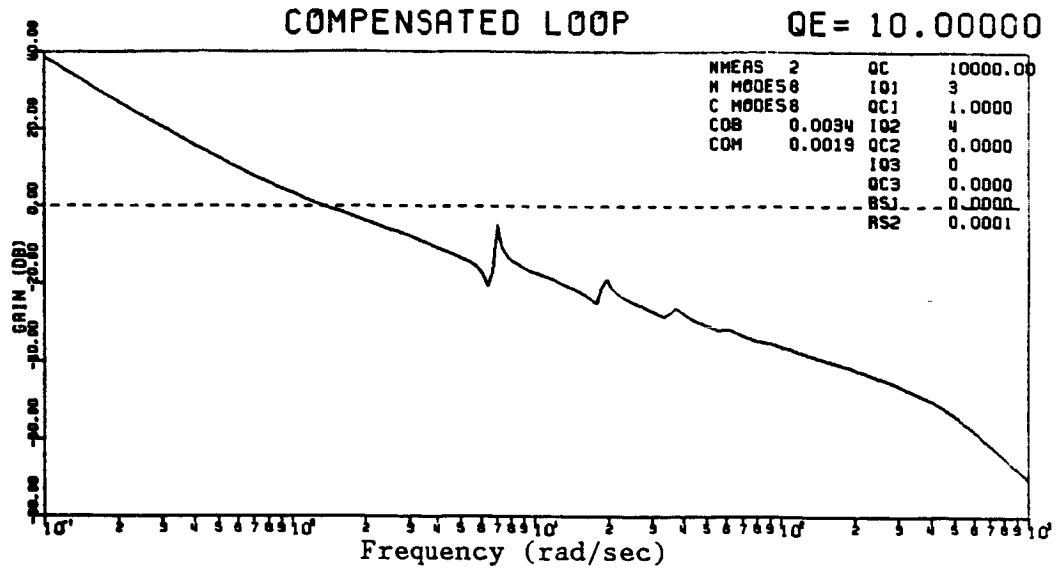

Figure 4.3.6 Loop Gain for Design # 4.3.2c

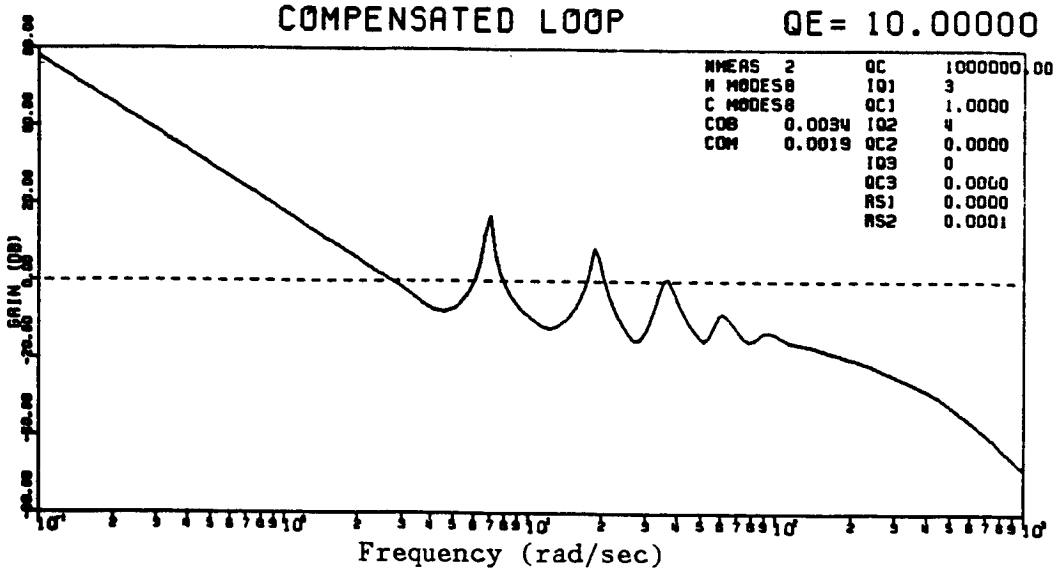

Figure 4.3.7 Loop Gain for Design # 4.3.2e

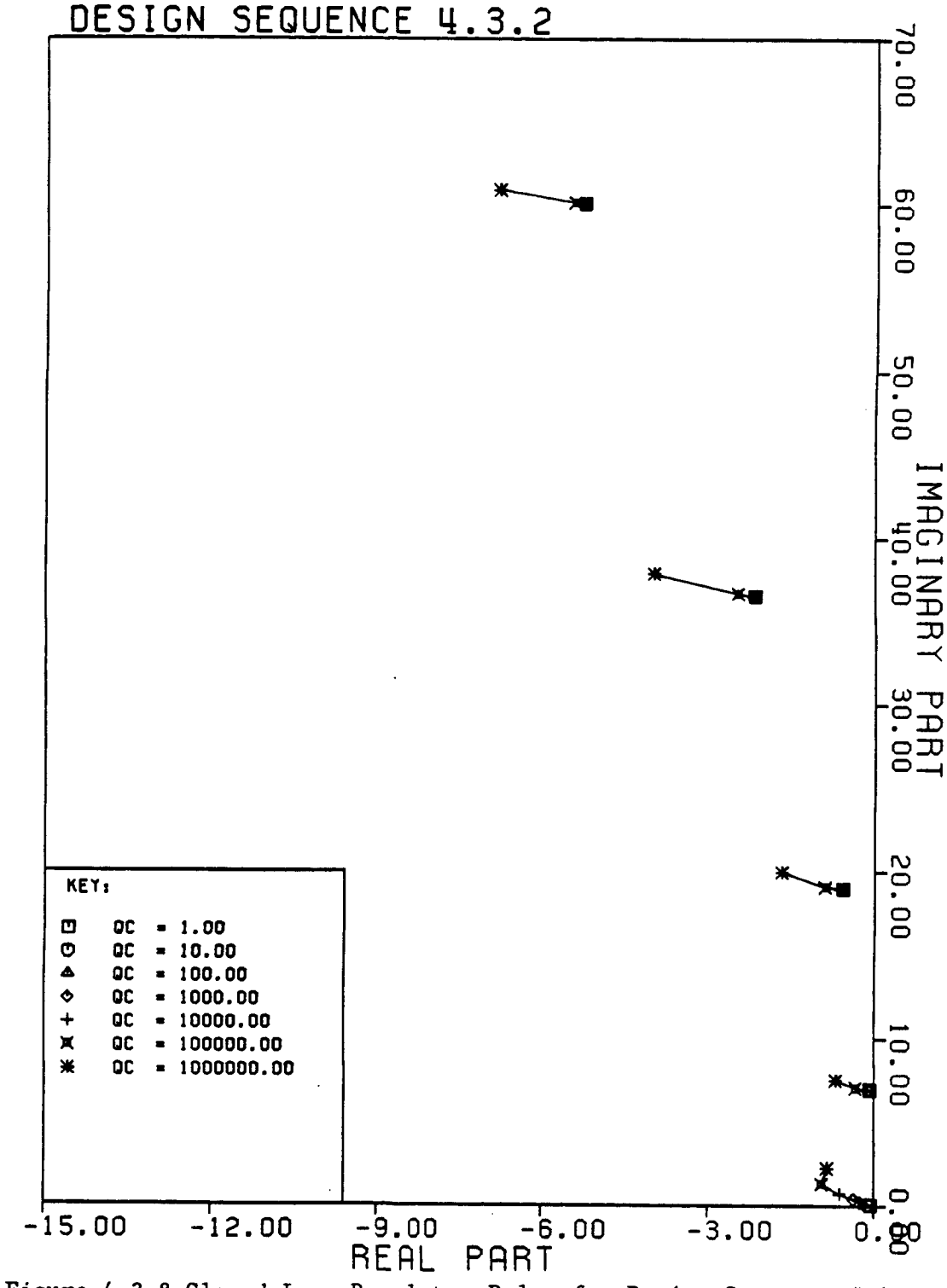

Figure 4.3.8 Closed Loop Regulator Poles for Design Sequence # 4.3.2

4.3.3 Designs with Increased Robustness -

The results of Section 2.2.3 suggest that increasing qc2 for a constant qc1 should improve robustness. Note that some weighting on qc1 must be included since no strain energy is associated with the rigid body mode. An LQR problem which weights only qc2 applies no control effort to the rigid body mode and this results in an unstable closed-loop system. Design sequence # 4.3.3 lets qc = 1.0, qc1 = 1.0 and increases qc2 from 1.0 to 10,000.0. The loop gains for qc2 = 1.0, 100.0 and 10,000.0 are illustrated in Figs. 4.3.9 - 4.3.11. The robustness results are presented in Table 4.3.3.

Table 4.3.3 Design Sequence 4.3.3 (qc=1.0, qc1=1.0, increase qc2)

Design #	qc2	Uniform Frequency Shifts	Mixed Frequency Shifts	GM	PM
4.3.3a)	1.	-15% to +48%	14% ---+	44db	66°
4.3.3b)	10.	-16% to +52%	15% --+-	42db	65°
4.3.3c)	100.	-22% to +68%	21% --++	33db	67°
4.3.3d)	1000.	-42% to +100%	37% ++-+	22db	83°
4.3.3e)	10000.	-55% to +100%	49% -+-+	15db	62°

As expected this sequence indicates increasing robustness. However, it is worthwhile examining the loop gains illustrated in Figs. 4.3.12 - 4.3.13. With qc2 = 1 the design is almost identical to # 4.3.1c. As qc2 is increased the loop gain at .1 rad/sec does not change much. On the other hand the loop gain in the range of the flexible frequencies increases considerably. The robust control

design is therefore placing no further control effort on the rigid body mode, while applying alot of effort to the flexible modes. This is confirmed by examining the locus of closed-loop pole locations, illustrated in Fig. 4.3.14. As qc2 is increased the poles corresponding to flexible modes move further into the left half plane while the poles corresponding to the rigid body mode actually move back towards the origin. For the robust designs, 4.3.3d and 4.3.3e, all poles corresponding to flexible modes are further to the left than poles corresponding to the rigid body mode. This suggests that designs which attempt a high performance control for the rigid body mode while ignoring flexible modes may be less robust with respect to frequency errors than those which emphasize control of the flexible modes.

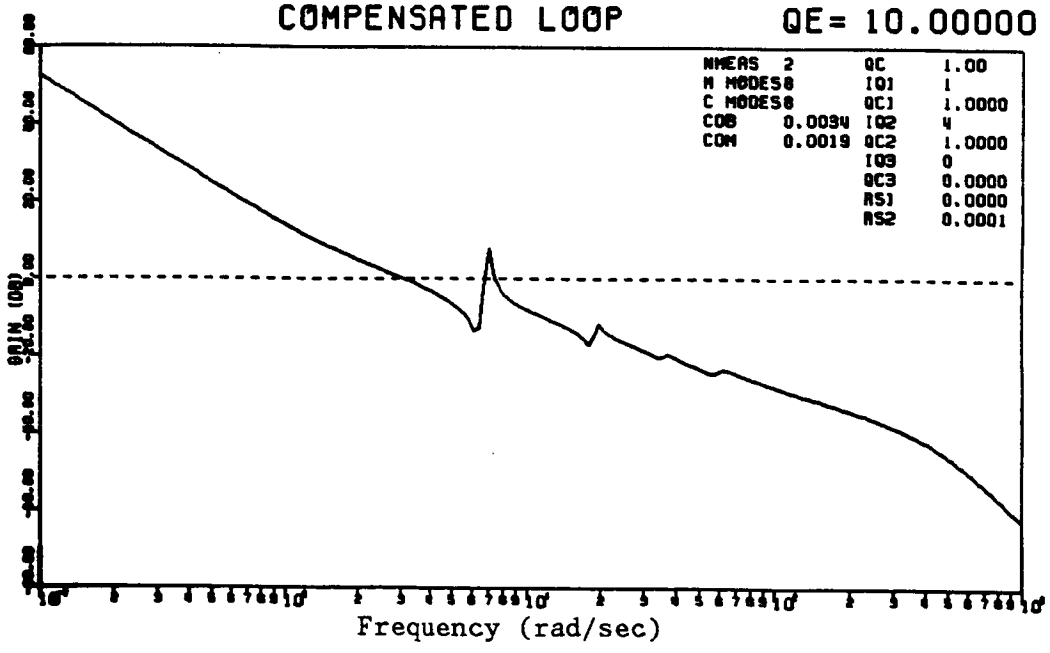

Figure 4.3.9 Loop Gain for Design # 4.3.3a

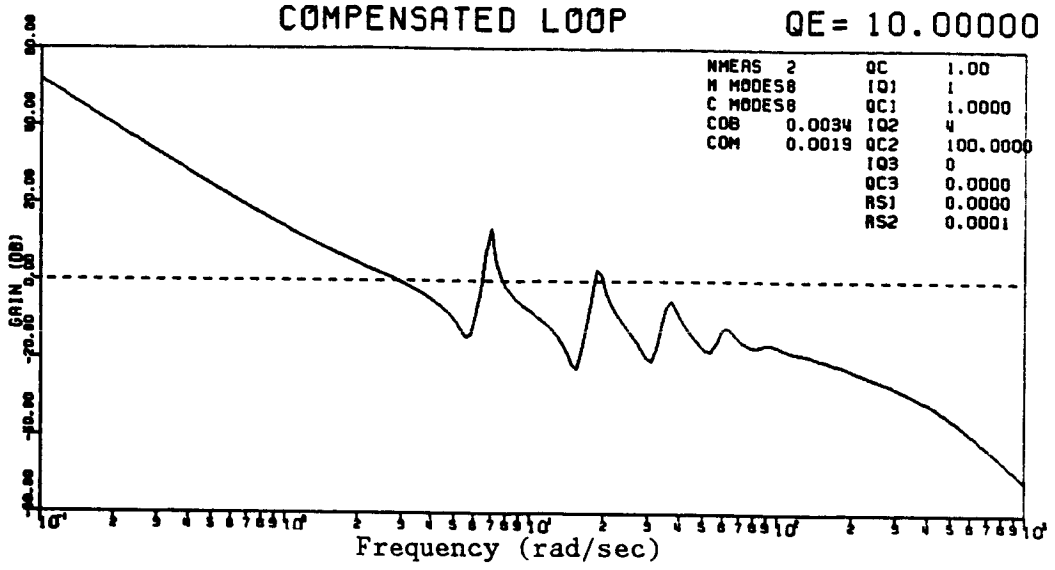

Figure 4.3.10 Loop Gain for Design # 4.3.3c

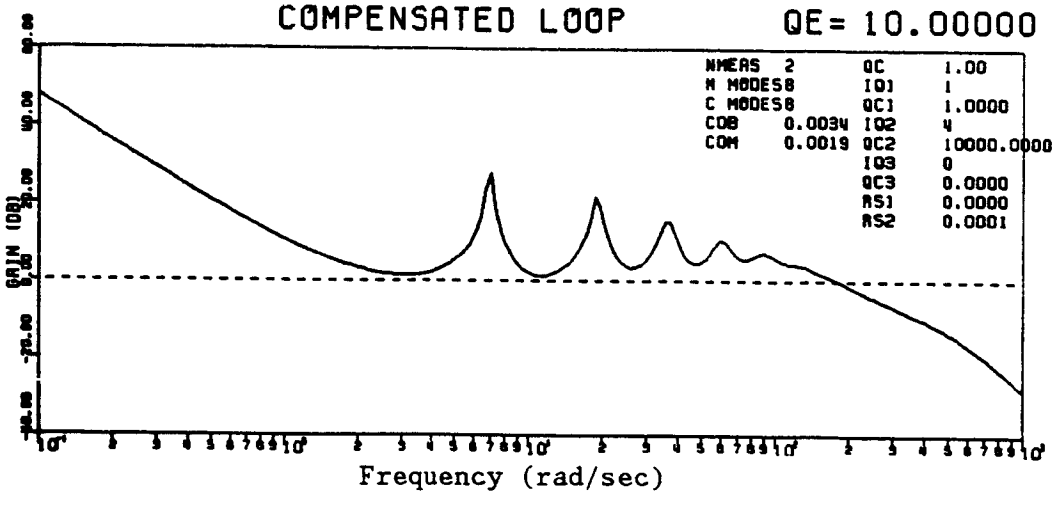

Figure 4.3.11 Loop Gain for Design # 4.3.3e

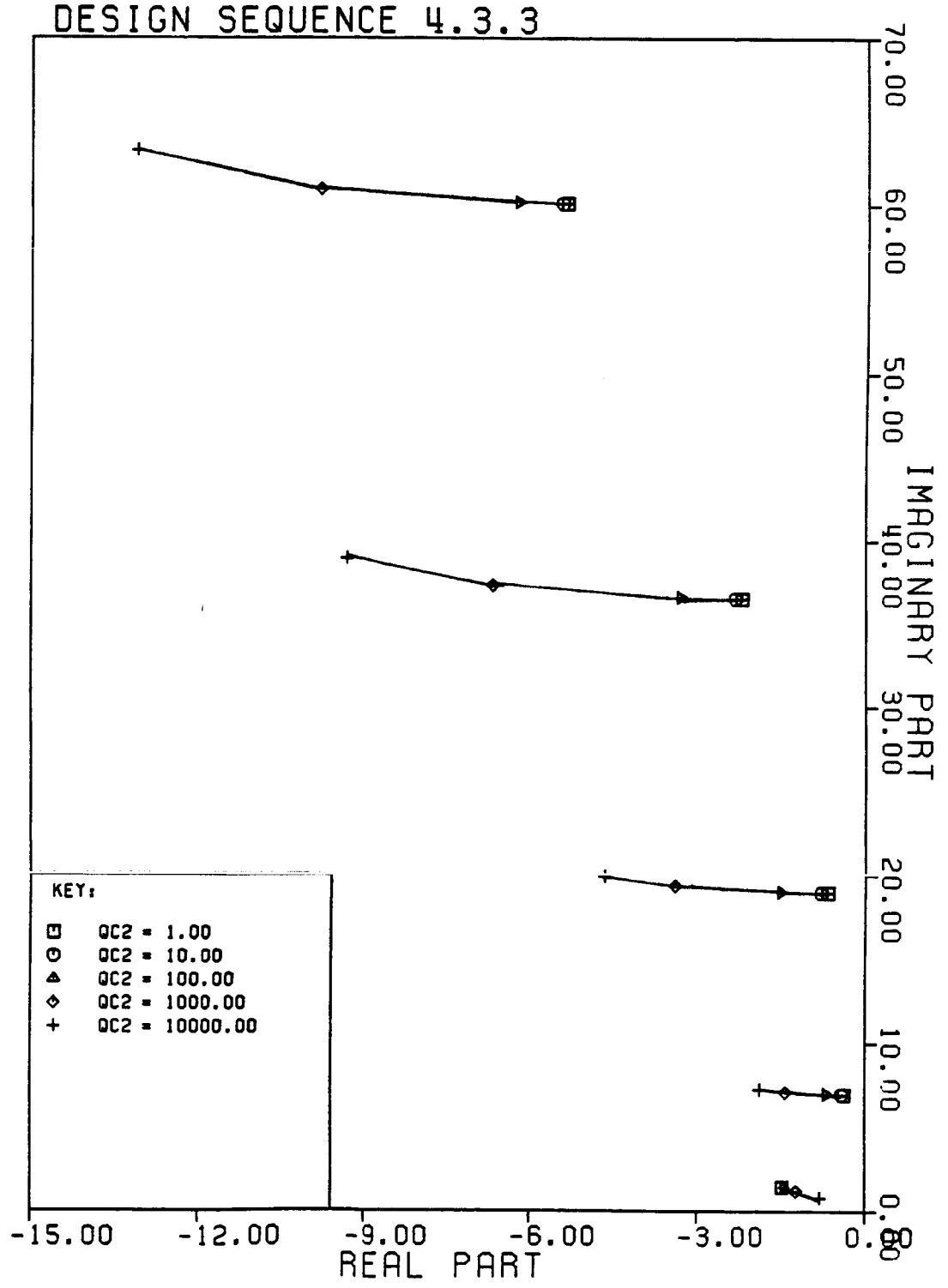

Figure 4.3.12 Closed Loop Regulator Poles for Design Sequence # 4.3.3

4.3.4 Increased Performance with Fixed Robustness -

The final sequence of LQR designs involves increasing the weighting on RMS error with a fixed weighting on robustness to see if performance can be improved without affecting robustness. In this case qc = 1.0, qc2=1,000.0 and qc1 is increased from .1 to 1,000.0. The loop gains for qc1 = .1, 10. and 1,000.0 are illustrated in Figs. 4.3.15 - 4.3.17, while robustness results are presented in Table 4.3.4.

Table 4.3.4 Design Sequence 4.3.4 (qc=1.0, qc2=1,000.0, increase qc1)

Design #	qc1	Uniform Frequency Shifts	Mixed Frequency Shifts	GM	PM
4.3.4a)	.1	-99% to +92%	44% -+-+	22db	80°
4.3.4b)	1.	-42% to +83%	37% ++-+	22db	83°
4.3.4c)	10.	-32% to +46%	31% ---+	22db	83°
4.3.4d)	100.	-29% to +29%	26% -+--	20db	85°
4.3.4e)	1000.	-32% to +29%	27% -+-+	17db	69°

In this case, performance clearly increases as indicated by the loop gain, but robustness decreases. Note that the loop gain in the region of the flexible frequencies does not change much, while the loop gain near .1 rad/sec increases from approximately 42db to approximately 78db. This indicates that the increasing robustness of design sequence 4.3.3 cannot be attributed only to the fact that loop gain is maintained above 0db throughout the region of flexible frequencies. It is also worthwhile noting that design # 4.3.4a is extremely robust

for uniform frequency increases and decreases, but can still go unstable for 44% mixed variations in frequency. This illustrates the danger in checking robustness with respect to increases and decreases of all frequencies together.

The emphasis that increasing qc1 places on the rigid body mode is illustrated in Fig. 4.3.18. This agrees with the previous observation that robustness is decreased when the real part of the poles corresponding to the rigid body mode lie significantly to the left of the real part of the poles corresponding to flexible modes.

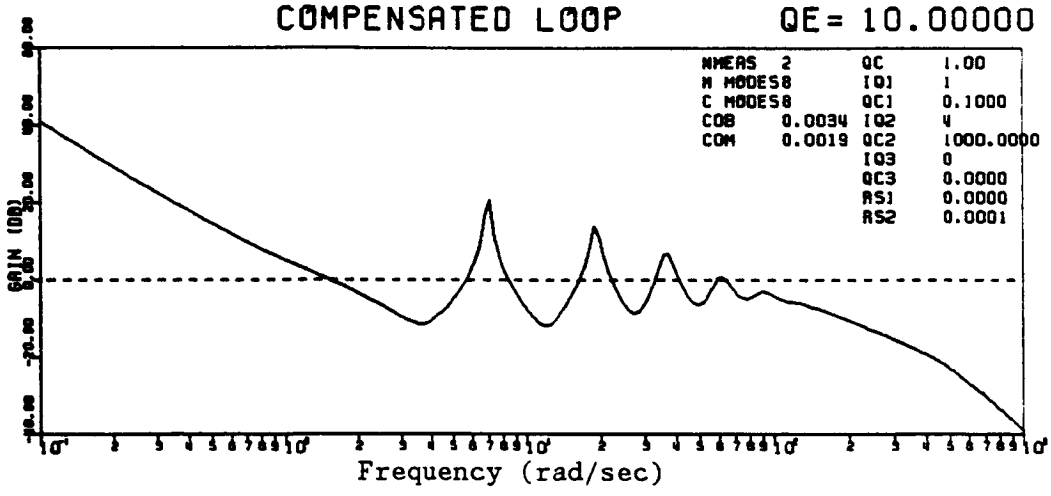

Figure 4.3.13 Loop Gain for Design # 4.3.4a

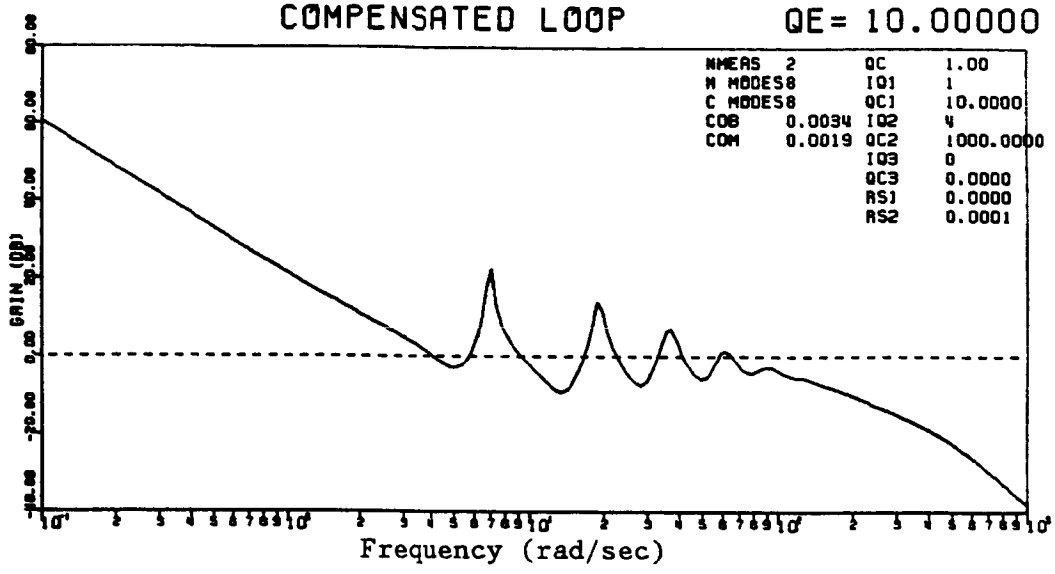

Figure 4.3.14 Loop Gain for Design # 4.3.4c

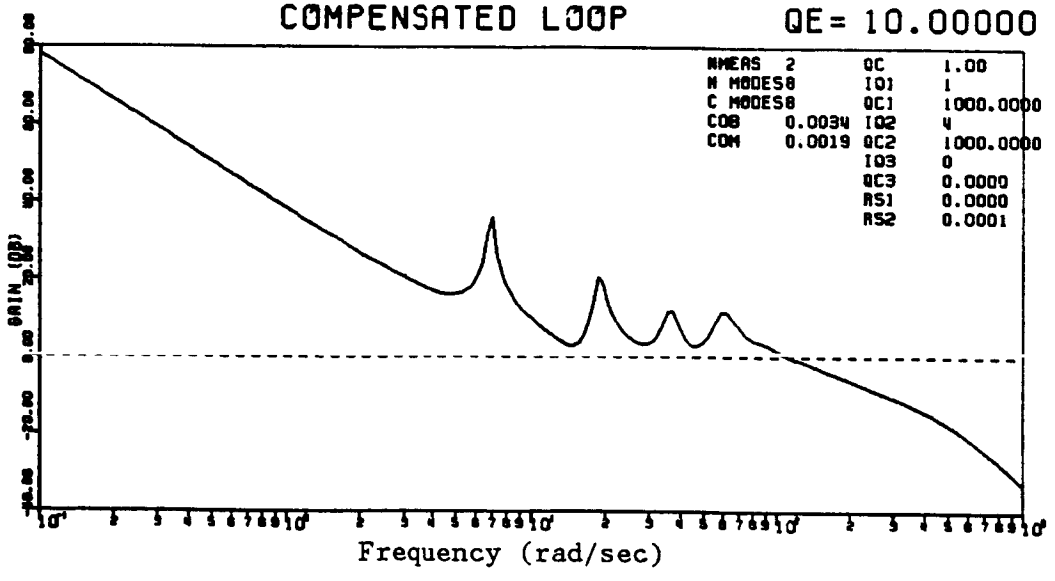

Figure 4.3.15 Loop Gain for Design # 4.3.4e

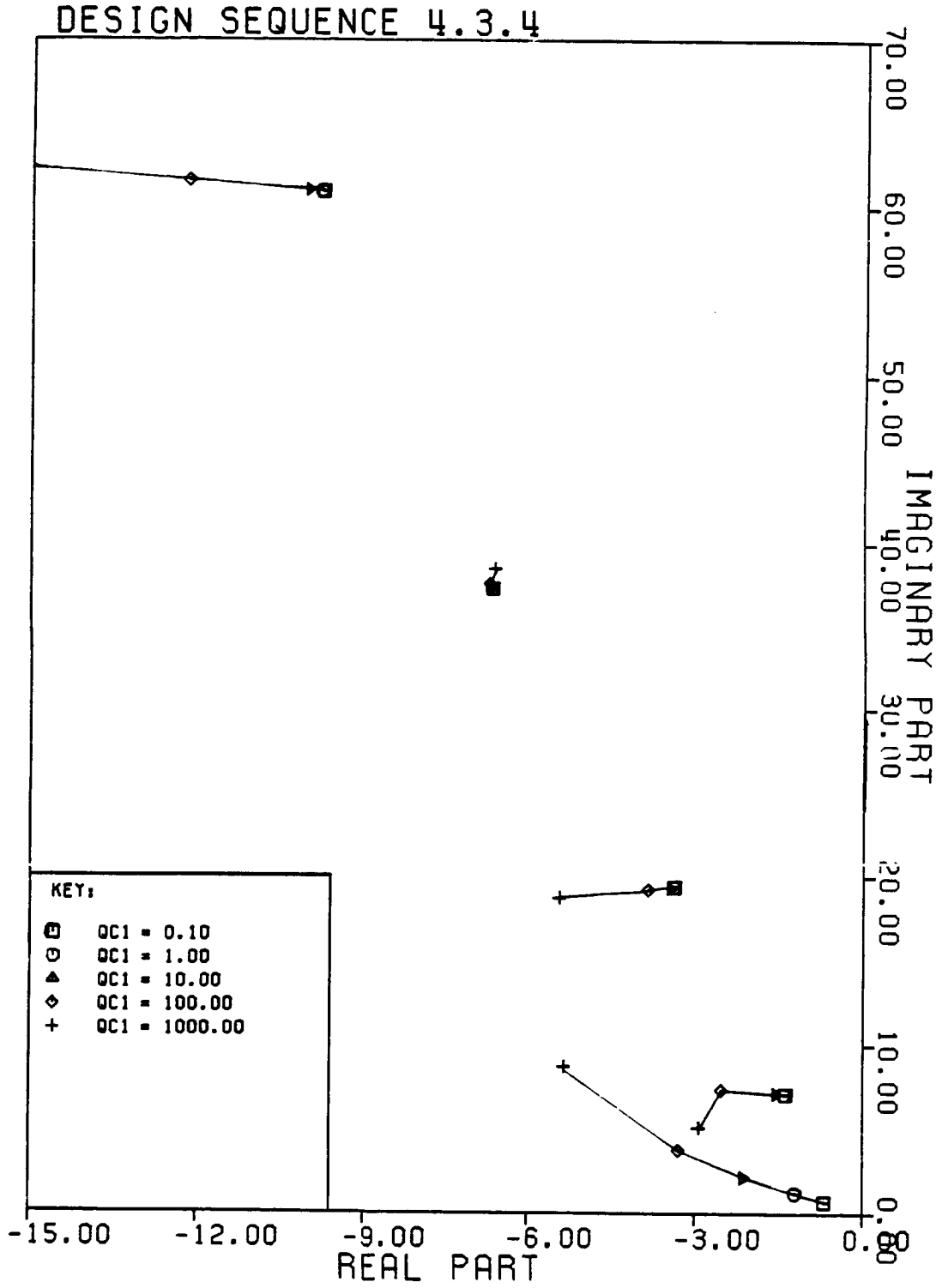

Figure 4.3.16 Closed Loop Regulator Poles for Design Sequence # 4.3.4

4.4 Estimator Design and Robustness

Now consider the effect of varying the estimator design within the context of the modified LTR approach. To achieve loop recovery, process noise must enter through the control input. On the other hand, the results of Section 2.2.3 suggest an alternate noise model to improve robustness, though this model does not necessarily result in loop recovery. Adding this alternate noise model constitutes a modified Loop Transfer Recovery approach to designing the estimator. To study the tradeoffs between loop recovery and robustness with this modified approach consider the following state space representation:

$$\dot{x} = Ax + Bu + Bw_1 + Ww_2 + w_3 \tag{4.10a}$$

$$y = Cx + n \tag{4.10b}$$

where $w^T = rs1*[\ 0\ \ \omega_1\ \ 0\ \ \omega_2\ \ \ldots\ \ 0\ \ \omega_n\ ]$

$$E[w_1^2] = E[w_2^2] = 10^8*qe, \quad E[nn^T] = I$$

$$E[w_3 w_3^T] = 10^8*rs2*\hat{Q}_r = 10^8*rs2* \begin{bmatrix} 0 & \cdots & \cdots & 0 \\ \vdots & \omega_1^2 & & \vdots \\ \vdots & & 0 & \vdots \\ 0 & \cdots & \cdots & \omega_n^2 \end{bmatrix}$$

qe is the parameter which is increased to achieve loop recovery. rs1

weights a particular choice of a second column of the B-matrix as suggested in Section 2.2.3. The point of including rs1 is to see if it approximates the effect of rs2 without affecting loop recovery. rs2 increases the effect of the noise model suggested in Section 2.2.3. Roughly qe can be thought of as a term which adjusts loop recovery/performance, rs2 as a term which adjusts robustness, and rs1 as an approximation to rs2. The factor 10^8 is included so that loop recovery is achieved for reasonable values of qe.

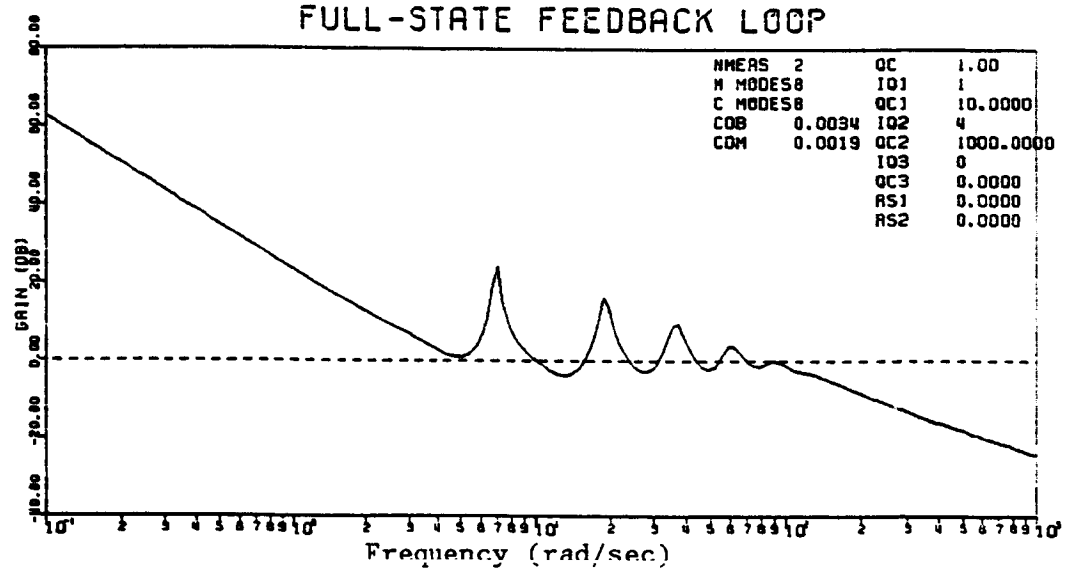

Figure 4.4.1 Full-State Feedback Loop Gain for Standard LQR Design

Again, to compare the various estimators, a standard LQR design is chosen and kept constant thoughout this section. Rather than choose a design which is stable for large frequency variations, a design with intermediate robustness is chosen. This allows a better test of the effect of estimator design on robustness. The design is # 4.3.4c which is stable for -32% to +46% frequency variations with the stan-

dard estimator. The loop gain for this design, again with the standard estimator, is illustrated in Fig. 4.3.16. As a reference, the loop gain for LQR design # 4.3.4c with full-state feedback is illustrated in Fig. 4.4.1. The full-state feedback design has 102° phase margin and infinite gain margin. Loop Transfer Recovery designs will approximate the loop shape and therefore the phase margin of the full-state feedback design. Modified Loop Transfer Recovery designs may exhibit lower gains, implying reduced performance, suggesting that an acceptable compromise can be found. The following sections describe various sequences of estimator designs. The format is similar to that followed in Section 4.3.

4.4.1 Straight Loop Transfer Recovery -

The simplest design from an LTR point of view is one which seeks straight asymptotic loop recovery. In this case rs1 = rs2 =0.0 and qe is increased from .01 to 100.0.

Table 4.4.1 Design Sequence 4.4.1 (rs1=0.0, rs2=0.0, increase qe)

Design #	qe	Uniform Frequency Shifts	Mixed Frequency Shifts	GM	PM
4.4.1a)	.01	-20% to +14%	14% ++++	24db	60°
4.4.1b)	.1	-26% to +9%	9% ++++	18db	66°
4.4.1c)	1.	-30% to +8%	8% ++++	18db	79°
4.4.1d)	10.	-33% to +9%	9% ++++	21db	85°
4.4.1e)	100.	-34% to +10%	10% ++++	26db	91°

The loop gains for qe = .01, 1.0 and 100.0 are illustrated in Figs. 4.4.2 - 4.4.4. Note that as qe is increased both the low fre-

quency loop gain and the bandwidth increase. This indicates that loop recovery improves performance, which provides some justification for the interpretation of qe as a performance term. Furthermore, gain and phase margins increase as expected, though the designs are not particularily robust. The full-state feedback design #4.3.4c has 102° phase margin and infinite gain margin. As qe is increased beyond 100.0 the phase margin will asymptotically approach 102°, but this will not necessarily imply a further improvement in robustness with respect to frequency errors. Loop recovery is achieved by qe = 100.0, but robustness does not improve significantly. This indicates that while straight loop recovery designs approach LQR performance levels they do not necessarily result in good robustness with respect to frequency variations.

The convergence of the closed-loop estimator poles to the plant zeros is illustrated in Fig. 4.4.5. As qe is increased, the estimator poles move to the right, converging on fixed points. Since the system is lightly damped, the plant zeros will lie close to the imaginary axis, and the closed-loop estimator poles will therefore converge on points close to the imaginary axis. The lightly damped estimator poles may contribute to the lack of robustness evidenced by the LTR design. A relationship between robustness and the closeness of estimator poles to the imaginary axis will be demonstrated by more robust estimator designs, as well as algebraic designs and optimal LTR designs, which allow direct manipulation of the pole locations.

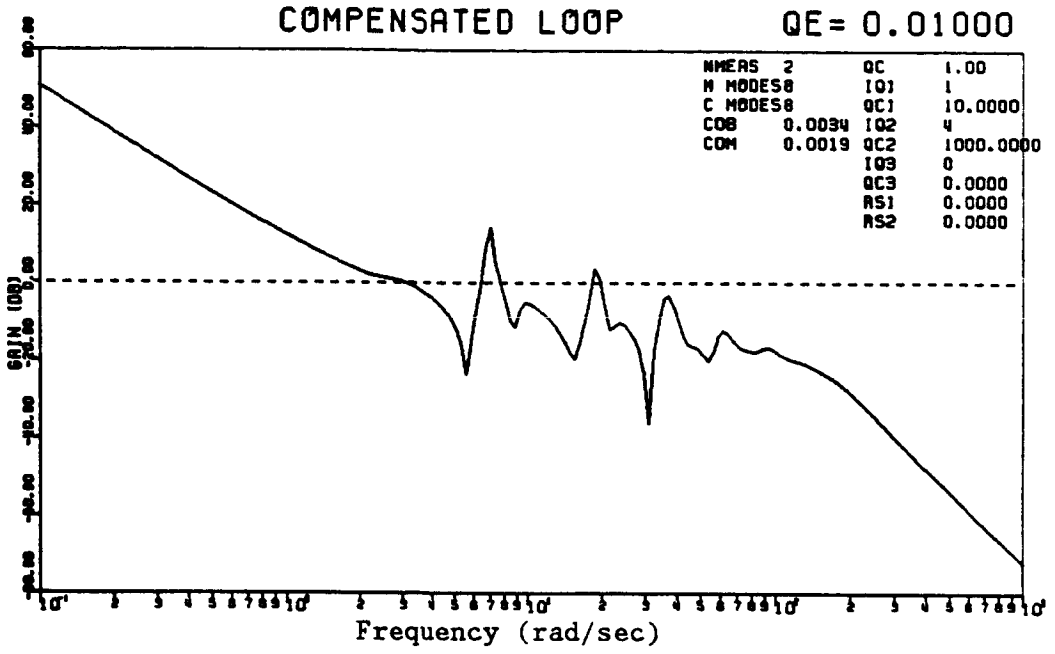

Figure 4.4.2 Loop Gain for Design # 4.4.1a

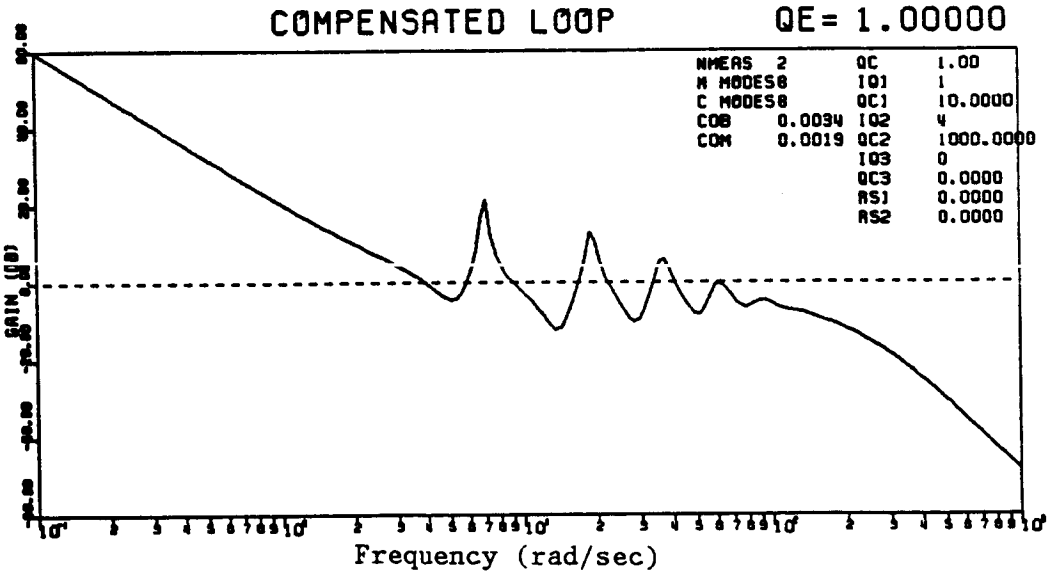

Figure 4.4.3 Loop Gain for Design # 4.4.1c

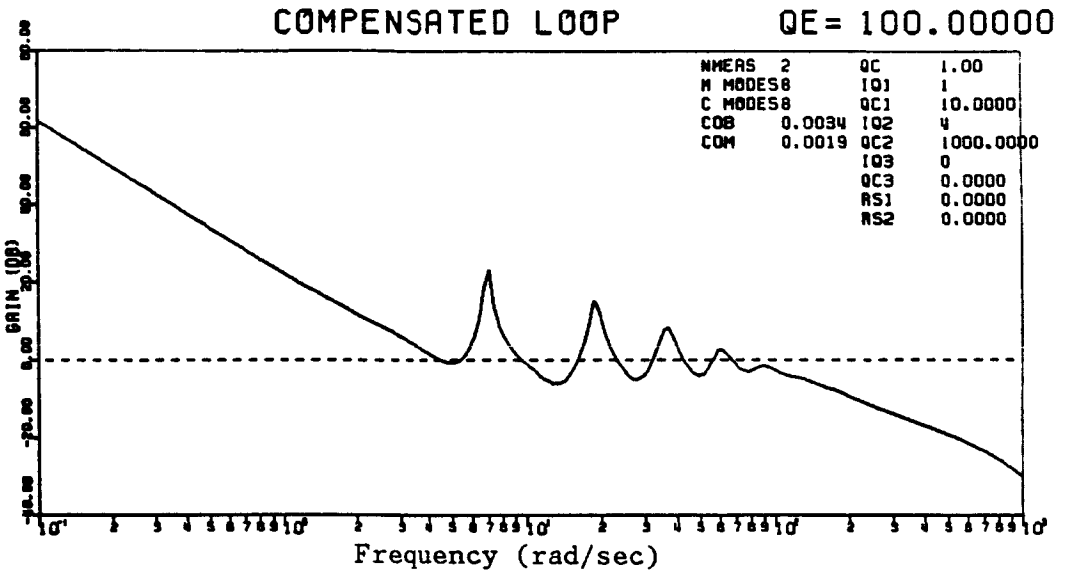

Figure 4.4.4 Loop Gain for Design # 4.4.1e

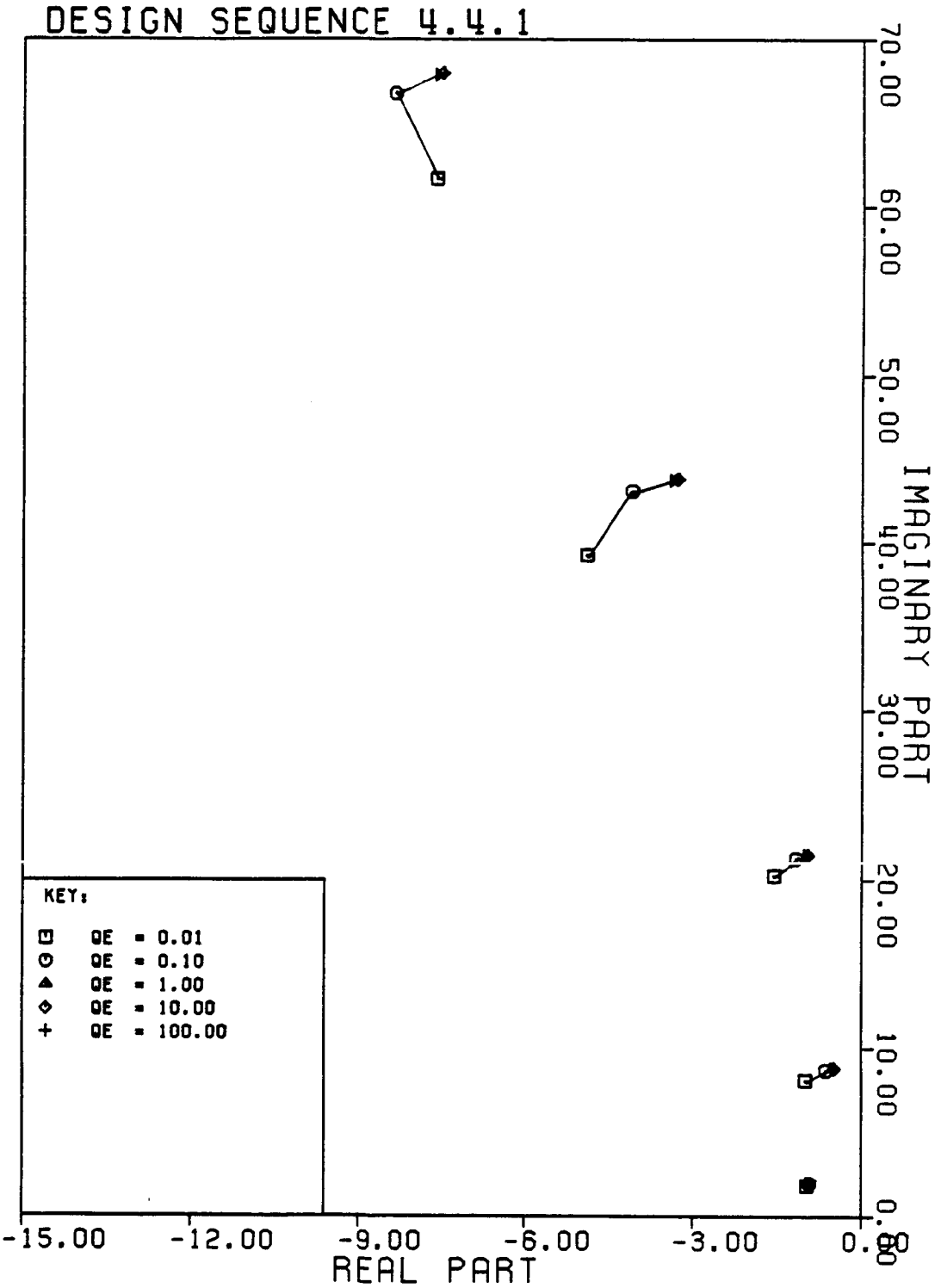

Figure 4.4.5 Closed Loop Estimator Poles for Design Sequence # 4.4.1

4.4.2 Modified Loop Transfer Recovery -

To examine the effect of rs2, increase qe and rs2 together. This is a modified Loop Transfer Recovery approach which should still approach loop recovery, but will also exhibit increased robustness. In this case rs1 = 0.0 and rs2 = qe.

Table 4.4.2 Design Sequence 4.4.2 (rs1=0.0, rs2=qe, increase qe)

Design #	qe	Uniform Frequency Shifts	Mixed Frequency Shifts	GM	PM
4.4.2a)	.00001	-24% to +33%	24% ----	23db	40°
4.4.2b)	.0001	-31% to +70%	29% +---	21db	33°
4.4.2c)	.001	-41% to +85%	28% +---	23db	33°
4.4.2d)	.01	-46% to +89%	29% ++--	27db	35°
4.4.2e)	.1	-48% to +91%	30% ++--	34db	36°
4.4.2f)	1.	-49% to +91%	31% ++--	51db	37°
4.4.2g)	10.	-50% to +91%	31% ++--	61db	38°

The loop gains for qe = .00001, .001, .1 and 10. are illustrated in Figs. 4.4.6 - 4.4.9. As qe and rs2 are increased together the low frequency loop gain does not increase substantially. This indicates that the rs2 term limits loop gain while improving robustness. It is worthwhile to compare this result to design sequence 4.3.3 where robustness was achieved by keeping all the flexible modes above 0db. Design sequence 4.4.2 achieves robustness with all the flexible modes near cross-over. This suggests that robustness is not necessarily achieved by maintaining modes above crossover, but is a complicated function of things other than loop shape. It should also be noted

that the increase of robustness with respect to softening and stiffening the structure is much more pronounced than the robustness with respect to corners of the parameter space. This indicates that the two measures of robustness used in this dissertation do not necessarily result in the same conclusions.

As illustrated in Fig. 4.4.10, increasing qe and rs2 together has little effect on the estimator poles corresponding to the rigid body mode, but shifts poles corresponding to flexible modes to the left. Note that these poles do not converge on plant zeros, indicating that loop recovery will not be achieved. These results are similar to those observed when varying LQR designs. In that case robustness was increased by shifting regulator poles corresponding to flexible modes to the left with respect to regulator poles corresponding to the rigid body mode. The results indicate that a similar relationship exists for the estimator poles.

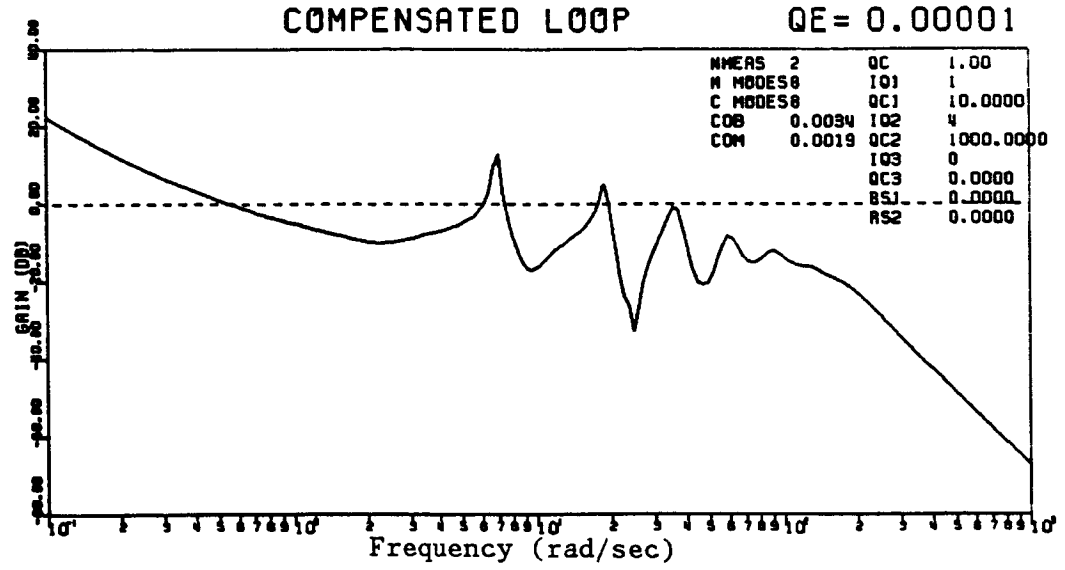

Figure 4.4.6 Loop Gain for Design # 4.4.2a

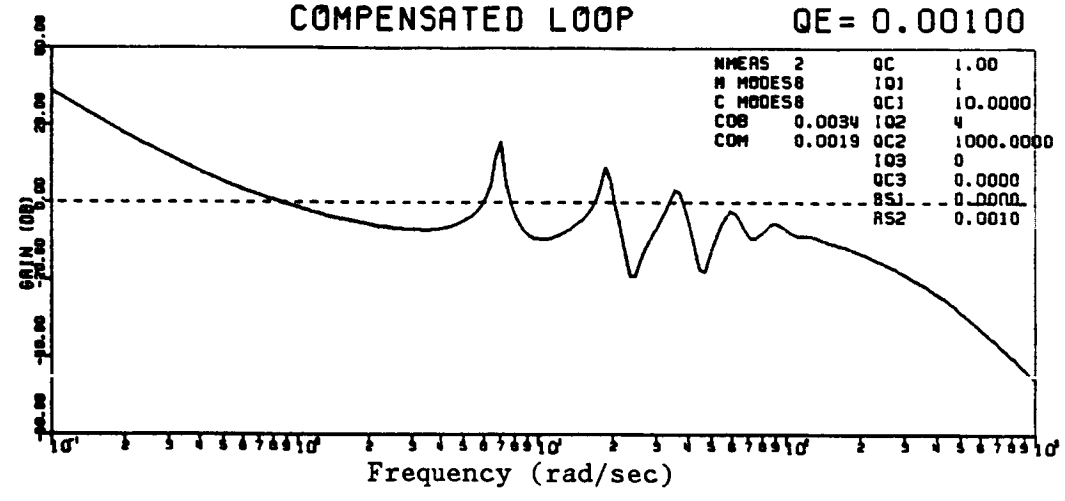

Figure 4.4.7 Loop Gain for Design # 4.4.2c

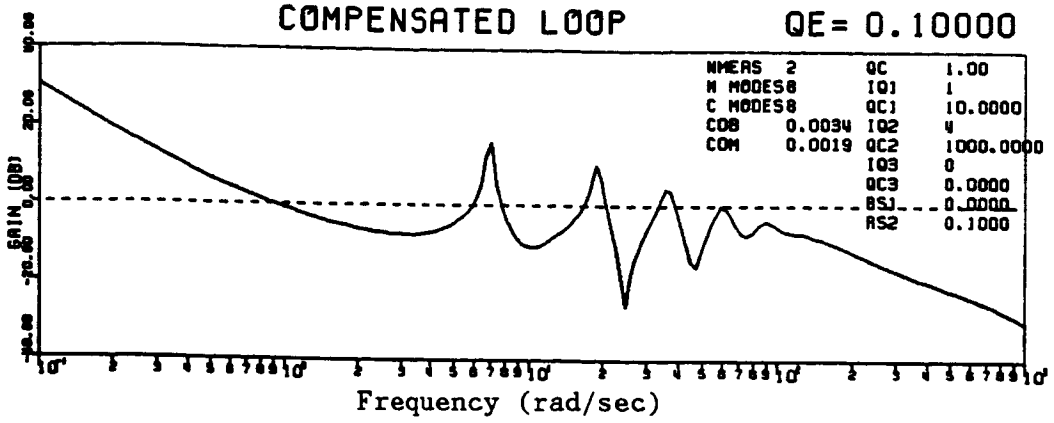

Figure 4.4.8 Loop Gain for Design # 4.4.2e

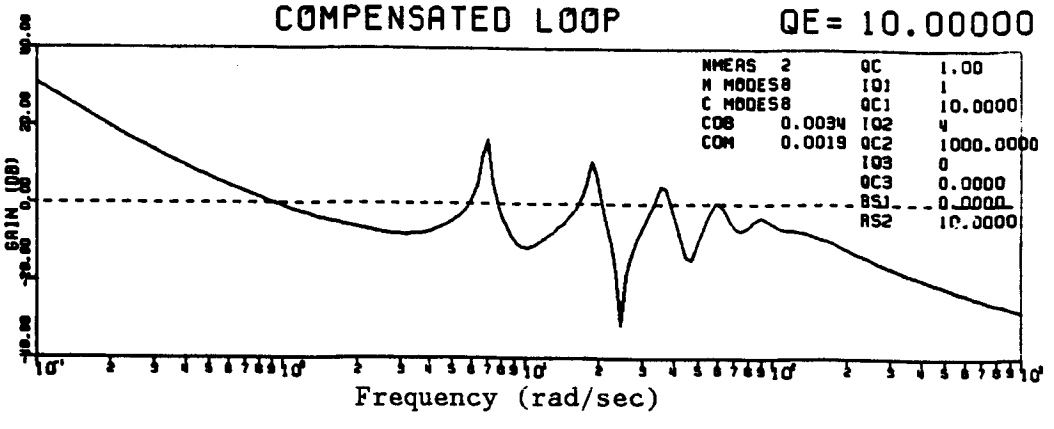

Figure 4.4.9 Loop Gain for Design # 4.4.2g

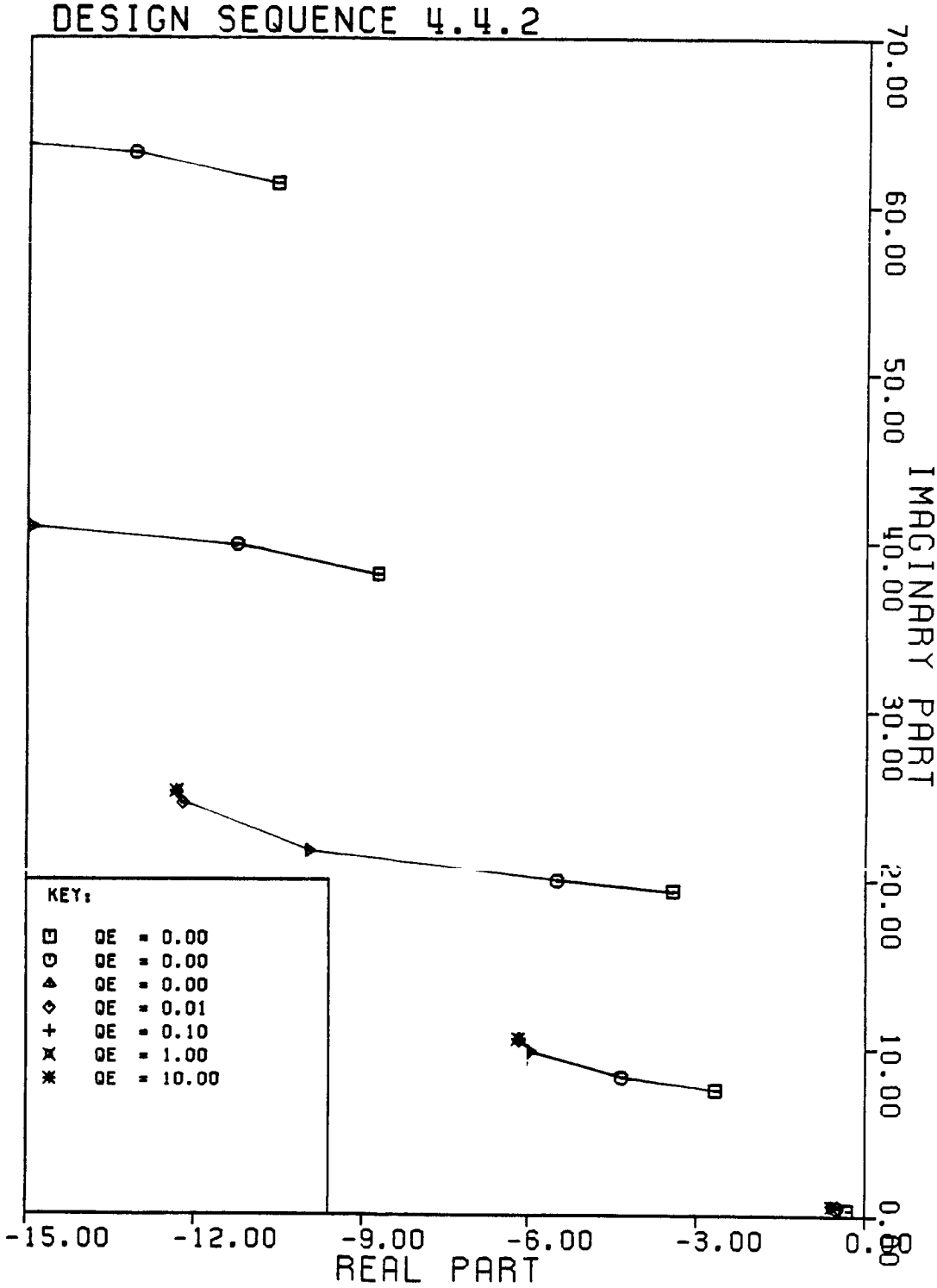

Figure 4.4.10 Closed Loop Estimator Poles for Design Sequence # 4.4.2

4.4.3 Fixed Robustness with Increasing Loop Recovery -

Next examine the effect of fixing rs2 while increasing qe. Let rs1 = 0.0, rs2 = .00001 and increase qe from .01 to 10.0. Again this is a modified Loop Transfer Recovery approach which attempts to increase performance without decreasing robustness.

Table 4.4.3 Design Sequence # 4.4.3 (rs1=0.0, rs2=.00001, increase qe)

Design #	qe	Uniform Frequency Shifts	Mixed Frequency Shifts	GM	PM
4.4.3a)	.01	-23% to +26%	23% ----	23db	38°
4.4.3b)	.1	-25% to +22%	22% ++++	19db	60°
4.4.3c)	1.	-30% to +24%	24% ++++	18db	77°
4.4.3d)	10.	-33% to +30%	30% ++++	21db	84°
4.4.3e)	100.	-34% to +36%	33% -+--	26db	91°

The loop gains for qe = .01, 1.0 and 100.0 are illustrated in Figs. 4.4.11 - 4.4.13. Loop recovery is achieved and performance is increased with a modest increase for both measures of robustness. This suggests that loop recovery and robustness to frequency errors can be simultaneously achieved, though a modification of the LTR approach must be used to attain this result. The modification simply involves adding a small rs2 term. In this case the estimator poles do converge on plant zeros as illustrated in Fig. 4.4.14. The phase margin also approaches the full-state feedback phase margin of 102°.

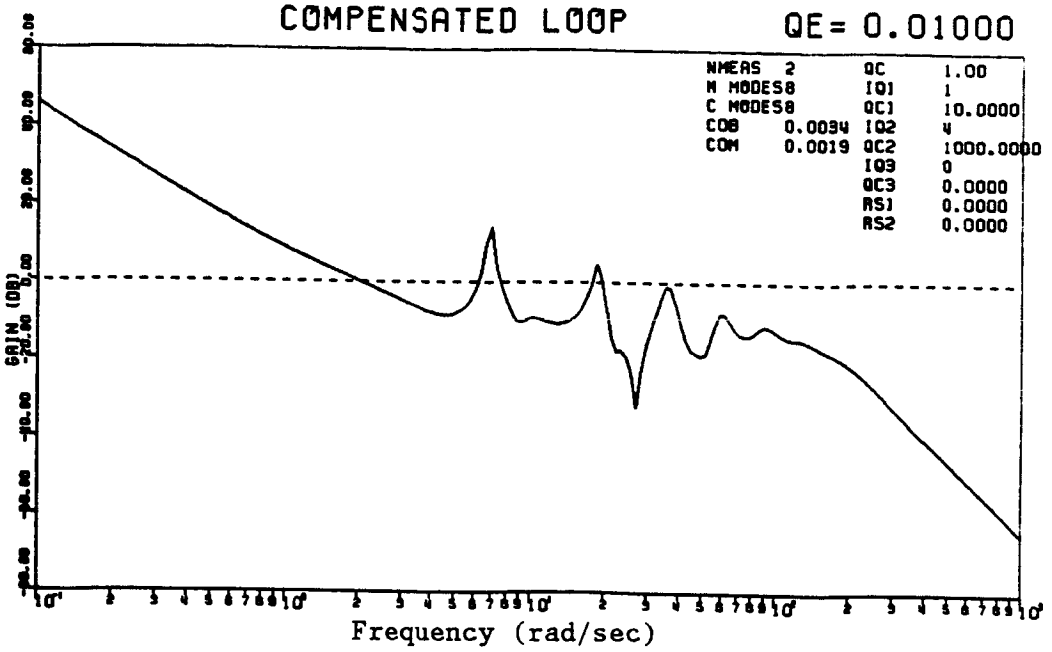

Figure 4.4.11 Loop Gain for Design # 4.4.3a

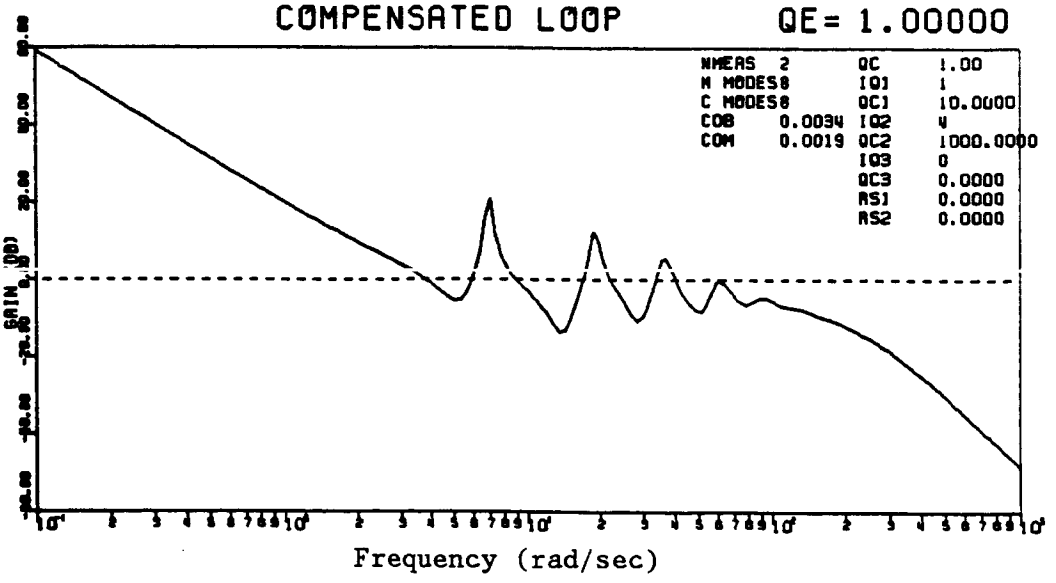

Figure 4.4.12 Loop Gain for Design # 4.4.3c

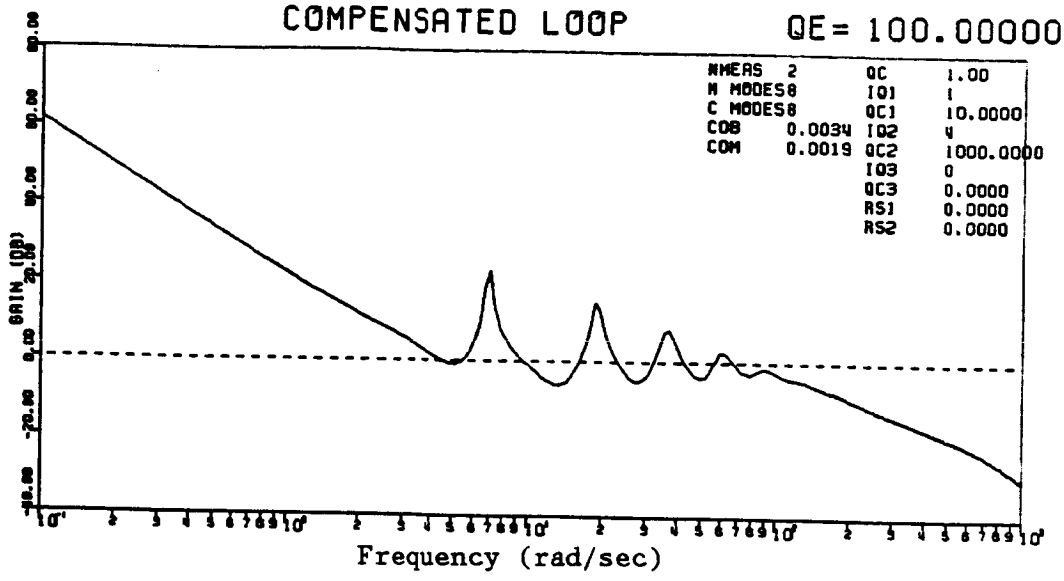

Figure 4.4.13 Loop Gain for Design # 4.4.3e

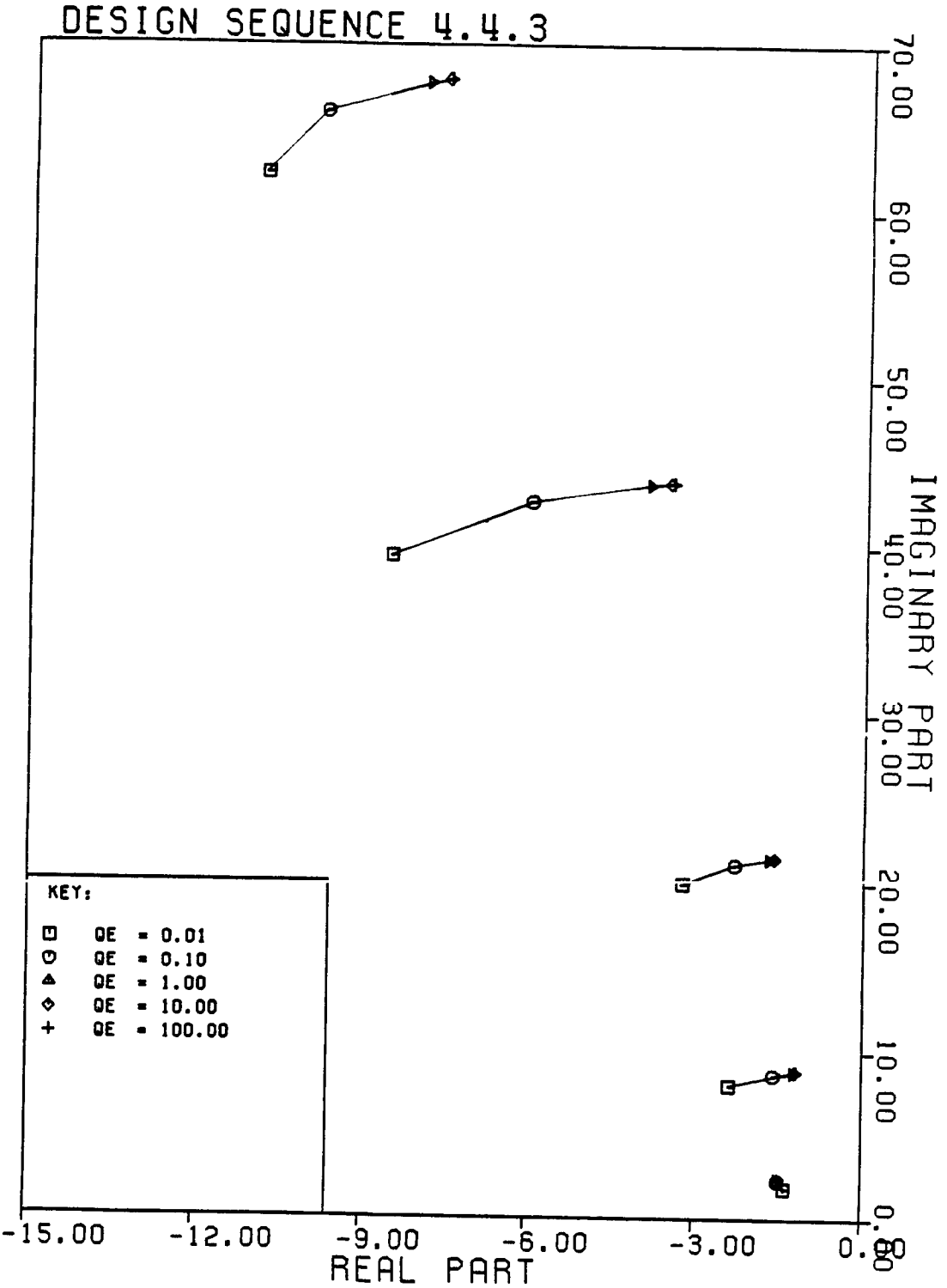

Figure 4.4.14 Closed Loop Estimator Poles for Design Sequence # 4.4.3

4.4.4 Fixed Loop Recovery with Increasing Robustness -

Now fix the loop recovery parameter qe at a level that achieves loop recovery and attempt to improve robustness by increasing rs2. Let qe = 10.0, rs1 = 0.0 and increase rs2 from .00001 to 10.0. This is another version of the modified Loop Transfer Recovery approach and should result in improved robustness.

Table 4.4.4 Design Sequence # 4.4.4 (qe=10.0, rs1=0.0, increase rs2)

Design #	rs2	Uniform Frequency Shifts	Mixed Frequency Shifts	GM	PM
4.4.4a)	.00001	-33% to +30%	30% ++++	21db	84°
4.4.4b)	.0001	-32% to +46%	31% ---+	22db	83°
4.4.4c)	.001	-32% to +55%	30% --++	22db	74°
4.4.4d)	.01	-38% to +70%	32% ++--	27db	42°
4.4.4e)	.1	-46% to +80%	32% ++--	32db	31°
4.4.4f)	1.	-51% to +88%	32% +---	39db	32°
4.4.4g)	10.	-50% to +91%	31% ++--	42db	38°

The results show that robustness with respect to stiffening and softening the structure does increase but robustness with respect to corners of the parameter space does not vary significantly. The loop gain actually decreases as illustrated in Figs. 4.4.15 - 4.4.18. For rs2 = .00001 the loop gain at .1 rad/sec is approximately 62db, while for rs2 = 10.0 the same loop gain is approximately 30db. This is a case where adding process noise to the KBF filter decreases rather than increases the loop gain. It is also another case where robustness with respect to uniform frequency shifts increases while phase

margin decreases, again illustrating the lack of correlation between actual robustness and the margins.

Fig. 4.4.19 indicates that increasing rs2 shifts poles corresponding to flexible modes to the left while shifting poles corresponding to the rigid body mode to the right. This results in decreased control effort applied to the rigid body mode and decreased low frequency loop gain. Again it illustrates the relationship between estimator pole location and robustness.

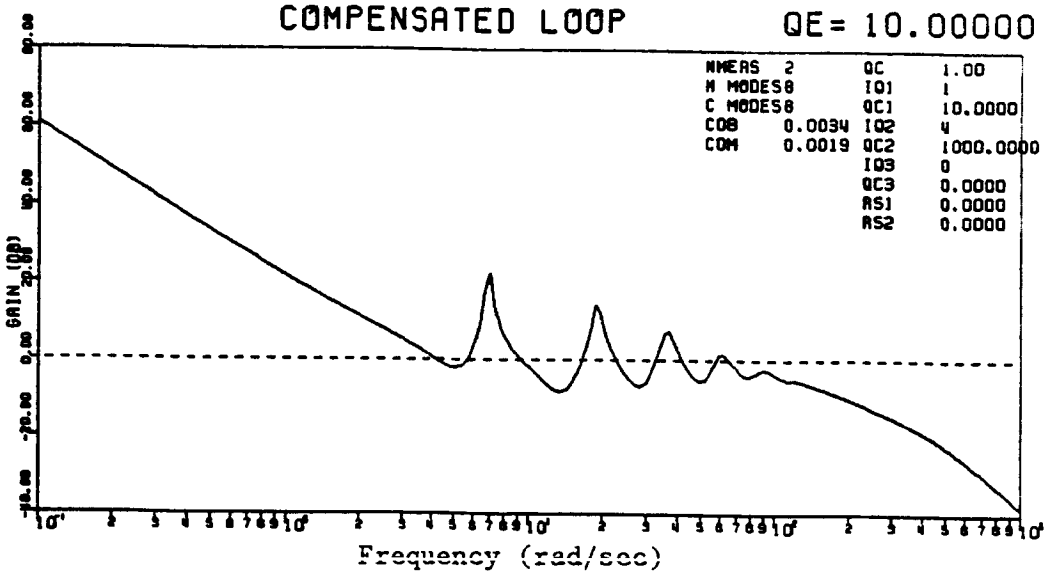

Figure 4.4.15 Loop Gain for Design # 4.4.4a

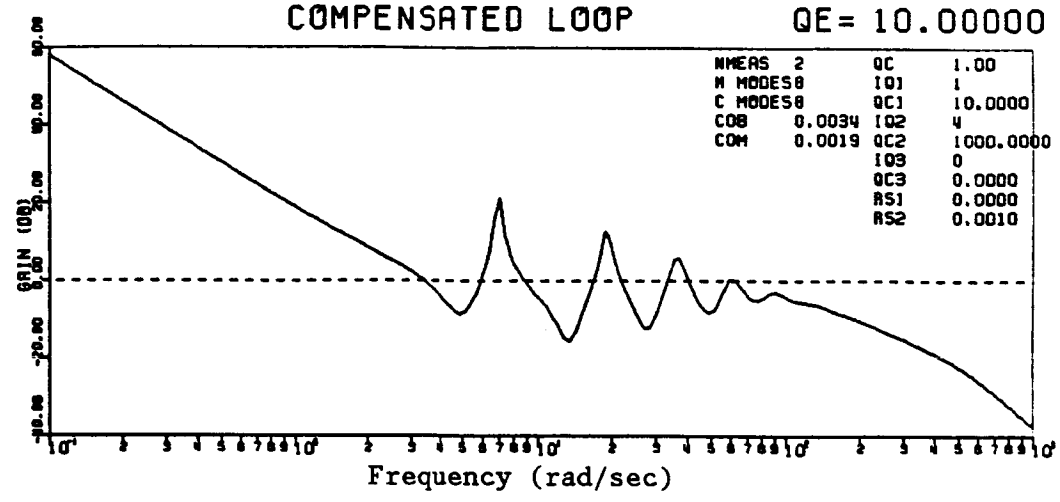

Figure 4.4.16 Loop Gain for Design # 4.4.4c

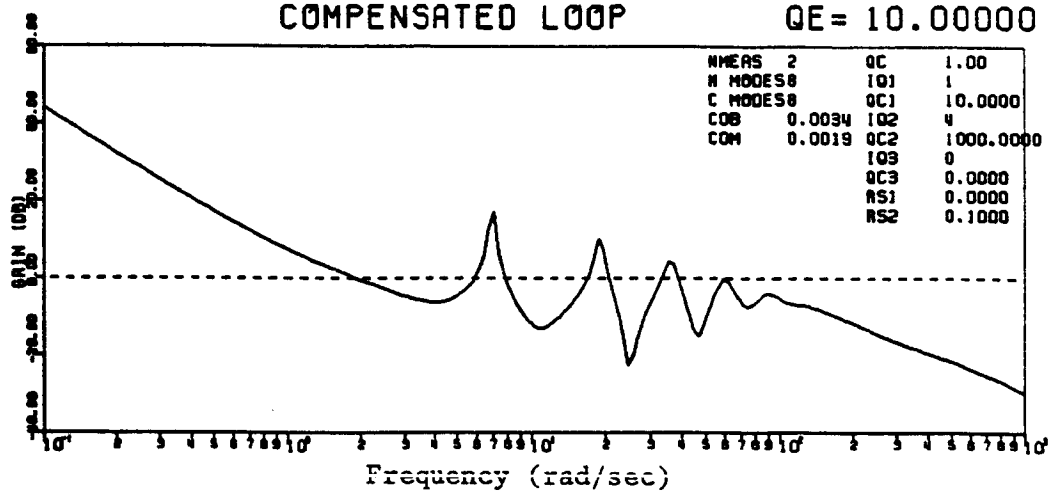

Figure 4.4.17 Loop Gain for Design # 4.4.4e

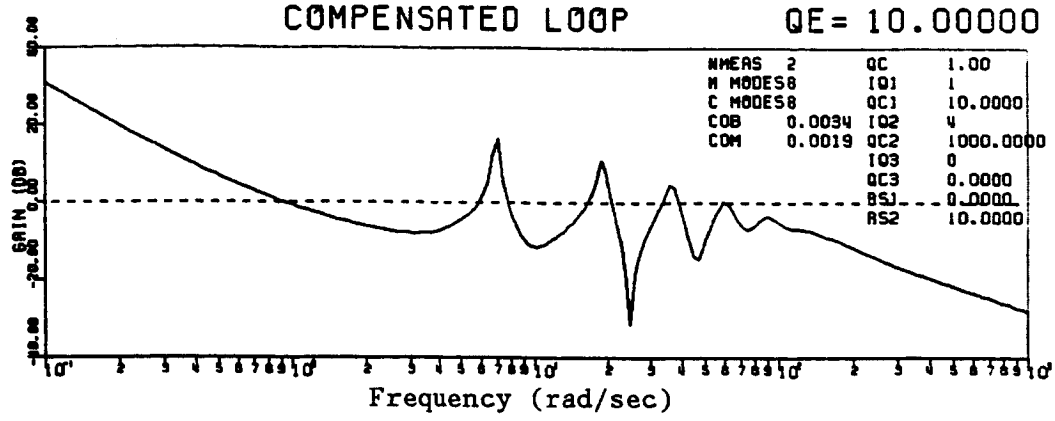

Figure 4.4.18 Loop Gain for Design # 4.4.4g

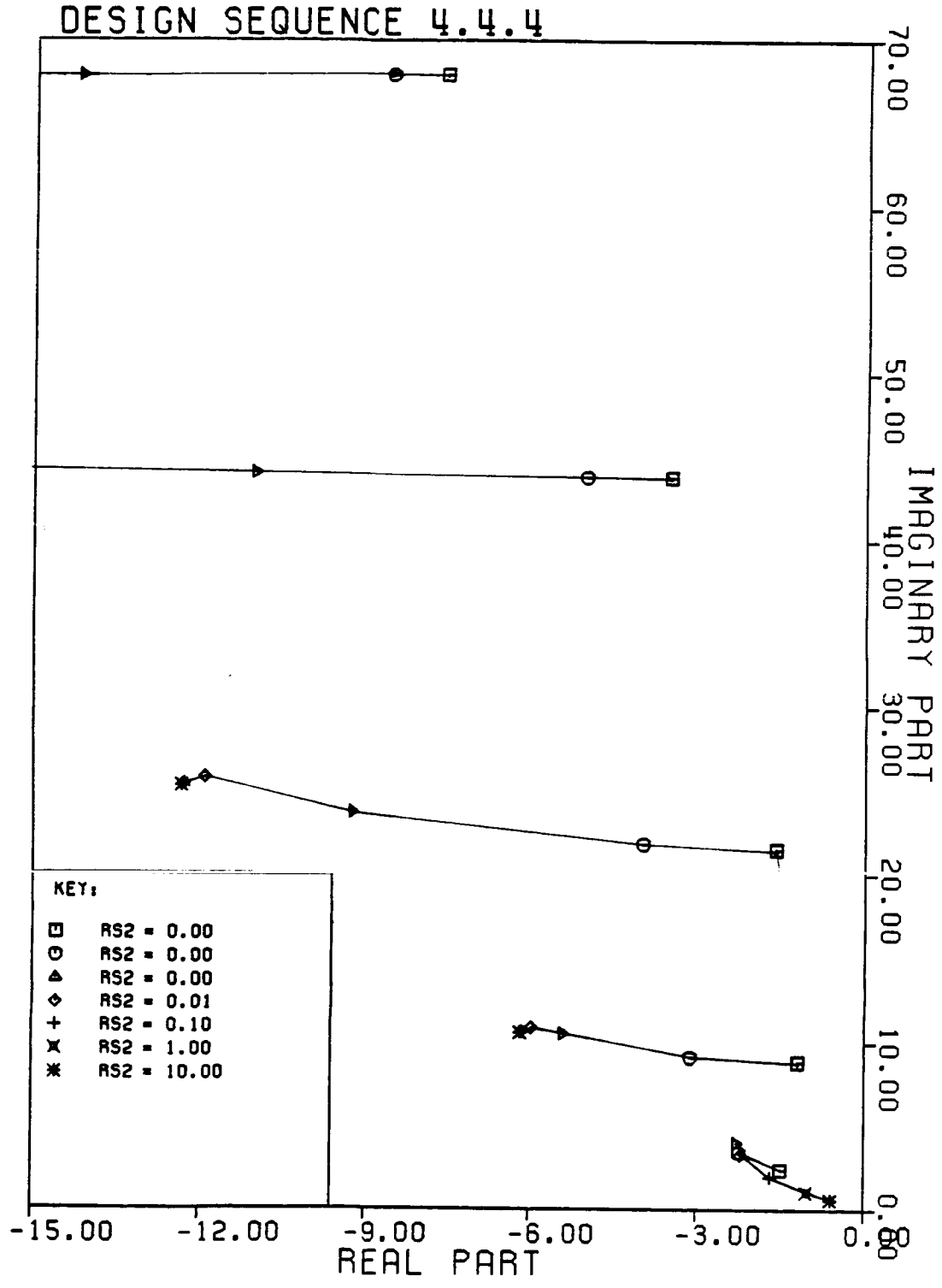

Figure 4.4.19 Closed Loop Estimator Poles for Design Sequence # 4.4.4

4.4.5 Addition of $W*W^T$ Term -

Section 2.3.3 suggests a diagonal noise covariance to improve robustness. This covariance is represented by Matrix Q_r and is controlled by the parameter rs2. One problem with increasing rs2 is that this decreases loop gain and therefore performance (see Section 4.4.3). Note that the noise model model represented by rs2 corresponds to an independent white noise input entering each mode, weighted by the frequency of that mode. A similar noise model might assume that the n independent inputs were actually a single noise input. In this case the noise would enter the modes though column vector W in Eq. 4.10. The advantage of considering the second noise model is that W can be regarded as an appended column to the B-matrix, as discussed in Section 3.2. Theoretically, for a plant with one more output than input, any column can be added to the B-matrix, as long as the resulting plant is minimum phase. Therefore increasing rs1 should approximate the affect of increasing rs2 without the corresponding decrease in loop gain. The robustness of these designs is presented in Table 4.4.5.

Surprisingly the introduction of W decreases rather than increases robustness. This indicates that approximating w_3 by a scalar noise input w_2 acting through the distribution matrix W (see Eq. 4.10) does not result in improved performance or robustness. The loop gains for

Table 4.4.5 Design Sequence # 4.4.5 (qe=10.0, rs2=0.0, increase rs1)

Design #	rs2	Uniform Frequency Shifts	Mixed Frequency Shifts	GM	PM
4.4.5a)	.001	-29% to +12%	12% ++++	21db	86°
4.4.5b)	.0032	-25% to +11%	11% ++++	22db	88°
4.4.5c)	.01	-15% to +10%	10% ++++	24db	67°
4.4.5d)	.032	-12% to +9%	9% ++++	28db	50°
4.4.5e)	.1	-11% to +9%	9% ++++	48db	48°
4.4.5f)	.32	-11% to +9%	9% ++++	55db	48°
4.4.5g)	1.	-11% to +9%	9% ++++	62db	48°

rs1 = .001, .01, .1 and 1.0 are illustrated in Figs. 4.4.20 - 4.4.23. Loop gain also decreases as rs1 is increased, but not to the extent that it does when rs2 is increased.

The locus of estimator poles of this sequence is illustrated in Fig. 4.4.24. As opposed to sequence # 4.4.4, increased weighting is placed on the rigid body mode. This contradicts the situations in which robustness is increased and indicates that increasing rs1 is not an acceptable substitute for increasing rs2. Adding process noise w_2 neither improves robustness or performance.

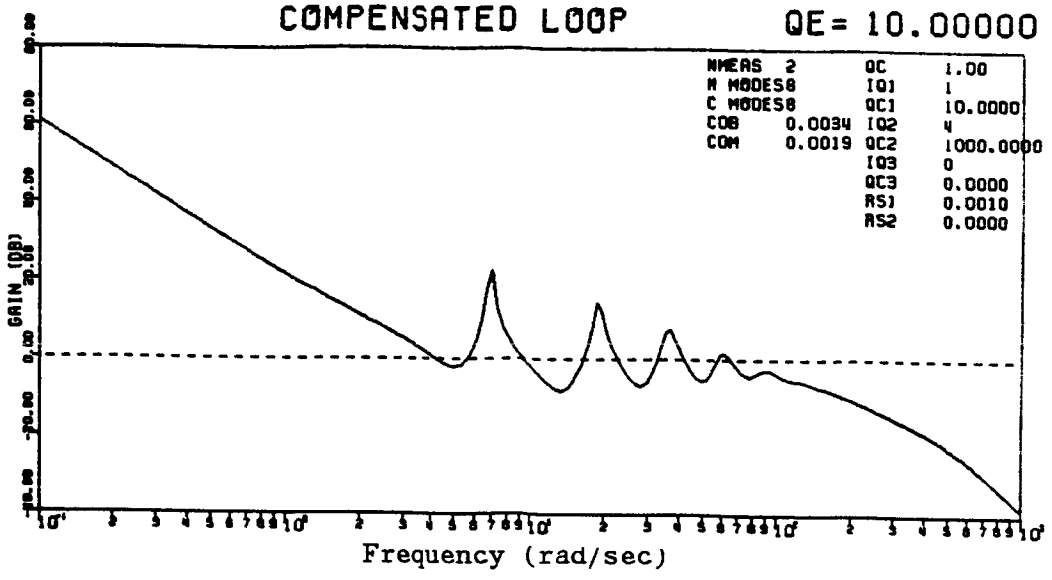

Figure 4.4.20 Loop Gain for Design # 4.4.5a

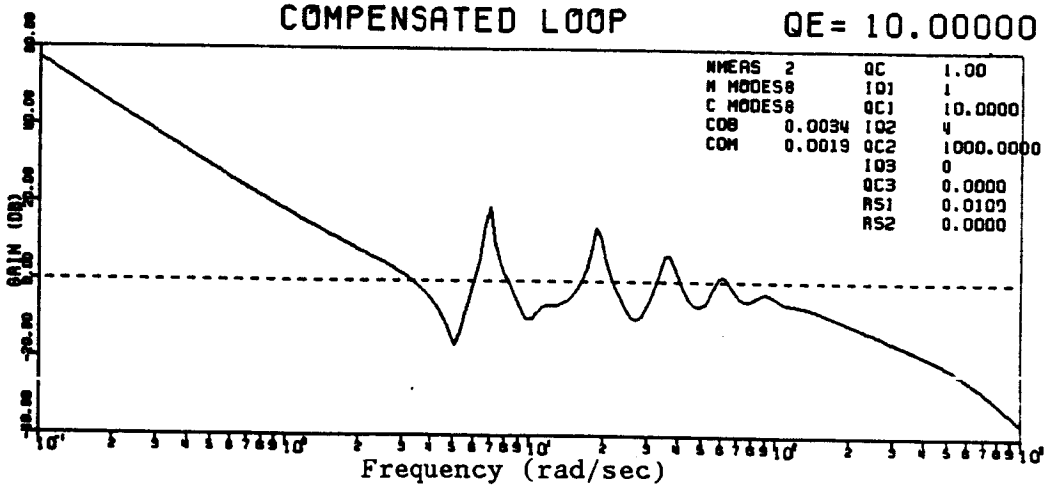

Figure 4.4.21 Loop Gain for Design # 4.4.5c

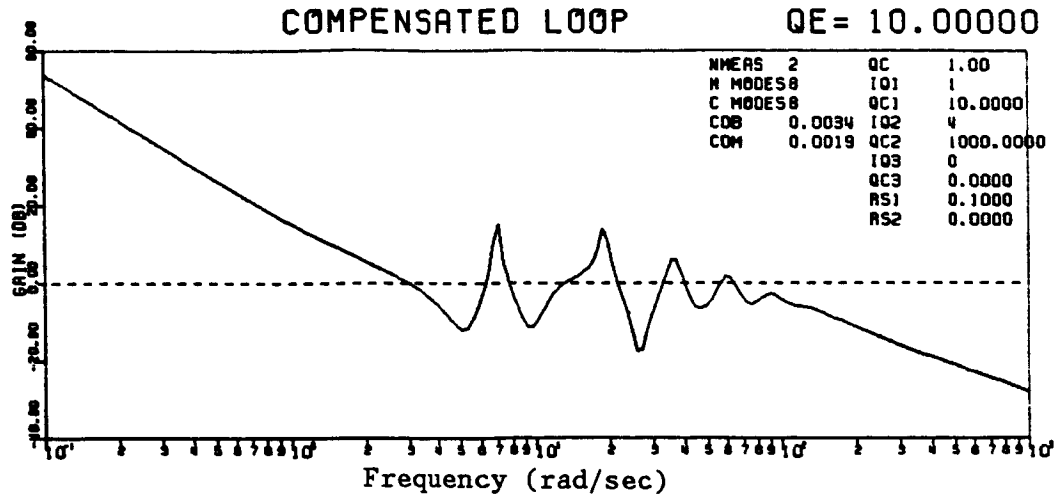

Figure 4.4.22 Loop Gain for Design # 4.4.5e

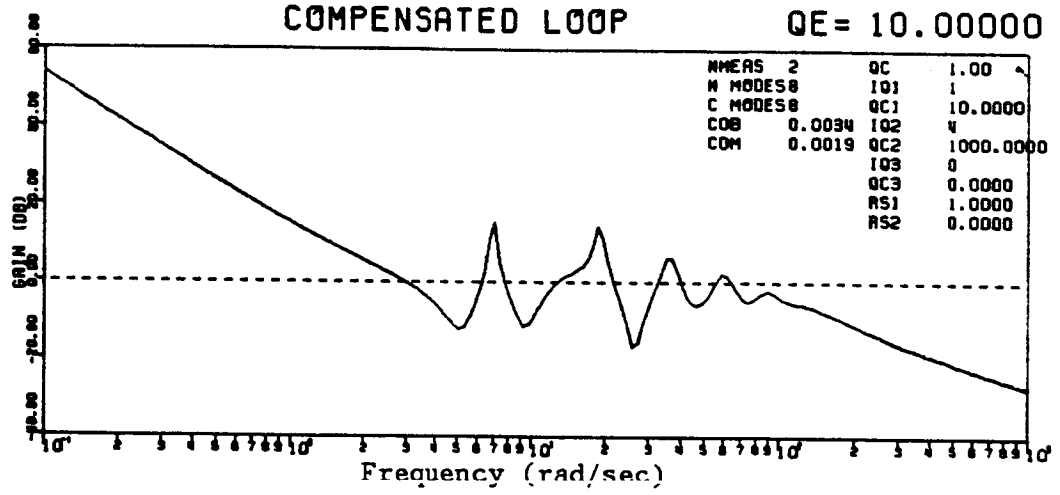

Figure 4.4.23 Loop Gain for Design # 4.4.5g

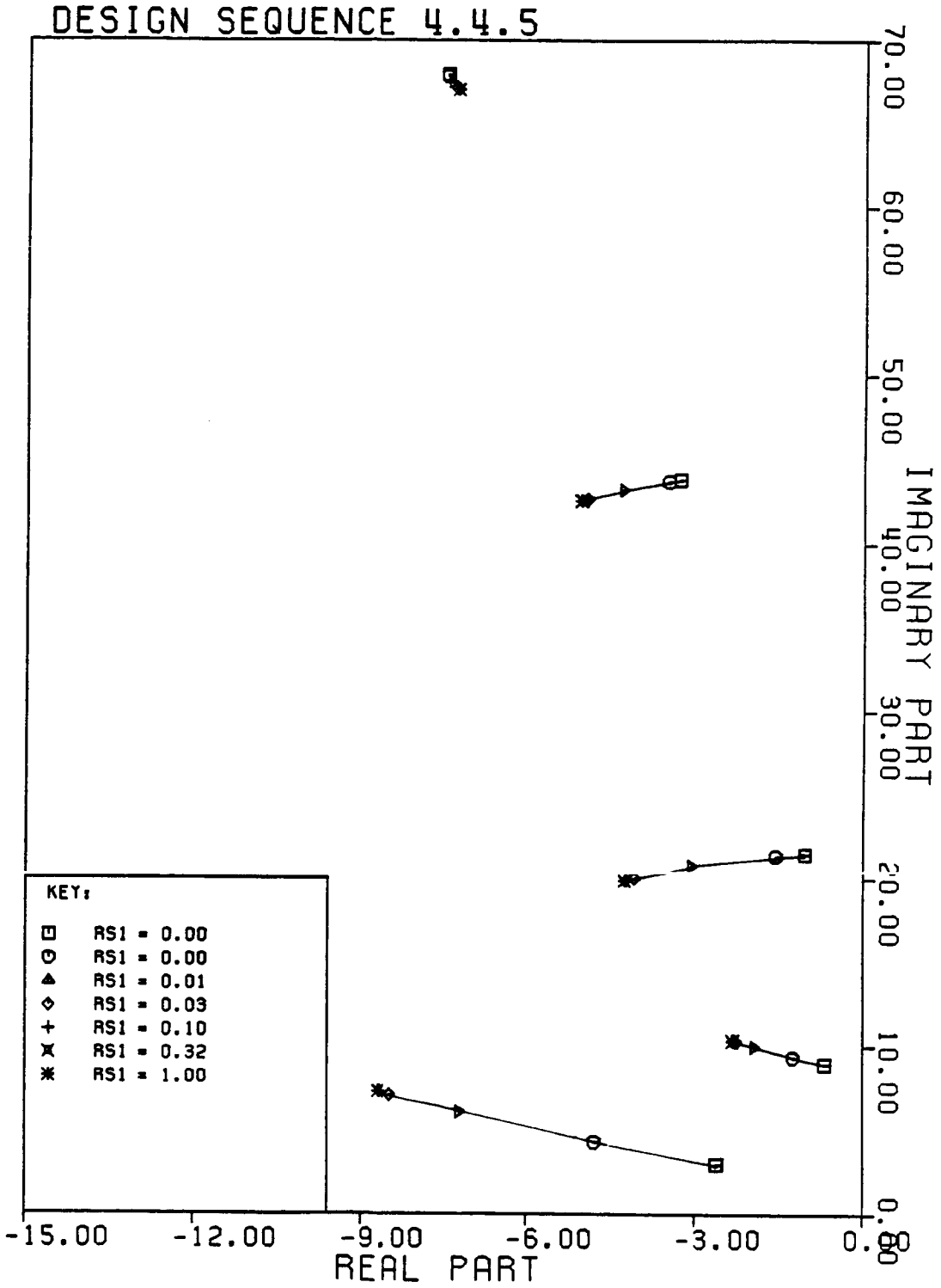

Figure 4.4.24 Closed Loop Estimator Poles for Design Sequence # 4.4.5

4.5 Algebraic Loop Recovery Designs

As indicated in Section 3.3, input loop recovery can be achieved for a system with more outputs than inputs with the freedom of arbitrary compensator pole placement. This is the algebraic loop recovery approach, which synthesizes a loop recovery compensator directly from the plant numerator and desired loop numerator polynomials. Not only is loop recovery achieved in one step, with arbitrary pole placement, but the resulting compensator is of lower order than the corresponding LTR design. As discussed in Section 3.3, the process requires that the plant numerator polynomials contain no repeated factors (i.e. the polynomials do not share roots). These are not the transmission zeros of the MIMO plant, but the zeros of each of the elements of the plant transfer function taken separately. In this regard the poles and zeros of the 2x1 plant transfer function matrix for an antenna model based on 8-modes are listed in Table 4.5.1.

While the zeros are not repeated exactly, there are zeros in the two channels which are very close. This indicates that while matrix S in Eq. (3.30) will not be singular, it will be close to singular (small minimum singular value). In this case the equation Sn = d will have well behaved solutions (small change in n for small change in d) for some d (corresponding to a particular choice of compensator pole location), but very poorly behaved solutions for other d (correspond-

Table 4.5.1 Plant Poles and Zeros for 8-mode model

Plant Poles	Zeros in Channel #1	Zeros in Channel #2
-44.620±155.949j		
-24.959±120.006j	-37.619±143.079j	-36.940±141.879j
-12.923 ±87.791j	-18.944±103.584j	-19.392±104.747j
-5.260 ±60.090j	-7.570 ±68.476j	-7.309 ±67.434j
-2.154 ±36.509j	-3.136 ±43.261j	-3.293 ±44.351j
-0.572 ±18.940j	-0.819 ±21.992j	-0.744 ±20.923j
-0.073 ±6.951j	-0.112 ±8.300j	-0.138 ±9.234j
0.000 ±0.000j	-0.009 ±2.733j	0.000 ±0.000j

ing to another choice of compensator pole location). This suggests that the the algebraic design procedure may be very sensitive to some compensator pole locations. As an example, consider LQR design # 4.3.4c and the compensator pole pattern illustrated in Fig. 4.5.1. These poles are placed in the pattern of a Butterworth low-pass filter, with a cut-off frequency of 10 rad/sec.[1] The loop shape of LQR design # 4.3.4c is recovered exactly, as illustrated in Fig. 4.5.3, but the closed loop system is unstable for ±1% variations in frequency. Therefore, while loop recovery can be achieved with arbitrary compensator pole location, the resulting designs can be very sensitive to frequency errors.

In order to achieve more robust designs consider the compensator poles resulting from design # 4.4.4f. The first 12 poles are listed in Table 4.5.2 and their location is illustrated in Fig. 4.5.2. These

---

[1] The algebraic LTR procedure also requires that another pair of poles be chosen. These poles are not cancelled and must be placed far enough into the left half plane so that they do not affect loop shape in the design region. For all the algebraic designs presented in this dissertation these poles are placed a -1000±1000j so that loop shape is fully recovered for all the designs.

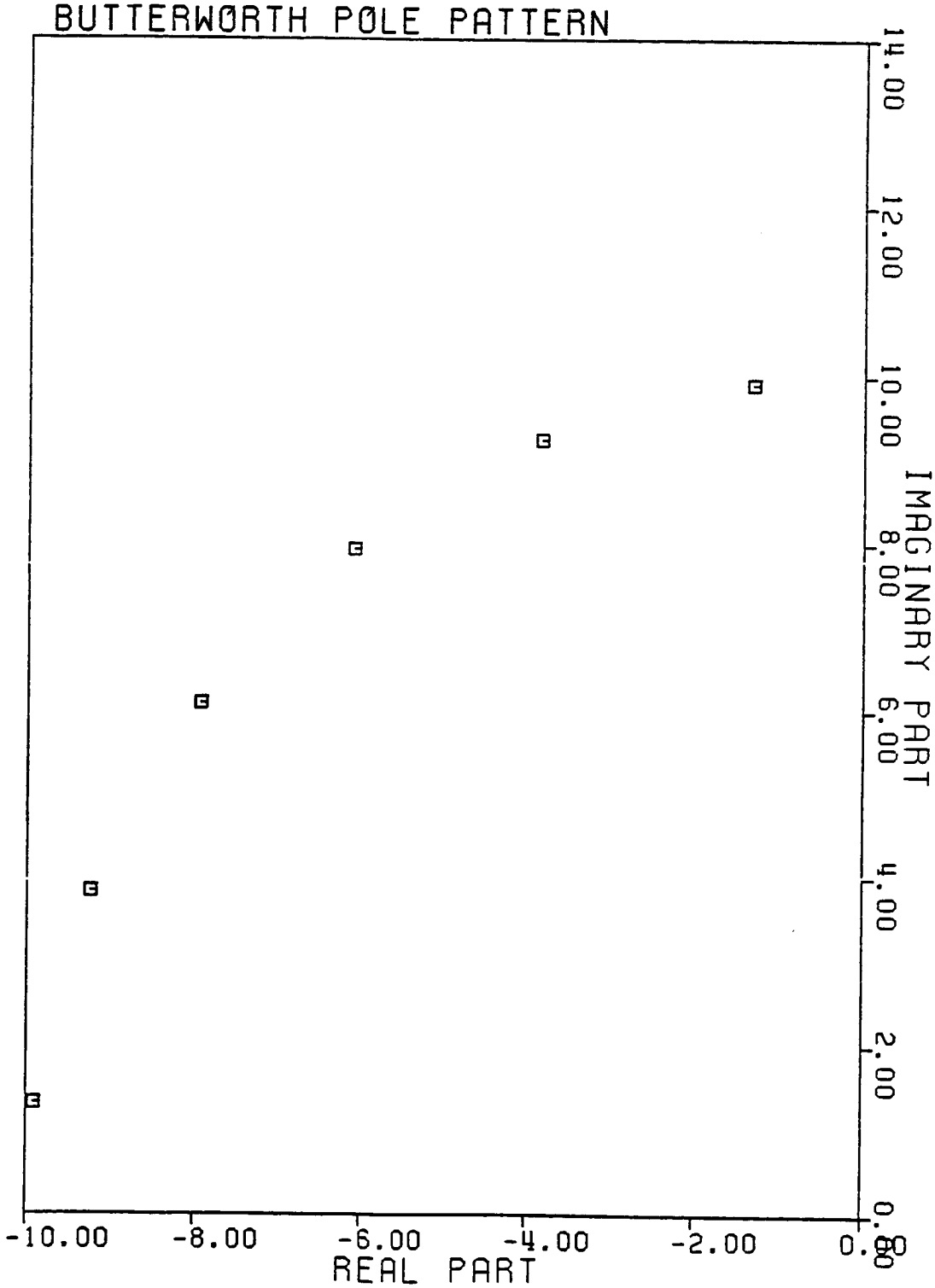

Figure 4.5.1 Compensator Poles in a Butterworth Pattern

are the poles which are cancelled in the algebraic design. The LQR/LTR version of this design is stable for -51% to +88% frequency variations. The corresponding loop gain is illustrated in Fig. 4.5.4. Compare this to Fig. 4.5.3 and note that the loop gain of the LQR/LTR design is considerably lower than the loop gain of the algebraic LTR design.[2] This is because the algebraic LTR design always recovers the LQR loop shape, independent of compensator pole location, while shifting the pole location to improve robustness in the LQR/LTR approach also affects loop shape.

The algebraic design is stable for -32% to +53% variations in frequency. While this is less robust than the corresponding modified LTR design, this would be expected from the increase in loop gain. It also compares favorably with fully loop recovered modified LTR designs (such as 4.4.1e, 4.4.3e and 4.4.4a).

Next the compensator poles are moved to the left and to the right in an attempt to improve robustness. The real part of all the poles are shifted together, one and two units to the left, and one and two units to the right (any further shift to the right would result in an unstable compensator pole). As indicated in Table 4.5.3 the robustness does not vary considerably, though moving poles to the left seems to improve robustness with respect to frequency increases while moving poles to the right seems to improve robustness with respect to fre-

---

[2] The loop shape of all the algebraic designs based on LQR design # 4.3.4g are identical.

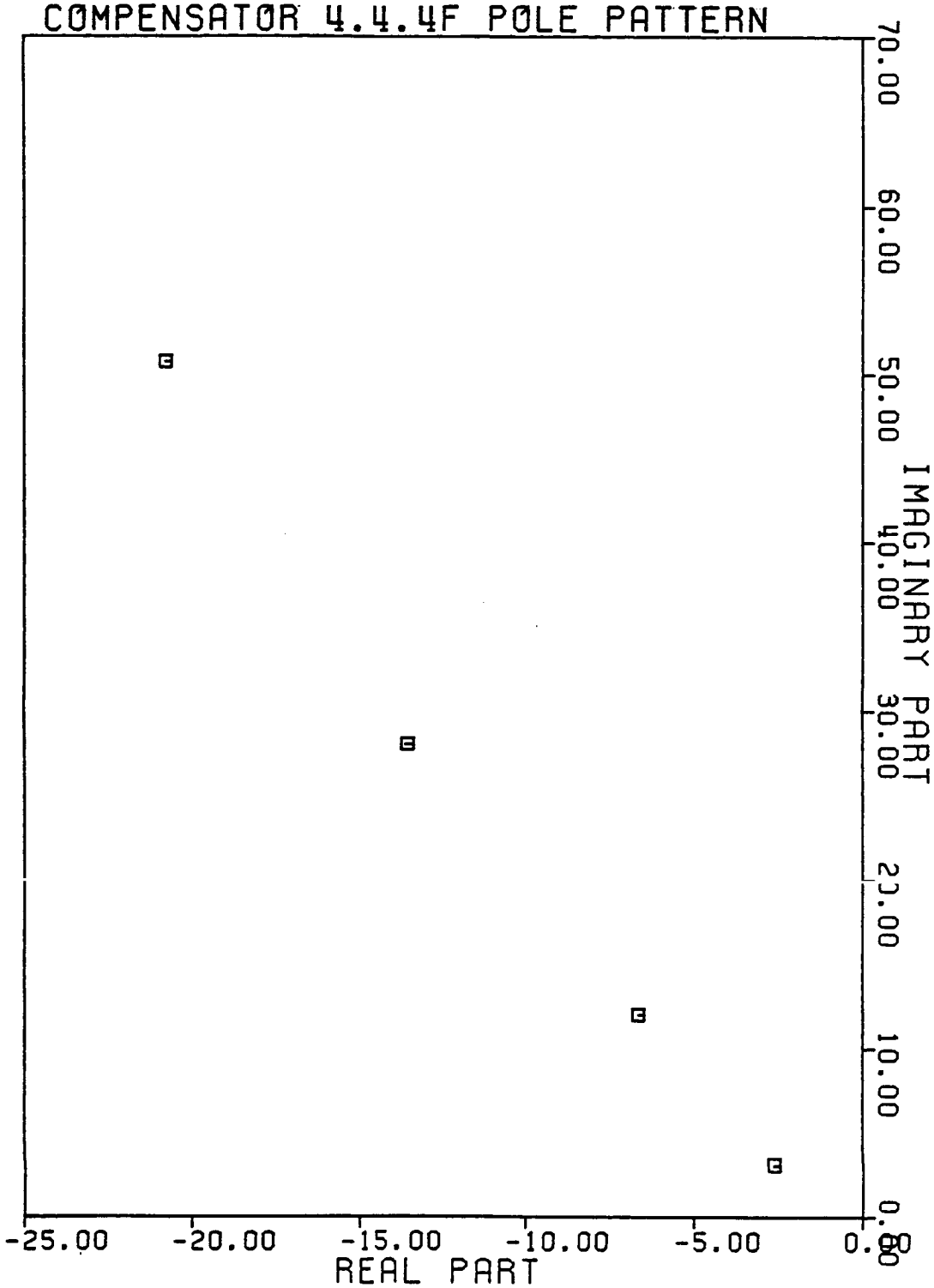

Figure 4.5.2 Compensator Poles for Design #4.4.4f

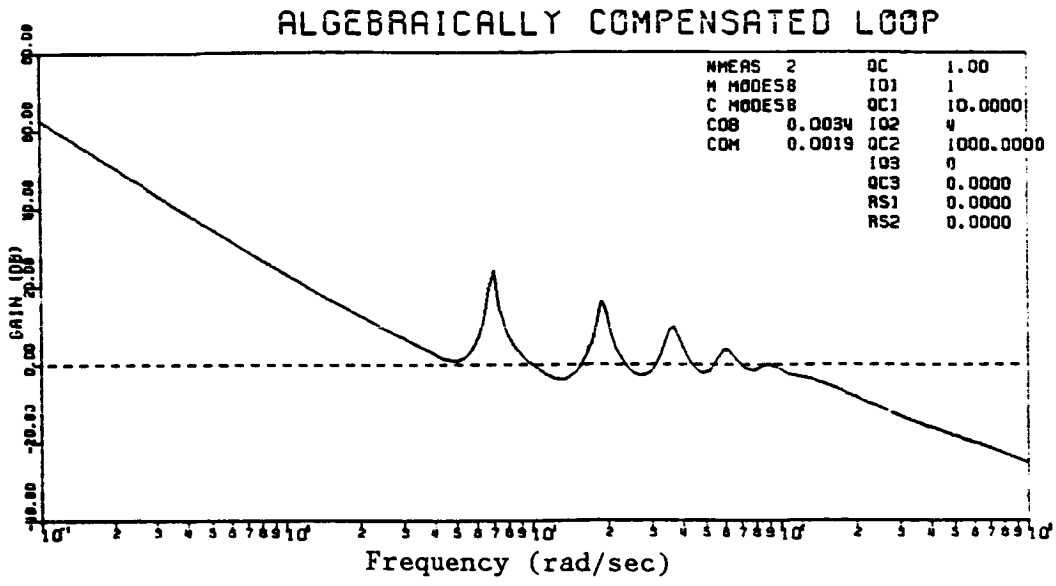

Figure 4.5.3 Loop Gain for Algebraic LTR Designs

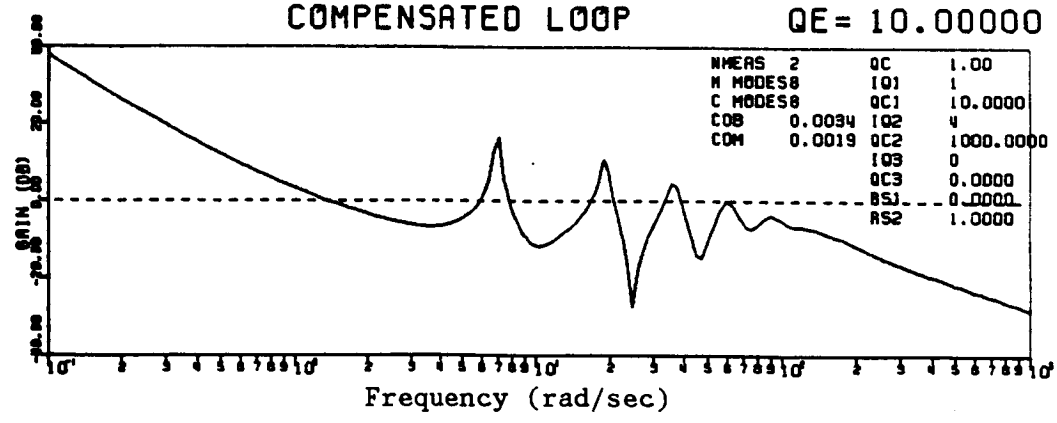

Figure 4.5.4 Loop Gain for Design # 4.4.4f

quency decreases.

Two other variations on the pole location are attempted, both based on the observation in Section 4.4 that designs where the estimator poles corresponding to the rigid body mode lie to the right of the other estimator poles seem to be more robust than others. In the first case the first compensator pole is moved to the right and to the

Table 4.5.2 Compensator Pole Locations for Design #4.4.4f

1) -44.069 ±113.11j
2) -28.412 ±77.489j
3) -20.787 ±50.690j
4) -13.498 ±27.980j
5) -6.6500 ±12.012j
6) -2.6367 ±3.2261j

Table 4.5.3 Robustness when moving all poles to right and left

Design #	Poles	Uniform Frequency Shifts	Mixed Frequency Shifts	GM	PM
4.5.1a)	2 to left	-31% to +59%	31% ----	18db	100°
4.4.5b)	1 to left	-31% to +58%	31% ----	18db	100°
4.4.5c)	nominal	-32% to +53%	32% ----	18db	100°
4.4.5d)	1 to right	-34% to +50%	33% -+-+	18db	100°
4.4.5e)	2 to right	-39% to +50%	32% -+-+	18db	100°

left. The results are listed in Table 4.5.4.

Table 4.5.4 Robustness when moving first pole to right and left

Design #	Poles	Uniform Frequency Shifts	Mixed Frequency Shifts	GM	PM
4.5.1a)	4 to left	-31% to +58%	29% ---+	18db	100°
4.5.1b)	3 to left	-31% to +56%	30% ---+	18db	100°
4.5.1c)	2 to left	-30% to +52%	30% ----	18db	100°
4.4.5d)	1 to left	-29% to +47%	29% ----	18db	100°
4.4.5e)	nominal	-32% to +53%	32% ----	18db	100°
4.4.5f)	1 to right	-34% to +39%	32% ++-+	18db	100°
4.4.5g)	2 to right	-38% to +30%	30% ++++	18db	100°

Again shifting the poles has little effect, though shifts to the left seem to improve robustness with respect to frequency increases while shifts to the right seem to improve robustness with respect to

frequency decreases. Finally all poles but the first are moved to the left and to the right. These results are illustrated in Table 4.5.6.

Table 4.5.5 Robustness when moving all but the first pole

Design #	Poles	Uniform Frequency Shifts	Mixed Frequency Shifts	GM	PM
4.5.1a)	4 to left	-32% to +50%	32% ----	18db	100°
4.5.1b)	3 to left	-32% to +51%	32% ----	18db	100°
4.5.1c)	2 to left	-32% to +51%	32% ----	18db	100°
4.4.5d)	1 to left	-32% to +52%	32% ----	18db	100°
4.4.5e)	nominal	-32% to +53%	32% ----	18db	100°
4.4.5f)	1 to right	-32% to +53%	32% ----	18db	100°
4.4.5g)	2 to right	-32% to +52%	32% ----	18db	100°
4.4.5h)	3 to right	-33% to +46%	32% ---+	18db	100°
4.4.5i)	4 to right	-33% to +39%	33% ----	18db	100°

In this case the variations are minimal, with some loss of robustness with respect to frequency increases when poles are moved to the right.

In conclusion, the algebraic method produces compensators which recover loop gain, but the robustness of these compensators is a strong function of pole location. Since all these compensators result in identical loop shapes, this dramatically illustrates the fact that robustness with respect to parameter errors is not a function of loop shape alone. In particular, arbitrary pole locations do not result in robust compensators, while pole locations near those for robust modified LTR compensators do much better. It is possible to vary robustness slightly by shifting poles from those of a robust modified LTR compensator, but no significant improvement has been found. While the

algebraic approach provides an interesting method for studying the effect of compensator pole location it does not result in more robust compensators than the modified LTR method. In order to fully exploit the potential for algebraic LTR designs, guidelines would be need for placing the compensator poles. Such guidelines have not been discovered in the present work, but this may be a worthwhile topic for future study.

Chapter V

CONCLUSIONS

Standard Loop Transfer Recovery methods are an effective way to achieve robust controller designs when the modeling errors of the plant are well characterized by a single unstructured uncertainty model. However, when these errors are not well described by such a model, then robustness is not necessarily achieved by recovering the full-state feedback loop shape. In this case a modified Loop Transfer Recovery procedure must be employed.

The approach taken in this dissertation overcomes some of the shortcomings of the standard LTR methods. It sets up the control design procedure in terms of structured uncertainties, and then minimizes the 2-norm of the resulting transfer function. Once performance and control cost penalties are appropriately adjusted, a well posed LQR problem is obtained which can be solved with standard numerical methods. As indicated in Section 4.3, robustness and performance can be easily traded off by adjusting only two parameters until a suitable compromise is found. (In this trade-off, robustness refers to the ability of the closed-loop system to remain stable in the presence of modeling errors, and performance to the achievement of a desired loop shape for disturbance rejection at low frequencies).

The estimator is designed by one of two procedures. The first is a modified LTR approach where the actual process noise is augmented by two types of fictitious noise, one of which improves robustness, while

the other is added at the control input to achieve loop recovery. Improved loop transfer recovery increases loop gain, implying better disturbance rejection (performance) and increased gain and phase margins, though the significance of these margins is questionable.

The second method designs the compensator directly via an algebraic cancellation procedure and achieves exact loop transfer recovery with arbitrary pole placement. This method, however, is extremely sensitive to pole location. For the examples examined in this dissertation the best pole locations were found to lie near the poles of compensators that produced robust designs via the modified LTR approach. In this case robustness of the algebraic design is approximately equal to that of a modified LTR design with similar loop gain, while the order of the compensator is lower.

In Chapter IV the entire design procedure is illustrated for a large flexible space antenna. This includes the selection of a reduced order model via approximate balanced singular values and also the application of the methods described above. The modified LTR design is found by varying four parameters, two in the LQR problem and two in the KBF problem. (In terms of the notation in Chapter IV these are qc1, qc2, qe and rs2).

The results of Chapter IV illustrate the inability of traditional robustness measures such as gain and phase margins or loop shape to deal with the complex problem studied in this dissertation. In particular, there is no apparent relationship between gain and phase mar-

gins and robustness with respect to frequency variations. The measures developed in this dissertation were found to provide a much better basis for synthesizing robust controllers. They lead to a control design procedure which effectively balances robustness and performance. The procedure also offers the advantage of a simple implementation involving widely available, efficient numerical tools. Alternative robustness measures and controller design methods are presently under development by other researchers (e.g., μ-synthesis), but difficult numerical problems must be solved before these methods will be ready for application to lightly damped flexible structures such as the example considered here.

A number of extensions and directions for further research are suggested by the results of this dissertation. Other parameter uncertainties, such as uncertain damping ratios or modal displacements could be taken into account by a simple generalization of the modified LTR method. The relationship between compensator pole location and robustness might be studied in greater depth by examining the algebraic design procedure. One approach would involve applying a numerical optimization to find optimal pole locations. Another direction would be to use the structured uncertainty model of this dissertation, but move towards synthesis methods that deal directly with this representation. A possibility is a hybrid H_2/μ-synthesis approach. The results for these more complex methods could then be compared to those presented in Chapter IV to determine if possible improvements would justify the increased complexity.

REFERENCES

AT-1) Athans, M., Kapasouris, P, Kappos, E., Spang, H.A., "Linear-Quadratic Gaussian with Loop-Transfer Recovery Methodology for the F-100 Engine," AIAA J. Guidance and Control, Vol. 9, pp. 45-52, 1986

BA-1) Barmish, B.R., Hollot, C.V., "Counter-Example to a Recent Result on the Stability of Interval Matrices by S. Bialas," Int. J. Control Vol. 39, pp. 1103-1104, 1984

BA-2) Barmish, B.R., "Invariance of the Strict Hurwitz Property for Polynomial with Perturbed Coefficients," IEEE Trans. Auto. Contr., Vol. AC-29, pp. 935-936, 1984

BI-1) Bialas, S., "A Necessary and Sufficient Condition for the Stability of Interval Matrices," Int. J. Control Vol. 37, pp. 717-722, 1983

BL-1) Blelloch, P.A., Mingori, D.L., Wei, J.D., "Perturbation Analysis of Internal Balancing for Lightly Damped Mechanical Systems," submitted to the Journal of Guidance and Control, 1986

BO-1) H.W. Bode, Network Analysis and Feedback Amplifier Design, Van Nostrand, New York, 1945

CH-1) Chen, C.T., Linear System Theory and Design, Holt, Rinehart and Winston, New York, 1984

CR-1) Cruz, J.B., Perkins, W.R., "A New Approach to the Sensitivity Problem in Multivariable Feedback System Design," IEEE Trans. Auto. Contr., Vol. AC-9, pp. 216-226, 1964

DO-1) Doyle, J.C., Stein, G., "Multivariable Feedback Design: Concepts for a Classical/Modern Synthesis," IEEE Trans. Auto. Contr., Vol. AC-26, No. 1, pp. 4-16, 1981

DO-2) Doyle, J.C., Stein, G., "Robustness with Observers," IEEE Trans. Auto. Contr., Vol. AC-24, No. 4, pp. 607-611, 1979

DO-3) Doyle, J.C., "Analysis of Feedback Systems with Structured Uncertainties," IEE Proc., Vol. 129, No. 6, pp. 242-250, 1982

DO-4) Doyle, J.C., Wall, J.E., Stein, G., "Performance and Robustness Analysis for Structured Uncertainty," Proc. 21st IEEE Conf. Dec. Contr., pp. 629-636, 1982

DO-5) Doyle, J.C., "Synthesis of Robust Controllers and Filters with Structural Plant Uncertainty," Proc. 22nd IEEE Conf. Dec. Contr., pp. 109-114, 1983

DO-6) Doyle, J.C., "Structured Uncertainty in Control System Design," Proc. 24th IEEE Conf. Dec. Contr., pp. 260-265, 1985

DO-7) Doyle, J.C., "Notes from short course on Structured Uncertainties," taught at TRW, Redondo Beach, California, Jan.-Mar. 1986.

EV-1) Evans, R.J., Xianya, X., "Robust Regulator Design," Int. J. Control Vol. 41, pp. 461-476, 1985

FA-1) Fan, M.K.H., Tits, A.L., "A New Formula for the Structured Singular Value," Proc. 24th IEEE Conf. Dec. Contr., pp. 595-596, 1985

FR-1) Freudenberg, J.S., Looze, D.P., "Relations between properties of Multivariable Feedback Systems at Different Loop-Breaking Points: Part I," Proc. 24th Conf. Dec. Contr., pp. 250-256, 1985

FR-2) Freudenberg, J., Looze, D., "A Generalization of Bode Gain-Phase Relations to Multiple-Loop Systems," Proc. Am. Contr. Conf., pp. 119-124, 1985

GA-1) de Gaston, R.R.E., "Nonconservative Calculation of the Multiloop Stability Margin," Ph.D. Thesis, University of Southern California, Department of Electrical Engineering, December 1985

GR-1) Gregory, C.Z., "Reduction of Large Flexible Spacecraft Models using Internal Balancing Theory," Proc. AIAA Guid. and Contr. Conf., pp. 805-814, 1983

HA-1) Harvey, C.A., Stein, G., "Quadratic Weights for Asymptotic Regulator Properties," IEEE Trans. Auto. Contr., Vol. AC-23, No. 3, pp. 378-387, 1978

HE-1) Heinen, J.A., "Sufficient Conditions for Stability of Interval Matrices," Int. J. Control Vol. 39, pp. 1323-1328, 1984

HO-1) Hollot, C.V., "Matrix Uncertainty Structures for Robust Stabilizability," Proc. Am. Contr. Conf., pp. 450-455, 1985

KA-1) Kailath, T., Linear Systems, Prentice-Hall Inc., New Jersey, 1980

KA-2) Kapasouris, P., Athans, M., Spang, H.A., III, "Gain-Scheduled Control for the GE-21 Turbofan Engine Using LQG/LTR Methodology," Proc. Am. Contr. Conf., pp. 109-118, 1985

KA-3) Kazerooni, H., Houpt, P.K., Sheridan, T.B., "An Approach to Loop Transfer Recovery Using Eigenstructure Assignment," Proc. Am. Contr. Conf., pp. 796-803, 1985

KA-4) Karl, W.C., Greschak, J.P., Verghese, G.C., "Comments on 'A Necessary and Sufficient Condition for the Stability of Interval Matrices'," Int. J. Control Vol. 39, pp. 849-851, 1984

KH-1) Khargonekar, P.P., Tannenbaum, A., "Non-Euclidean Metrics and the Robust Stabilization of Systems with Parameter Uncertainty," IEEE Trans. Auto. Contr., Vol. AC-30, pp. 1005-1013, 1985

KL-1) Klema, V.C., Laub, A.J., "The Singular Value Decomposition: Its Computation and Some Applications," IEEE Trans. Auto. Contr., Vol. AC-25, No. 2, pp. 164-176, 1980

KO-1) Kouvaritakis, B., Postlethwaite, I., "Principal Gain and Phases: Insensitive Robustness Measures for Assessing Closed-Loop Stabliity Property," IEE Proc., Vol. 129, No. 1, pp. 233-241, 1982

KW-1) Kwakernaak, H., "Optimal Low-Sensitivity Linear Feedback Systems," Automatica, Vol. 5, pp. 279-285, 1969

KW-2) Kwakernaak, H., "Minimax Frequency Domain Performance and Robustness Optimization of Linear Feedback Systems," IEEE Trans. Auto. Contr., Vol. AC-30, No. 10, pp.994-1004, 1985

KW-3) Kwakernaak, H., Sivan, R., Linear Optimal Control Systems, Wiley, New York, 1972

LA-1) Laub, A.J., "Numerical Linear Algebra Aspects of Control Design Computations," IEEE Trans. Auto. Contr., Vol. AC-30, No. 2, pp. 97-108, 1985

LE-1) Lehtomaki, N.A., "Practical Robustness Measures for Multivariable Control System Analysis," Ph.D. Thesis, Massachusetts Institute of Technology, May, 1981

LE-2) Lehtomaki, N.A., Sandell, N.R., Jr., Athans, M., "Robustnesss Results in Linear-Quadratic Gaussian Based Multivariable Control Designs," IEEE Trans. Auto. Contr., Vol. AC-26, No. 2, pp. 75-92, 1981

LE-3) Lehtomaki, N.A., Castanon, D., Levy, B., Stein, G., Sandell, N.R., Jr., Athans, M., "Robustness Tests Utilizing the Structure of Modelling Error," Proc. 20th IEEE Conf. Dec. Contr., pp. 1173-1190, 1981

LE-4) Lehtomaki, N.A., Castanon, D.A., Levy, B.C., Stein, G., Sandell, N.R., Jr., Athans, M., "Robustness and Modeling Error Characterization," IEEE Trans. Auto. Contr., Vol. AC29, No. 3, pp. 212-220, 1984

MA-1) Madiwale, A.N., Williams, D.E., "Some Extensions of Loop Transfer Recovery," Proc. Am. Contr. Conf., pp. 790-795, 1985

MO-1) Morton, B.G., McAfoos, R.M., "A Mu-Test for Robustness Analysis of a Real-Parameter Variation Problem," Proc. Am. Contr. Conf., pp. 135-138, 1985

MO-2) Morton, B.G., "New Applications of Mu to Real-Parameter Variation Problems," Proc. 24th IEEE Conf. Dec. Contr., pp. 233-238, 1985

MO-3) Moore, B.C., "Principal Component Analysis in Linear Systems: Controllability, Observability, and Model Reduction," IEEE Trans. Auto. Contr., Vol. AC-26, No.1, Feb. 1981, pp. 17-32

OP-1) Opdenacker, P.C., Jonckheere, E.A., Safonov, M.G., "Reduced Order Compensator Design for an Experimental Large Flexible Structure," Proc. 24th IEEE Conf. Dec. Contr., pp. 1799-1805, 1985

OW-1) Owens, D.H., "Gain-Phase Structures for Linear Multivariable Systems," Proc. Am. Contr. Conf., pp. 806-811, 1985

PL-1) Plaut, R.H., Huseyin, K., "Derivatives of Eigenvalues and Eigenvectors in Non-Self-Adjoint Systems," AIAA Journal, Vol. 11, No. 2, pp. 250-251, 1973

PO-1) Postlethwaite, I., "Gain and Phase Margins for Linear Multivariable Feedback Systems," Proc. 18th Allerton Conf. on Comm., Contr. and Comp., pp. 396-403, 1980

PO-2) Postlethwaite, I., Edmunds, J.M., MacFarlane, A.G.J., "Principal Gains and Principal Phases in the Analysis of Linear Multivariable Feedback Systems," IEEE Trans. Auto. Contr., Vol. AC-26, No. 1, pp. 32-46, 1981

RO-1) Rosenbrock, H.H., "The Stability of Mutivariable Systems," IEEE Trans. Auto. Contr., Vol. AC-17, No. 2, pp. 105-107, 1972

SA-1) Safonov, M.G., Stability and Robustness of Multivariable Feedback Systems, MIT Press, Cambridge Massachusetts, 1980

SA-2) Safonov, M.G., "Robustness and Stability Aspects of Stochastic, Multivariable Feedback System Design," Ph.D. Thesis, Massachusetts Institute of Technology, May 1977

SA-3) Safonov, M.G., Laub, A.J., Hartmann, G.L., "Feedback Properties of Multivariable Systems: The Role and Use of the Return Difference Difference Matrix," IEEE Trans. Auto. Contr., Vol. AC-26, No. 1, pp. 47-65, 1981

SA-4) Safonov, M.G., Athans, M., "Gain and Phase Margin for Multiloop LQG Regulators," IEEE Trans. Auto. Contr., Vol. AC-22, No. 2, pp. 173-179, 1977

SA-5) Safonov, M.G., "Tight Bounds on the Response of Multivariable Systems with Component Uncertainty," Proc. 16th Allerton Conf. on Comm., Contr.and Comp., 1978

SA-6) Safonov, M.G., "Stability Margins of Diagonally Perturbed Multivariable Feedback Systems," IEE Proc., Vol. 129, No. 6, pp. 251-256, 1982

SA-7) Safonov, M.G., "Stability Margins of Diagonally Perturbed Multivariable Feedback Systems," Proc. 20th IEEE Conf. Dec. Contr., pp. 1472-1478, 1981

SA-8) Safonov, M.G., "Exact Calculation of the Multivariable Structured-Singular-Value Stability Margin," Proc. 23rd IEEE Conf. Dec. Contr., pp. 1224-1225, 1984

SA-9) Safonov, M.G., "Optimal Diagonal Scaling for Infinity Norm Optimization," Proc. Am. Contr. Conf., pp. 125-128, 1985

SH-1) Shaked, U., Soroka, E., "On the Stability Robustness of Continuous Time LQG Optimal Control," IEEE Trans. Auto. Contr., Vol. AC-30, No. 10, pp.1039-1043, 1985

SO-1) Soh, C.B., Berger, C.S., Dabke, K.P., "On the Stability Properties of Polynomials with Perturbed Coefficients," IEEE Trans. Auto. Contr., Vol. AC30, pp. 1033-1036, 1985

SO-2) Soh, Y.C., Evans, R.J., "Robust Multivariable Regulator Design - General Cases," Proc. 24th IEEE Conf. Dec. and Contr., pp. 1323-1327, 1985

SO-3) Soh, Y.C., Evans, R.J., "Robust Multivariable Regulator Design - Special Cases," Proc. 24th IEEE Conf. Dec. and Contr., pp. 1328-1332, 1985

ST-1) Stewart, G.W., Introduction to Matrix Computations, Academic Press, New York, 1973

SU-1) Sundararajan, N., Joshi, S.M., Armstrong, E.S., "Robust Controller Synthesis for a Large Flexible Space Antenna," Proc. 23rd Conf. Dec. Contr., pp.202-208, 1984

YE-1) Yedavalli, R.K., Banda, S.S., Ridgely, D.B., "Time-Domain Stability Robustness Measures for Linear Regulators," AIAA J. Guidance and Control, Vol. 8, pp. 520-524, 1985

ZA-1) Zames, G., "On the Input-Output Stability of Time-Varying Nonlinear Feedback Systems - Part I: Conditions Derived Using Concepts of Loop Gain, Conicity, and Positivity," IEEE Trans. Auto. Contr., Vol. AC-11, No. 2, pp. 228-238, 1966

ZA-2) Zames, G., "On the Input-Output Stability of Time-Varying Nonlinear Feedback Systems - Part II: Conditions Involving Circles in the Frequency Plane and Sector Nonlinearities," IEEE Trans. Auto. Contr., Vol. AC-11, No. 3, pp. 465-476, 1966

Appendix A

SINGULAR VALUES

Singular values measure the "size" of a complex matrix, and are equivalent to the concept of the modulus of a complex scalar. The singular values of a matrix transfer function can therefore be thought of as the MIMO equivalents of the gain of a scalar transfer function.

Any n x m complex matrix A can be decomposed in the following fashion:

$$A = U\Sigma V^* = \sum_{i=1}^{k} \sigma_i u_i v_i^*$$

where:

$k = \min(n,m)$

$\sigma_i = \sqrt{\lambda_i[AA^*]} = \sqrt{\lambda_i[A^*A]}$,

$\sigma_i \geq \sigma_{i+1}$

$U = [u_1\ u_2\ \ldots\ u_n]$, $UU^* = U^*U = I$

$V = [v_1\ v_2\ \ldots\ v_n]$, $VV^* = V^*V = I$

The σ_i's are the singular values of A, the vectors u_i are the left singular vectors of A and the vectors v_i are the right singular vectors of A. The largest singular value σ_1 is denoted by $\bar{\sigma}$ and the

smallest singular value σ_k by $\underline{\sigma}$. $\bar{\sigma}[A]$ is the l_2 induced operator norm of A in the following sense:

$$\bar{\sigma}[A] = \max_{x \neq 0} \frac{\|Ax\|_2}{\|x\|_2} = \max_{\|x\|_2=1} \|Ax\|_2$$

while $\underline{\sigma}[A]$ is a measure of the closeness of A to singularity in the following sense:

$$\underline{\sigma}[A] = \min_{x \neq 0} \frac{\|Ax\|_2}{\|x\|_2} = \min_{\|x\|_2=1} \|Ax\|_2$$

$\underline{\sigma}[A]$ is the only computationally reliable tool for the determination of near singularity, or rank of a matrix [KL-1,LA-1].

The following table includes a number of useful properties of singular values:

1) $\underline{\sigma}[A] > 0 \Longrightarrow \sigma[A] = 1/\sigma[A^{-1}]$

2) $\sigma_i[\alpha A] = |\alpha| \sigma_i[A]$

3) $\underline{\sigma}[A] \leq |\lambda_i[A]| \leq \bar{\sigma}[A]$

4) $A=A^* \Longrightarrow \sigma_i[A] = |\lambda_i[A]|$

5) $A=A^* \geq 0 \Longrightarrow \sigma_i[A] = \lambda_i[A]$

6) $\bar{\sigma}[A + B] \leq \bar{\sigma}[A] + \bar{\sigma}[B]$

7) $\bar{\sigma}[AB] \leq \bar{\sigma}[A]\bar{\sigma}[B]$

8) $\underline{\sigma}[AB] \geq \underline{\sigma}[A]\underline{\sigma}[B]$

9) $\underline{\sigma}[A] - 1 \leq \underline{\sigma}[I + A] \leq \underline{\sigma}[A] + 1$

10) $\bar{\sigma}[E] < \underline{\sigma}[A] \Longrightarrow \underline{\sigma}[A + E] > 0$

11) $\bar{\sigma}[A] < 1 \Longrightarrow \underline{\sigma}[I + A] \geq 1 - \bar{\sigma}[A]$

Another slight variation on the singular value decompostion is the polar decompostion, used extensively by Postlethwaite [PO-1,2,KO-1]. Write the singular value decompostion as:

$$A = U\Sigma V^* = UV^*(V\Sigma V^*) = (U\Sigma V^*)UV^*$$

where $U\Sigma V^*$ is the usual singular value decomposition, $UV^*(V\Sigma V^*)$ is the right polar decomposition and $(U\Sigma U^*)UV^*$ is the left polar decomposition. Postlethwaite defines the principal gains as the eigenvalues of $V\Sigma V^*$ or $U\Sigma U^*$, which are of course just the singular values of A, and the principal phases as the arguments of the eigenvalues of the unitary matrix UV^*. This decomposition is useful in separating a transfer function into a gain part and a phase part and will be used the proof of Theorems 2.1 and 2.2 in Appendix B.

Appendix B

PROOF OF UNSTRUCTURED UNCERTAINTY THEOREMS

Theorems 2.1 and 2.2 are standard in the literature [LE-1,2,3,4], but the proofs presented here are somewhat different, and are included for completeness. Theorem 2.1 will be proved in detail. The changes that need to be made for Theorem 2.2 will not be extensive and will be described in less detail.

Theorem 2.1:

The Multivariable Nyquist Criterion requires that det[I + KG'], evaluated on the standard Nyquist D-contour, encircle the origin counterclockwise as many times as KG' has unstable open-loop poles. If it is assumed that KG' has the same number of unstable open-loop poles as KG, the encirclement count of the origin must not change as G is warped continuously towards any allowable G'. For the Nyquist Contour to remain fixed as G is warped towards G', it is also necessary to assume that any poles on the jω-axis be identical for G and G'. Any plant that has an uncertain frequency on the jω-axis will have an infinite unstructured error in the neighborhood of that frequency, so it is reasonable to assume that the only poles on the jω-axis are at the origin, or equivalently, that the model have some positive damping. Furthermore, practical plants will be strictly proper, implying that $\lim_{s\to\infty} K(s)G(s)=0$. The Nyquist D-contour can therefore be replaced

by the $j\omega$-axis, with the possibility of an indentation about the origin, which will not have any effect on the results for uncertain modal data.

Since $KG(I+\varepsilon\Delta_m)$ is a continuous function of ε, requiring that the encirclement count of $\det[I + KG]$ not change as G is warped towards G' is equivalent to requiring that:

$$\det[I + KG(I+\varepsilon\Delta_m)] \neq 0 \text{ for } 0 \leq \varepsilon \leq 1$$

or in terms of the minimum singular value:

$$\underline{\sigma}[I + K(s)G(s)(I+\varepsilon\Delta_m(s))] > 0, \text{ for } 0\leq\varepsilon\leq 1, \ \overline{\sigma}[\Delta(s)] < \ell_m(s), \ s\varepsilon\Omega_R \quad (B.1)$$

Dropping the dependence on s, and noting that if $\overline{\sigma}[\Delta(s)]\leq\ell_m$, then $\overline{\sigma}[\varepsilon\Delta(s)]\leq\ell_m$, allows us to replace (B.1) by:

$$\underline{\sigma}[I + KG + KG\Delta_m] > 0 \text{ for } \overline{\sigma}[\Delta] \leq \ell_m \quad (B.2)$$

Assume that $\underline{\sigma}[(I + KG)^{-1}]=1/(\overline{\sigma}[I + KG]) > 0$. This is true whenever $\overline{\sigma}[KG] < \infty$, which in turn is true by the definition of the Nyquist D-contour. Multiply (B.2) by $\underline{\sigma}[(I + KG)^{-1}]$:

$$0 < \underline{\sigma}[(I+KG)^{-1}]\underline{\sigma}[I + KG + KG\Delta_m] \leq \underline{\sigma}[I + (I + KG)^{-1}KG\Delta_m] \quad (B.3)$$

Now let $(I + KG)^{-1}KG$ have the singular value decompostion given by $U\Sigma V^*$ or equivalently the polar decompostion given by $UV^*(V\Sigma V^*)$. Let

$\Delta = -\varepsilon \ell_m V U^*$ for $0 \le \varepsilon \le 1$. $\underline{\sigma}[\Delta] = \overline{\sigma}[\Delta] = \varepsilon \ell_m \le \ell_m$, so this is an uncertainty that falls within the specified bounds. Substitute this in:

$$0 < \underline{\sigma}[I + (I + KG)^{-1} KG \Delta_m] = \underline{\sigma}[I - \varepsilon \ell_m V \Sigma V^*] \tag{B.4}$$

but $(I - \varepsilon \ell_m V \Sigma V^*)$ is hermitian, positive semi-definite, so the singular values can be treated as eigenvalues to get:

$$0 < 1 - \varepsilon \ell_m \sigma_i (V \Sigma V^*) = 1 - \varepsilon \ell_m \sigma_i [(I + KG)^{-1} KG] \tag{B.5}$$

$$1 - \varepsilon \ell_m \overline{\sigma}[(I + KG)^{-1} KG] > 0 \tag{B.6}$$

$$\overline{\sigma}[(I + KG)^{-1} KG] > 1/(\varepsilon \ell_m) \ge 1/(\ell_m) \tag{B.7}$$

Before continuing to prove sufficiency it is worth noting that the particular uncertainty that will destabilize the system must have a phase characteristic given by $-VU^*$. An uncertainty with some other phase characteristic might require that $\overline{\sigma}[\Delta_m(j\omega)] >> \ell_m(\omega)$ before the system would go unstable. This indicates that if there is a some specified relationship between gain uncertainty and phase uncertainty, the unstructured uncertainty representation of Theorem 2.1 can be arbitrarily conservative. This point is discussed by Lehtomaki [LE-1,3,4] in the context of most sensitive directions of the perturbation.

Now prove sufficiency by working backwards:

$$\bar{\sigma}[(I + KG)^{-1}KG] < 1/(\ell_m) \tag{B.8}$$

$$1 > \ell_m \sigma[(I + KG)^{-1}KG] \geq \bar{\sigma}[\Delta]\bar{\sigma}[(I + KG)^{-1}KG] \tag{B.9}$$

$$\underline{\sigma}[I + (I + KG)^{-1}KG\Delta_m] \geq 1 - \bar{\sigma}[(I + KG)^{-1}KG\Delta_m] > 0 \tag{B.10}$$

Now assume that $\underline{\sigma}[I + KG] > 0$, which is true whenever the nominal feedback system is stable. Multiply by $\underline{\sigma}[I + KG]$:

$$0 < \underline{\sigma}[I + (I + KG)^{-1}KG\Delta_m]\underline{\sigma}[I + KG] \leq \underline{\sigma}[I + KG + KG\Delta_m] \tag{B.11}$$

$$\underline{\sigma}[I + KG + KG\Delta_m] > 0 \tag{B.12}$$

and Theorem 2.1 is proved[1].

Theorem 2.2:

The major difference in the proof of theorem 2.2 is in ascertaining the continuity of $L(\varepsilon,s)$ as ε varies from 0 to 1. In particular $KG(I+\varepsilon\Delta_d)^{-1}$ must be a continuous function of ε for $0 \leq \varepsilon \leq 1$, or equiva-

---

[1] The only difference between our result and the result stated in Ref. [DO-1] is that we've replaced $\sigma[\Delta(j\omega)] < \ell_m$ by $\sigma[\Delta(j\omega)] \leq \ell_m$. This is a minor variation, and it was corrected in later papers by Doyle [DO-3,4,5]. Furthermore, for practical purposes, the results are identical.

lently that $L(s)=(I+\Delta_d)^{-1}$ have no zero or strictly negative real eigenvalues. This is true since if L(s) has no zero or negative eigenvalues, then neither does $(I+\Delta_d)$, and thus Δ_d can have no eigenvalues in the interval $(-\infty,-1]$, so $\varepsilon\Delta_d$ never has eigenvalues of -1 and $(I+\varepsilon\Delta_d)$ is never singular. If the first requirement is met it is then necessary that:

$$0 < \underline{\sigma}[I + KG(I+\Delta_d)^{-1}] \quad \forall s\varepsilon\Omega_R,\ 0 \leq \varepsilon \leq 1 \tag{B.13}$$

which in turn is equivalent to:

$$0< \underline{\sigma}[I + KG + \Delta_d] \quad \forall s\varepsilon\Omega_R \tag{B.14}$$

The proof then continues as with Theorem 2.1.

Appendix C

NUMERICAL CONSIDERATIONS IN ALGEBRAIC LTR

There are essentially five steps in solving for an LTR compensator by the algebraic method. This appendix will describe the numerical considerations important in each step.

1) Calculation of the Plant Numerator Polynomials -

The plant transfer function is as follows:

$$G(s) = C(sI-A)^{-1}B \tag{C.1}$$

where C is an mxn matrix, A is an nxn matrix, B is an nx1 vector and G(s) is an mx1 vector function of s. To use the algebraic approach the numerator polynomials of G(s) must be found. I have used two methods, the Fadeeva method, which finds the coefficients directly based upon the Cayley Hamilton Theorem [CH-1], and a method based on the transfer function zeros. The Fadeeva method works well for small systems but not for large. The first reason for this is that the number of steps is proportional to n^4, which can become computationally very expensive. The second reason is that the algorithm involves raising the matrix A to the (n-1)th power. This works well for discrete time systems, since the eigenvalues of A lie inside the unit circle, but it is very poorly conditioned for continuous time problems, since the eigenvalues of A may be very large.

The second approach is far more reliable. It is based on calculating the zeros in each channel of the plant, calculating a constant that will premultiply the numerator polynomial and then multiplying out the zeros. The zeros of a plant are defined as values of s which result in a zero output for a non-zero input. In terms of the state space representation of the plant for the ith channel, this can be defined as follows:

$$\begin{bmatrix} (sI-A) & -B \\ C_i & 0 \end{bmatrix} \begin{Bmatrix} x \\ u \end{Bmatrix} = \begin{Bmatrix} 0 \\ y \end{Bmatrix} \tag{C.2}$$

where C_i is the ith row of C and the plant zeros are the values of s which are a solution to (C.2) for y = 0. This can in turn be transformed into the following generalized eigenvalue problem:

$$\begin{bmatrix} A & B \\ -C & 0 \end{bmatrix} \begin{Bmatrix} x \\ u \end{Bmatrix} = s \begin{bmatrix} I & 0 \\ 0 & 0 \end{bmatrix} \begin{Bmatrix} x \\ u \end{Bmatrix} \tag{C.3}$$

The generalized eigenvalue problem can be solved accurately and efficiently by the QZ-algorithm [ST-1], where the computational cost is proportional to n^3. The only tricky step is the separation of finite zeros from infinite zeros. The QZ-algorithm will result in one complex vector α and one real vector β. The eigenvalues are found by dividing the elements of α by the corresponding non-zero elements of β. The first step in separating finite zeros is to eliminate all elements where β is zero. There are two possibilities for eliminating further infinite zeros. The first is to place a threshold on the elements of β, eliminating elements lying below this threshold. This

method ,however, proves to be very sensitive to the threshold. A more reliable method involves dividing all the remaining elements of α by the corresponding non-zero elements of β and then placing an upper bound on the magnitude of the resulting zeros. The upper bound is easily estimated, with some knowledge of the problem, and this method has proved to work very well. As a final check, the number of zeros for a SISO flexible system will almost always be n-2.

The ith numerator polynomial will have the following form:

$$n_i(s) = k_i(s-z_1)(s- z_2)\ldots(s-z_{n-2}) \qquad (C.4)$$

The next step therefore involves computing k_i This is most easily done by noting the following equality:

$$C_i(sI-A)^{-1}B = \frac{k_i(s-z_1)(s-z_2)\ldots(s-z_{n-2})}{(s-p_1)(s-p_2)\ldots(s-p_{n-2})(s-p_{n-1})(s-p_n)} \qquad (C.5)$$

where p_j is the jth pole. (C.5) is valid for any s which is not a pole of the system. k_i can therefore be found by evaluating (C.5) for some $s = s_o$ (e.g., $s_o = 1$) and then solving for k_i. Also note that only $(s_oI-A)^{-1}B$ need be evaluated, using a linear equation solver, rather than $(s_oI-A)^{-1}$. The above method was used in Ref. ED-1 to evaluate plant transfer functions for $s = j\omega$.

The final step in solving for the plant numerator polynomials is to multiply out (C.4), but this is a simple and effecient calculation. The approach based on plant zeros is more complex than the Faddeva

method and must be carried out for each channel separately, but it is far more computationally reliable.

2) Solution to the LQR Problem -

The major step in the calculation of full-state feedback control gains is the solution of a Riccati equation for the LQR problem. This is solved by Potter's method [KA-1] which involves finding the eigenvalues and eigenvectors of the following Hamiltonian matrix:

$$H = \begin{bmatrix} A & -Q \\ -BR^{-1}B^T & -A^T \end{bmatrix} \tag{C.6}$$

Finding an accurate solution to the Riccati equation therefore reduces to finding accurate eigenvalues and eigenvectors for (C.6). Inaccuracies can develop when Q is made very large in comparison with BB^T. This becomes especially important in the solution of the near singular Kalman filter problem for the asymptotic LTR method, since Q may be very large before loop recovery is achieved. This difficulty can be overcome by multiplying both Q and BB^T by the square root of q_c, and then multiplying the final Riccati solution matrix P by the same number, rather than simply multiplying Q by q_c. This procedure keeps H from becoming too "unbalanced" and results in accurate solutions to the Riccati equation, even for very large q_c. A similar apprach involves calling EISPACK routine BALANCE to balance H in the sense of Osbourne. This also improves the accuracy of the solution.

The numerator polynomial for the optimal LQR transfer function $K(sI-A)^{-1}B$ is found by the same methods used to find the plant numerator polynomials.

3) Compensator Order Determination -

The compensator order is found very simply by counting the maximum degree of the plant numerator polynomials and applying equation (3.24). If a proper compensator is required the compensator order will be identical to n_N in (3.24), while if a strictly proper compensator is required, the compensator order will be $n_N + 1$. The only problem in determining the compensator order is dealing with cases in which the matrix S in (3.30) is singular. This will occur when some plant numerators contain identical zeros. This could be checked, but it essentially corresponds to a poorly posed problem.

4) Solution of Compensator Numerator Polynomials -

Once the plant numerator polynomials, the optimal loop gain polynomial, and the compensator order are found; a set of compensator poles are chosen and the compensator numerator polynomials are found by solving the $m(n_N+1)$ set of linear equations defined by (3.30). The solution of these equations depends on the condition number of the matrix S, which is discussed in Section 3.3. Assuming that a solution does exist, I use a standard IMSL iterative inversion routine. This is performed only once per design, and since the accuracy of the pole/zero cancellations depends heavily on an accurate solution, the

extra computational cost and storage required for the iterative solution is considered worthwhile.

5) State-Space Realization of the LTR Compensator -

Since the compensator is found in polynomial form it must be transformed to a state space form. I use a observable-canonical representation [CH-1] which is as follows:

$$A = \begin{bmatrix} 0 & \cdots & 0 & -D_0 \\ 1 & \cdots & 0 & \cdot \\ 0 & 1 \cdots & 0 & \cdot \\ & & & \\ \cdot & \cdot & \cdot & \cdot \\ 0 & 0 \cdots & 1 & -D_{n_N} \end{bmatrix}, \qquad B = \begin{bmatrix} n_{1,0} & \cdots & n_{m,0} \\ \cdot & \cdots & \cdot \\ \cdot & \cdots & \cdot \\ & & \\ \cdot & \cdots & \cdot \\ n_{1,n_N} & \cdots & n_{m,n_N} \end{bmatrix} \tag{C.7}$$

$$C = [\, c \; 0 \; \cdots \cdots \; 0 \,]$$

where D_i is the ith coefficient of the compensator denominator polynomial, $n_{i,j}$ is the jth coefficient of the ith compensator numerator polynomial, and c is the product of the compensator poles which are not cancelled.

Since the polynomial coefficients are sometimes very large, and will possibly contribute to later numerical problems, the state-space representation is balanced so as to minimize the 1-norm of the matrix. This is a relatively cheap operation (computational cost proportional to n^2), and does result in better numerical properties for the robustness calculations.

Appendix D

ANTENNA MODEL DATA

The antenna model is described in Chapter IV. The purpose of this appendix is to list the model data so that the results of this dissertation may be duplicated or compared. Table D.1 lists the physical parameters of the system, while all further data are based on a structural model of the antenna quadrant. This corresponds to the following second order differential equation:

$$\ddot{x} + D\dot{x} + \Omega^2 x = Bu, \quad y = Cx \tag{D.1}$$

All data is based on a 63-mode structural model. Of the original 63-modes, however, approximately 31 are uncontrollable/unobservable from the sensor/actuator positions chosen for this dissertation, as indicated by approximate balanced singular values (see Section 4.2). From an input/output point of view this indicates that a 32-mode model is essentially identical to the 63-mode model, so all data is for the first 32-modes. Table D.2 lists frequency and damping ratio ordered on the basis of of approximate balanced singular values. Table D.3 lists the input matrix B, while D.4 lists the output matrix C. Table D.5 lists the damping matrix D and finally Table D.6 lists the matrix Q_{RMS} such that $x^T Q_{RMS} x$ is the square of the RMS surface error. All information for the examples described in Chapter IV is contained in this data.

Table D.1 Antenna Model Data

Item	Value	Unit
Hub Mass Moment of Inertia	85.58	$lb.in.sec^2$
Hub Radius	46.00	in
Beam Length	1036.7	in
Beam Mass Density	8.00×10^{-5}	$lb.sec^2/in^2$
Beam Stiffness	4.05×10^{6}	lb/in
Mesh Mass Density	9.59	$lb.sec^2/in^3$
Mesh Tension (radial)	1.00×10^{-3}	lb
(tangential)	1.80	lb
Damping Coefficient (beam)	.00345	sec
(mesh)	.00192	sec

Table D.2 Frequency, Damping and Approximate Balanced Singular Values

Mode #	Frequency (rad/sec)	Damping Ratio (% Critical)	Approximate Balanced Singular Value
1	0.00000	0.0%	INFINITE
2	6.95179	1.1%	0.2283233791E+00
3	36.57027	5.9%	0.9497325943E-01
4	18.94830	3.0%	0.8458939640E-01
5	60.31645	8.7%	0.5315266075E-01
6	88.73099	14.6%	0.5528646096E-01
7	122.58242	20.4%	0.3278469507E-01
8	162.23076	27.0%	0.2105883068E-01
9	59.62264	6.4%	0.1266272318E-01
10	51.89005	5.2%	0.1050968921E-01
11	208.83459	35.7%	0.1007722723E-01
12	262.78830	45.1%	0.6011596893E-02
13	55.32309	5.4%	0.2993721983E-02
14	62.18559	6.1%	0.5265596729E-02
15	323.82510	55.7%	0.2963382299E-02
16	392.30962	67.6%	0.1996830257E-02
17	469.48279	80.9%	0.1355287359E-02
18	64.85598	6.3%	0.9801454944E-03
19	120.64193	11.7%	0.7189551663E-03
20	79.12612	7.6%	0.6302797578E-03
21	74.92353	7.2%	0.4360248329E-03
22	57.70021	5.6%	0.1726167648E-03
23	115.53350	11.1%	0.1514403122E-03
24	132.45230	12.7%	0.1073543331E-03
25	102.98778	9.9%	0.1056754992E-03
26	71.18703	6.9%	0.8743073515E-04
27	139.28540	13.4%	0.7292762316E-04
28	67.84885	6.5%	0.5989437099E-04
29	126.27082	12.1%	0.3596155921E-04
30	110.92685	10.7%	0.2675764704E-04
31	146.86891	14.1%	0.9382695966E-05
32	107.05644	10.3%	0.1708525827E-05

Table D.3 Input Matrix B

COLUMN 1

0.93232941E-01
-0.12264582E+00
-0.51061561E+00
-0.28537016E+00
-0.97870307E+00
-0.65160771E+00
-0.11015151E+01
-0.11259166E+01
-0.27375730E+00
-0.19977346E+00
-0.10570916E+01
-0.97602427E+00
-0.11122365E+00
-0.17318549E+00
-0.89571392E+00
-0.83593602E+00
-0.87737986E+00
0.77353996E-01
0.12183550E+00
-0.73710178E-01
-0.57412321E-01
-0.25647807E-01
0.53449162E-01
0.50889322E-01
-0.37706533E-01
-0.23696058E-01
0.44393740E-01
0.20734734E-01
0.27591842E-01
0.21996120E-01
0.17429700E-01
-0.42419404E-02

Table D.4 Output Matrix C

COLUMN 1	COLUMN 2	COLUMN 3	COLUMN 4
0.93232941E-01	-0.12264582E+00	-0.51061561E+00	-0.28537016E+00
0.00000000E+00	0.24335795E+00	0.61749390E+00	0.18318503E+00
COLUMN 5	**COLUMN 6**	**COLUMN 7**	**COLUMN 8**
-0.97870307E+00	-0.65160771E+00	-0.11015151E+01	-0.11259166E+01
0.10835038E+01	0.55838278E+00	0.99704163E+00	0.12321333E+01
COLUMN 9	**COLUMN 10**	**COLUMN 11**	**COLUMN 12**
-0.27375730E+00	-0.19977346E+00	-0.10570916E+01	-0.97602427E+00
0.22422917E+00	0.20085667E+00	0.95020516E+00	0.10860521E+01
COLUMN 13	**COLUMN 14**	**COLUMN 15**	**COLUMN 16**
-0.11122365E+00	-0.17318549E+00	-0.89571392E+00	-0.83593602E+00
0.11487366E+00	0.15370534E+00	0.78891834E+00	0.95115708E+00
COLUMN 17	**COLUMN 18**	**COLUMN 19**	**COLUMN 20**
-0.87737986E+00	0.77353996E-01	0.12183550E+00	-0.73710178E-01
0.77878650E+00	-0.67831847E-01	-0.11314490E+00	0.72486687E-01
COLUMN 21	**COLUMN 22**	**COLUMN 23**	**COLUMN 24**
-0.57412321E-01	-0.25647807E-01	0.53449162E-01	0.50889322E-01
0.58941248E-01	0.34724757E-01	-0.49331841E-01	-0.49704958E-01
COLUMN 25	**COLUMN 26**	**COLUMN 27**	**COLUMN 28**
-0.37706533E-01	-0.23696058E-01	0.44393740E-01	0.20734734E-01
0.42910304E-01	0.27135897E-01	-0.42185051E-01	-0.15009767E-01
COLUMN 29	**COLUMN 30**	**COLUMN 31**	**COLUMN 32**
0.27591842E-01	0.21996120E-01	0.17429700E-01	-0.42419404E-02
-0.28839699E-01	-0.18512671E-01	-0.13913096E-01	0.77825443E-02

Table D.5 Damping Matrix D

COLUMN 1	COLUMN 2	COLUMN 3	COLUMN 4
0.00000000E+00	0.00000000E+00	0.00000000E+00	0.00000000E+00
0.00000000E+00	0.14638437E+00	-0.50403864E-01	-0.30499319E-01
0.00000000E+00	-0.50403864E-01	0.43079375E+01	-0.15115725E+00
0.00000000E+00	-0.30499319E-01	-0.15115725E+00	0.11440055E+01
0.00000000E+00	-0.96051567E-01	-0.50519897E+00	-0.28374255E+00
0.00000000E+00	-0.64761062E-01	-0.40646664E+00	-0.17942450E+00
0.00000000E+00	-0.10757214E+00	-0.59225094E+00	-0.32090525E+00
0.00000000E+00	-0.11019300E+00	-0.60448869E+00	-0.32712396E+00
0.00000000E+00	-0.28117977E-01	-0.72046680E-01	-0.72937681E-01
0.00000000E+00	-0.16068441E-01	-0.92852435E-02	-0.95720628E-01
0.00000000E+00	-0.10341279E+00	-0.56754228E+00	-0.30713846E+00
0.00000000E+00	-0.95527870E-01	-0.52376478E+00	-0.28426118E+00
0.00000000E+00	-0.88294531E-02	-0.94783629E-01	-0.49483060E-01
0.00000000E+00	-0.16863195E-01	-0.21291377E+00	-0.44504431E-01
0.00000000E+00	-0.87586191E-01	-0.48263768E+00	-0.26058077E+00
0.00000000E+00	-0.81945184E-01	-0.44992022E+00	-0.24288004E+00
0.00000000E+00	-0.85808601E-01	-0.47167806E+00	-0.25555047E+00
0.00000000E+00	0.77615037E-02	0.16422412E+00	0.13418431E-01
0.00000000E+00	0.12065249E-01	0.52677988E-01	0.36269594E-01
0.00000000E+00	-0.57102945E-02	-0.11721112E-01	-0.33739170E-01
0.00000000E+00	-0.44285185E-02	0.28275500E-01	-0.29849041E-01
0.00000000E+00	-0.12790714E-02	-0.85951736E-01	-0.14795521E-01
0.00000000E+00	0.55117068E-02	0.21295666E-01	0.14956000E-01
0.00000000E+00	0.49177136E-02	0.12023530E-01	0.17493581E-01
0.00000000E+00	-0.29948857E-02	-0.59774351E-03	-0.16677566E-01
0.00000000E+00	-0.14402934E-02	0.75244409E-01	-0.19920489E-01
0.00000000E+00	0.41919961E-02	0.11070899E-01	0.16046914E-01
0.00000000E+00	0.25716347E-02	0.12172107E+00	-0.56398774E-02
0.00000000E+00	0.27459402E-02	-0.60432359E-03	0.99205552E-02
0.00000000E+00	0.25603561E-02	0.12025279E-01	0.42554055E-02
0.00000000E+00	0.14789512E-02	0.93794112E-03	0.83025561E-02
0.00000000E+00	0.10151803E-03	0.60223775E-02	-0.48136680E-02

D (cont.)

COLUMN 5	COLUMN 6	COLUMN 7	COLUMN 8
0.00000000E+00	0.00000000E+00	0.00000000E+00	0.00000000E+00
-0.96051567E-01	-0.64761062E-01	-0.10757214E+00	-0.11019300E+00
-0.50519897E+00	-0.40646664E+00	-0.59225094E+00	-0.60448869E+00
-0.28374255E+00	-0.17942450E+00	-0.32090525E+00	-0.32712396E+00
0.25846961E+02	-0.67036902E+00	-0.12441595E+01	-0.12637859E+01
-0.67036902E+00	0.10519942E+02	-0.85700581E+00	-0.73630140E+00
-0.12441595E+01	-0.85700581E+00	0.49918619E+02	-0.14171384E+01
-0.12637859E+01	-0.73630140E+00	-0.14171384E+01	0.89238053E+02
-0.82294032E+00	0.16741648E+01	-0.35669112E+00	-0.58832570E+00
-0.22115186E+00	0.83854036E+00	0.13619481E+00	-0.17708274E+00
-0.12271264E+01	-0.84540448E+00	-0.13565030E+01	-0.13257525E+01
-0.10769157E+01	-0.67819016E+00	-0.12710761E+01	-0.12965739E+01
0.22061337E+00	0.41918747E+00	-0.79699219E-01	0.21219101E+00
0.30866078E+00	0.75983362E+00	-0.11863941E+00	-0.83902243E-01
-0.10089703E+01	-0.62711973E+00	-0.11313962E+01	-0.11807640E+01
-0.95656393E+00	-0.68915568E+00	-0.10783901E+01	-0.10598043E+01
-0.97957931E+00	-0.55299806E+00	-0.11166330E+01	-0.11530837E+01
-0.34115156E+00	-0.23575097E+00	-0.18902100E+00	0.10569110E+00
-0.58050773E-01	0.12791185E+00	-0.21865088E+01	0.32660691E+00
0.36647841E+00	0.36227628E+00	-0.43861694E+00	-0.63969795E+00
0.26644261E+00	0.31197621E+00	-0.62001030E+00	-0.33854901E+00
0.41561674E+00	-0.28632101E-01	-0.45102015E-01	0.28867957E+00
-0.15645428E+00	0.64868177E-01	-0.87211122E+00	0.38778673E+00
0.32889958E-01	0.57725248E-01	-0.79801809E+00	-0.36409171E+00
0.23777302E+00	-0.95528736E-01	0.43881264E+00	-0.18151580E+00
0.34280941E-01	0.20981601E+00	-0.61539617E+00	-0.57432491E-01
0.10500231E+00	0.35996553E-01	-0.70732005E+00	-0.40794111E+00
-0.19630530E+00	0.36223743E-01	-0.45103535E+00	0.94898692E-01
-0.87896274E-01	0.51784136E-01	-0.37508757E+00	-0.99071555E-01
-0.12577410E+00	0.18310980E-01	-0.29766037E+00	0.29100065E+00
0.11545757E+00	-0.39317319E-03	-0.45606966E+00	0.11889891E+00
-0.11093549E-01	-0.28989149E-01	0.96217342E-01	0.89167638E-01

D (cont.)

COLUMN 9	COLUMN 10	COLUMN 11	COLUMN 12
0.00000000E+00	0.00000000E+00	0.00000000E+00	0.00000000E+00
-0.28117977E-01	-0.16068441E-01	-0.10341279E+00	-0.95527870E-01
-0.72046680E-01	-0.92852435E-02	-0.56754228E+00	-0.52376478E+00
-0.72937681E-01	-0.95720628E-01	-0.30713846E+00	-0.28426118E+00
-0.82294032E+00	-0.22115186E+00	-0.12271264E+01	-0.10769157E+01
0.16741648E+01	0.83854036E+00	-0.84540448E+00	-0.67819016E+00
-0.35669112E+00	0.13619481E+00	-0.13565030E+01	-0.12710761E+01
-0.58832570E+00	-0.17708274E+00	-0.13257525E+01	-0.12965739E+01
0.76503011E+01	0.40344857E+00	-0.48154585E+00	-0.35515553E+00
0.40344857E+00	0.53849061E+01	0.42986876E-01	-0.13542488E+00
-0.48154585E+00	0.42986876E-01	0.14910184E+03	-0.11610500E+01
-0.35515553E+00	-0.13542488E+00	-0.11610500E+01	0.23707070E+03
0.18020995E+00	0.99284754E-01	-0.15890190E+00	0.22615722E+00
0.33104659E+00	0.17570832E+00	0.61450148E-01	-0.25081353E+00
-0.51293751E+00	0.10956457E-01	-0.11038452E+01	-0.98959215E+00
-0.21915347E+00	-0.10439742E+00	-0.10271764E+01	-0.95785436E+00
-0.51286710E+00	-0.18592858E-01	-0.10574638E+01	-0.10051085E+01
-0.86524213E-01	-0.53828825E-01	-0.29427909E+00	0.11734967E+00
0.61570842E-01	-0.40827822E-02	0.23832486E+00	0.44778812E-01
0.15766222E+00	0.81028934E-01	0.87100258E-03	-0.25008331E+00
0.13846525E+00	0.68142928E-01	0.12490886E-01	-0.46131715E+00
-0.39504416E-01	-0.11416819E-01	-0.12462226E-01	0.17083517E+00
0.35573213E-01	0.17864543E-02	-0.37135533E-01	0.16030759E+00
0.28113839E-01	0.10437037E-02	0.38392645E+00	0.19176870E-01
-0.54853196E-01	-0.14719426E-01	0.12300764E+00	-0.12470831E+00
0.10141112E+00	0.45318810E-01	-0.14449470E+00	-0.40677658E+00
0.15223052E-01	-0.38758805E-02	0.14485717E+00	0.27913999E+00
0.31926880E-01	0.71467195E-02	-0.29959442E+00	-0.14613640E+00
0.28164514E-01	0.71098133E-02	0.32745084E+00	-0.15140199E+00
0.13172814E-01	-0.10428367E-03	-0.10696807E+00	0.21277751E+00
-0.63385091E-02	-0.94073005E-02	-0.24077618E+00	0.36562724E+00
-0.13191413E-01	-0.47703679E-02	-0.33957402E-01	0.10633908E+00

D (cont.)

COLUMN 13	COLUMN 14	COLUMN 15	COLUMN 16
0.00000000E+00	0.00000000E+00	0.00000000E+00	0.00000000E+00
-0.88294531E-02	-0.16863195E-01	-0.87586191E-01	-0.81945184E-01
-0.94783629E-01	-0.21291377E+00	-0.48263768E+00	-0.44992022E+00
-0.49483060E-01	-0.44504431E-01	-0.26058077E+00	-0.24288004E+00
0.22061337E+00	0.30866078E+00	-0.10089703E+01	-0.95656393E+00
0.41918747E+00	0.75983362E+00	-0.62711973E+00	-0.68915568E+00
-0.79699219E-01	-0.11863941E+00	-0.11313962E+01	-0.10783901E+01
0.21219101E+00	-0.83902243E-01	-0.11807640E+01	-0.10598043E+01
0.18020995E+00	0.33104659E+00	-0.51293751E+00	-0.21915347E+00
0.99284754E-01	0.17570832E+00	0.10956457E-01	-0.10439742E+00
-0.15890190E+00	0.61450148E-01	-0.11038452E+01	-0.10271764E+01
0.22615722E+00	-0.25081353E+00	-0.98959215E+00	-0.95785436E+00
0.59404951E+01	0.10526167E+00	-0.17351093E+00	0.21272362E+00
0.10526167E+00	0.76159037E+01	0.13730200E+00	-0.20682669E+00
-0.17351093E+00	0.13730200E+00	0.36078019E+03	-0.83559901E+00
0.21272362E+00	-0.20682669E+00	-0.83559901E+00	0.53010861E+03
-0.13596495E+00	-0.44863237E-02	-0.92706941E+00	-0.82568860E+00
-0.41096281E-01	-0.76972262E-01	-0.10719129E+00	-0.13957629E+00
0.87134134E-02	0.15072994E-01	0.32540102E+00	-0.39939289E-01
0.49387878E-01	0.90492050E-01	-0.51197222E+00	0.55703788E-02
0.40896632E-01	0.73799009E-01	-0.19334825E+00	0.48746786E-01
0.12982190E-01	0.16254822E-01	0.72721887E-01	0.30819071E-01
0.41223744E-02	0.35229546E-02	0.79846718E-01	0.95363647E-02
0.23484288E-02	0.10099643E-01	-0.56778261E-03	0.27744150E+00
-0.54044759E-02	-0.87549399E-02	0.80833998E-01	-0.10049172E+00
0.22753506E-01	0.39915611E-01	0.76403008E-01	-0.20222029E+00
0.25088608E-02	0.72564018E-02	-0.17002760E+00	0.20884561E+00
-0.40491722E-02	-0.97596100E-02	0.66721161E-01	-0.33867808E+00
0.10790900E-02	0.75798611E-02	0.20586809E+00	0.28864774E-01
0.10092969E-02	-0.32293414E-02	-0.86320441E-01	0.16211056E+00
0.37383120E-02	0.16135216E-02	-0.42874246E-01	-0.11747420E+00
-0.22085961E-02	-0.68611338E-02	-0.72876769E-01	0.13157002E+00

D (cont.)

COLUMN 17	COLUMN 18	COLUMN 19	COLUMN 20
0.00000000E+00	0.00000000E+00	0.00000000E+00	0.00000000E+00
-0.85808601E-01	0.77615037E-02	0.12065249E-01	-0.57102945E-02
-0.47167806E+00	0.16422412E+00	0.52677988E-01	-0.11721112E-01
-0.25555047E+00	0.13418431E-01	0.36269594E-01	-0.33739170E-01
-0.97957931E+00	-0.34115156E+00	-0.58050773E-01	0.36647841E+00
-0.55299806E+00	-0.23575097E+00	0.12791185E+00	0.36227628E+00
-0.11166330E+01	-0.18902100E+00	-0.21865088E+01	-0.43861694E+00
-0.11530837E+01	0.10569110E+00	0.32660691E+00	-0.63969795E+00
-0.51286710E+00	-0.86524213E-01	0.61570842E-01	0.15766222E+00
-0.18592858E-01	-0.53828825E-01	-0.40827822E-02	0.81028934E-01
-0.10574638E+01	-0.29427909E+00	0.23832486E+00	0.87100258E-03
-0.10051085E+01	0.11734967E+00	0.44778812E-01	-0.25008331E+00
-0.13596495E+00	-0.41096281E-01	0.87134134E-02	0.49387878E-01
-0.44863237E-02	-0.76972262E-01	0.15072994E-01	0.90492050E-01
-0.92706941E+00	-0.10719129E+00	0.32540102E+00	-0.51197222E+00
-0.82568860E+00	-0.13957629E+00	-0.39939289E-01	0.55703788E-02
0.75947492E+03	0.12176257E+00	0.28170445E+00	-0.16856010E+00
0.12176257E+00	0.81195796E+01	0.22378238E-01	-0.33618648E-01
0.28170445E+00	0.22378238E-01	0.28176400E+02	0.39501550E-01
-0.16856010E+00	-0.33618648E-01	0.39501550E-01	0.12090169E+02
-0.42274938E+00	-0.22187292E-01	0.61127080E-01	0.58981436E-01
0.17262835E+00	-0.17140204E-01	-0.72709889E-03	0.76215948E-02
0.17695749E+00	0.13701167E-01	0.95513142E-01	0.83543967E-02
-0.96432706E-01	0.28672262E-02	0.81767175E-01	0.24991558E-01
0.51517417E-01	-0.80333715E-02	-0.50771260E-01	-0.47790429E-02
-0.27942107E+00	-0.28513859E-02	0.64867992E-01	0.35163388E-01
0.10240079E+00	0.23886979E-02	0.70136334E-01	0.24255339E-01
0.39084788E-01	0.19677161E-01	0.50279996E-01	0.36738538E-02
-0.14542906E-01	0.18675985E-02	0.41372769E-01	0.91801472E-02
-0.30294206E-01	0.84882084E-02	0.33846094E-01	-0.23323846E-02
0.26915315E+00	0.35098953E-02	0.45614584E-01	0.84669307E-02
-0.86057467E-01	0.18750037E-02	-0.10110822E-01	-0.58575041E-02

D (cont.)

COLUMN 21	COLUMN 22	COLUMN 23	COLUMN 24
0.00000000E+00	0.00000000E+00	0.00000000E+00	0.00000000E+00
-0.44285185E-02	-0.12790714E-02	0.55117068E-02	0.49177136E-02
0.28275500E-01	-0.85951736E-01	0.21295666E-01	0.12023530E-01
-0.29849041E-01	-0.14795521E-01	0.14956000E-01	0.17493581E-01
0.26644261E+00	0.41561674E+00	-0.15645428E+00	0.32889958E-01
0.31197621E+00	-0.28632101E-01	0.64868177E-01	0.57722248E-01
-0.62001030E+00	-0.45102015E-01	-0.87211122E+00	-0.79801809E+00
-0.33854901E+00	0.28867957E+00	0.38778673E+00	-0.36409171E+00
0.13846525E+00	-0.39504416E-01	0.35573213E-01	0.28113839E-01
0.68142928E-01	-0.11416819E-01	0.17864543E-02	0.10437037E-02
0.12490886E-01	-0.12462226E-01	-0.37135533E-01	0.38392645E+00
-0.46131715E+00	0.17083517E+00	0.16030759E+00	0.19176870E-01
0.40896632E-01	0.12982190E-01	0.41223744E-02	0.23484288E-02
0.73799009E-01	0.16254822E-01	0.35229546E-02	0.10099643E-01
-0.19334825E+00	0.72721887E-01	0.79846718E-01	-0.56778261E-03
0.48746786E-01	0.30819071E-01	0.95363647E-02	0.27744150E+00
-0.42274938E+00	0.17262835E+00	0.17695749E+00	-0.96432706E-01
-0.22187292E-01	-0.17140204E-01	0.13701167E-01	0.28672262E-02
0.61127080E-01	-0.72709889E-03	0.95513142E-01	0.81767175E-01
0.58981436E-01	0.76215948E-02	0.83543967E-02	0.24991558E-01
0.10834181E+02	0.46900440E-02	0.19469292E-01	0.28586230E-01
0.46900440E-02	0.64142488E+01	-0.30617007E-02	-0.19744084E-02
0.19469292E-01	-0.30617007E-02	0.25671157E+02	0.29515948E-01
0.28586230E-01	-0.19744084E-02	0.29515948E-01	0.33720614E+02
-0.10541929E-01	0.77237708E-02	-0.24960413E-01	-0.15423285E-01
0.39164821E-01	-0.30440835E-02	0.25441613E-01	0.23888779E-01
0.25315755E-01	0.88654574E-03	0.24600951E-01	0.32265721E-01
0.12088164E-01	-0.11276379E-01	0.23453207E-01	0.14168221E-01
0.12604543E-01	-0.42606329E-02	0.16188069E-01	0.17540870E-01
0.29716983E-02	-0.24543676E-02	0.17449714E-01	0.81803915E-02
0.11211752E-01	0.61270179E-02	0.18721351E-01	0.14496870E-01
-0.57275830E-02	0.33274696E-03	-0.32100371E-02	-0.48483373E-02

D (cont.)

COLUMN 25	COLUMN 26	COLUMN 27	COLUMN 28
0.00000000E+00	0.00000000E+00	0.00000000E+00	0.00000000E+00
-0.29948857E-02	-0.14402934E-02	0.41919961E-02	0.25716347E-02
-0.59774351E-03	0.75244409E-01	0.11070899E-01	0.12172107E+00
-0.16677566E-01	-0.19920489E-01	0.16046914E-01	-0.56398774E-02
0.23777302E+00	0.34280941E-01	0.10500231E+00	-0.19630530E+00
-0.95528736E-01	0.20981601E+00	0.35996553E-01	0.36223743E-01
0.43881264E+00	-0.61539617E+00	-0.70732005E+00	-0.45103535E+00
-0.18151580E+00	-0.57432491E-01	-0.40794111E+00	0.94898692E-01
-0.54853196E-01	0.10141112E+00	0.15223052E-01	0.31926880E-01
-0.14719426E-01	0.45318810E-01	-0.38758805E-02	0.71467195E-02
0.12300764E+00	-0.14449470E+00	0.14485717E+00	-0.29959442E+00
-0.12470831E+00	-0.40677658E+00	0.27913999E+00	-0.14613640E+00
-0.54044759E-02	0.22753506E-01	0.25088608E-02	-0.40491722E-02
-0.87549399E-02	0.39915611E-01	0.72564018E-02	-0.97596100E-02
0.80833998E-01	0.76403008E-01	-0.17002760E+00	0.66721161E-01
-0.10049172E+00	-0.20222029E+00	0.20884561E+00	-0.33867808E+00
0.51517417E-01	-0.27942107E+00	0.10240079E+00	0.39084788E-01
-0.80333715E-02	-0.28513859E-02	0.23886979E-02	0.19677161E-01
-0.50771260E-01	0.64867992E-01	0.70136334E-01	0.50279996E-01
-0.47790429E-02	0.35163388E-01	0.24255339E-01	0.36738538E-02
-0.10541929E-01	0.39164821E-01	0.25315755E-01	0.12088164E-01
0.77237708E-02	-0.30440835E-02	0.88654574E-03	-0.11276379E-01
-0.24960413E-01	0.25441613E-01	0.24600951E-01	0.23453207E-01
-0.15423285E-01	0.23888779E-01	0.32265721E-01	0.14168221E-01
0.20382429E+02	-0.14954188E-01	-0.12104470E-01	-0.14647226E-01
-0.14954188E-01	0.97639583E+01	0.19895722E-01	0.19835065E-01
-0.12104470E-01	0.19895722E-01	0.37279276E+02	0.11464226E-01
-0.14647226E-01	0.19835065E-01	0.11464226E-01	0.88614906E+01
-0.97343984E-02	0.12281662E-01	0.13422882E-01	0.82428871E-02
-0.11150663E-01	0.77095768E-02	0.66444198E-02	0.98257913E-02
-0.83910502E-02	0.11095041E-01	0.15171810E-01	0.84183435E-02
0.18330651E-02	-0.42973248E-02	-0.40760473E-02	-0.16614473E-02

D (cont.)

COLUMN 29	COLUMN 30	COLUMN 31	COLUMN 32
0.00000000E+00	0.00000000E+00	0.00000000E+00	0.00000000E+00
0.27459402E-02	0.25603561E-02	0.14789512E-02	0.10151803E-03
-0.60432359E-03	0.12025279E-01	0.93794112E-03	0.60223775E-02
0.99205552E-02	0.42554055E-02	0.83025561E-02	-0.48136680E-02
-0.87896274E-01	-0.12577410E+00	0.11545757E+00	-0.11093549E-01
0.51784136E-01	0.18310980E-01	-0.39317319E-03	-0.28989149E-01
-0.37508757E+00	-0.29766037E+00	-0.45606966E+00	0.96217342E-01
-0.99071555E-01	0.29100065E+00	0.11889891E+00	0.89167638E-01
0.28164514E-01	0.13172814E-01	-0.63385091E-02	-0.13191413E-01
0.71098133E-02	-0.10428367E-03	-0.94073005E-02	-0.47703679E-02
0.32745084E+00	-0.10696807E+00	-0.24077618E+00	-0.33957402E-01
-0.15140199E+00	0.21277751E+00	0.36562724E+00	0.10633908E+00
0.10790900E-02	0.10092969E-02	0.37383120E-02	-0.22085961E-02
0.75798611E-02	-0.32293414E-02	0.16135216E-02	-0.68611338E-02
0.20586809E+00	-0.86320441E-01	-0.42874246E-01	-0.72876769E-01
0.28864774E-01	0.16211056E+00	-0.11747420E+00	0.13157002E+00
-0.14542906E-01	-0.30294206E-01	0.26915315E+00	-0.86057467E-01
0.18675985E-02	0.84882084E-02	0.35098953E-02	0.18750037E-02
0.41372769E-01	0.33846094E-01	0.45614584E-01	-0.10110822E-01
0.91801472E-02	-0.23323846E-02	0.84669307E-02	-0.58575041E-02
0.12604543E-01	0.29716983E-02	0.11211752E-01	-0.57275830E-02
-0.42606329E-02	-0.24543676E-02	0.61270179E-02	0.33274696E-03
0.16188069E-01	0.17449714E-01	0.18721351E-01	-0.32100371E-02
0.17540870E-01	0.81803915E-02	0.14496870E-01	-0.48483373E-02
-0.97343984E-02	-0.11150663E-01	-0.83910502E-02	0.18330651E-02
0.12281662E-01	0.77095768E-02	0.11095041E-01	-0.42973248E-02
0.13422882E-01	0.66444198E-02	0.15171810E-01	-0.40760473E-02
0.82428871E-02	0.98257913E-02	0.84183435E-02	-0.16614473E-02
0.30623530E+02	0.48475420E-02	0.49900730E-02	-0.26324657E-02
0.48475420E-02	0.23633730E+02	0.69464732E-02	-0.25868390E-03
0.49900730E-02	0.69464732E-02	0.41428718E+02	-0.14946290E-02
-0.26324657E-02	-0.25868390E-03	-0.14946290E-02	0.22006422E+02

Table D.6 RMS Weighting Matrix Q_{RMS}

COLUMN 1	COLUMN 2	COLUMN 3	COLUMN 4
0.21661648E+05	0.38525240E+04	-0.75452277E+04	-0.31339031E+04
0.38525240E+04	0.16185685E+05	0.42800883E+03	-0.63298086E+04
-0.75452277E+04	0.42800883E+03	0.73720163E+05	-0.77189888E+04
-0.31339031E+04	-0.63298086E+04	-0.77189888E+04	0.15984954E+05
0.33884648E+04	0.76829167E+04	-0.10089972E+05	-0.23654820E+04
0.20649768E+04	0.14744351E+05	0.18577737E+05	-0.19409698E+05
0.15763914E+04	0.15295111E+04	-0.29302618E+04	0.17482218E+04
-0.61666046E+03	0.32088046E+05	-0.13355857E+04	-0.18444160E+03
0.39802456E+05	0.25140537E+05	-0.41391739E+05	-0.11382489E+05
-0.59800629E+05	-0.59762348E+04	-0.52952185E+05	0.68033214E+05
-0.16757605E+04	0.35051176E+04	-0.19784647E+04	-0.13483292E+03
-0.49048947E+03	0.18608633E+01	-0.14624230E+04	0.11385155E+04
0.15133825E+01	0.11767824E+04	-0.38391867E+00	-0.92600441E+00
-0.32378475E+05	-0.58816611E+04	0.57257529E+05	-0.12332910E+05
-0.13074169E+04	0.20302772E+04	-0.67285070E+03	0.31563402E+03
-0.19648788E+04	0.25843001E+04	-0.81704179E+03	-0.21659067E+03
-0.10924042E+04	0.18124357E+04	-0.10061082E+04	0.73642790E+03
0.33168790E+05	0.18628003E+04	-0.59979992E+05	0.18414489E+05
-0.80425386E+04	-0.39023116E+04	0.64484834E+04	-0.19938900E+04
0.26973742E+05	-0.18846468E+05	-0.13817635E+05	0.24725786E+05
0.28153099E+05	-0.13843846E+05	-0.29404122E+05	0.26215824E+05
-0.38595127E+05	-0.23618456E+05	0.35472053E+05	0.12416932E+05
-0.84523047E+04	-0.57319224E+04	0.35868363E+04	0.71809721E+03
-0.68899534E+04	-0.37300713E+03	0.75533207E+04	-0.54449434E+04
-0.97249078E+04	-0.11599333E+05	-0.99776882E+04	0.10297910E+05
0.29922439E+05	-0.88746053E+04	-0.43646534E+05	0.25917274E+05
-0.63792202E+04	0.10891202E+04	0.63071289E+04	-0.62831538E+04
0.31762190E+05	-0.35730364E+04	-0.54578073E+05	0.23315627E+05
-0.73678266E+04	-0.19676778E+04	0.75143206E+04	-0.39239651E+04
-0.86803842E+04	-0.74921923E+04	-0.26756527E+03	0.36442780E+04
-0.58735051E+04	0.24010430E+04	0.41107252E+04	-0.64609785E+04
-0.87720668E+04	-0.89831921E+04	-0.43152696E+04	0.63450540E+04

$\underline{Q}_{RMS}$ (cont.)

COLUMN 5	COLUMN 6	COLUMN 7	COLUMN 8
0.33884648E+04	0.20649768E+04	0.15763914E+04	-0.61666046E+03
0.76829167E+04	0.14744351E+05	0.15295111E+04	0.32088046E+04
-0.10089972E+05	0.18577737E+05	-0.29302618E+04	-0.13355857E+04
-0.23654820E+04	-0.19409698E+05	0.17482218E+04	-0.18444160E+03
0.13569239E+07	0.26915783E+03	0.34126847E+04	-0.65147272E+03
0.26915783E+03	0.28749350E+06	-0.17592564E+04	-0.12800686E+04
0.34126847E+04	-0.17592564E+04	0.38489251E+06	0.19746300E+03
-0.65147272E+03	-0.12800686E+04	0.19746300E+03	0.92491539E+04
0.46981148E+05	-0.35253662E+06	-0.11308487E+04	0.68022070E+04
0.12243293E+04	-0.18319527E+06	-0.18688072E+05	-0.17114507E+04
0.19169076E+04	0.36700932E+04	-0.13406687E+04	0.15307199E+04
0.19595549E+04	-0.54617535E+03	-0.93950599E+02	-0.17609535E+04
0.84344081E+00	0.26222226E+01	0.77464873E-01	0.26727715E+00
-0.42113691E+05	-0.16739588E+06	-0.51665287E+04	-0.33703391E+04
0.84651169E+03	0.54123216E+03	0.10673600E+04	0.68850100E+03
0.10678876E+04	0.22062986E+04	0.29993679E+03	0.26726608E+04
0.15049361E+04	0.14253753E+03	-0.25534632E+02	0.15855482E+03
0.36464201E+05	0.56152033E+05	0.13138152E+05	-0.15393100E+03
0.16620742E+05	-0.62934175E+04	0.10582877E+06	-0.43736730E+04
-0.38019844E+05	-0.76829928E+05	0.15469741E+05	0.14296930E+05
-0.28028571E+05	-0.64898906E+05	0.24613692E+05	0.70621300E+04
-0.38246642E+05	0.21130505E+04	0.61871963E+03	-0.83606924E+04
0.18661653E+05	-0.43907381E+04	0.42439347E+05	-0.82067041E+04
0.20145246E+04	-0.38991393E+04	0.38981838E+05	0.11047901E+05
-0.24224728E+05	0.13049357E+05	-0.21925167E+05	0.33990648E+04
-0.49684220E+04	-0.40995970E+05	0.26361035E+05	0.89353054E+03
-0.48636649E+04	-0.67345882E+03	0.34541855E+05	0.11930430E+05
0.18923882E+05	-0.24008828E+04	0.21556630E+05	-0.16367580E+04
0.10274277E+05	-0.61074252E+04	0.18484255E+05	0.34770222E+04
0.13005011E+05	-0.14337242E+03	0.14672135E+05	-0.67605737E+04
-0.83883978E+04	0.26520623E+04	0.21670700E+05	-0.25447058E+04
0.55483557E+03	0.50615705E+04	-0.46023407E+04	-0.24417456E+04

Q_{RMS} (cont.)

COLUMN 9	COLUMN 10	COLUMN 11	COLUMN 12
0.39802456E+05	-0.59800629E+05	-0.16757605E+04	-0.49048947E+03
0.25140537E+05	-0.59762348E+05	0.35051176E+04	0.18608633E+04
-0.41391739E+05	-0.52952185E+05	-0.19784647E+04	-0.14624230E+04
-0.11382489E+05	0.68033214E+05	-0.13483292E+03	0.11385155E+04
0.46981148E+05	0.12243293E+04	0.19169076E+04	0.19595549E+04
-0.35253662E+06	-0.18319527E+06	0.36700932E+04	-0.54617535E+03
-0.11308487E+04	-0.18688072E+05	-0.13406687E+04	-0.93950599E+02
0.68022070E+04	-0.17114507E+04	0.15307199E+04	-0.17609535E+04
0.87441423E+07	-0.84824935E+05	0.35574521E+04	0.34045331E+03
-0.84824935E+05	0.98137606E+06	-0.37947728E+04	-0.99548143E+03
0.35574521E+04	-0.37947728E+04	0.36467003E+07	0.74163758E+03
0.34045331E+03	-0.99548143E+03	0.74163758E+03	0.72723435E+04
0.10812865E+01	0.85323219E+00	-0.28704662E-01	0.10234946E+00
-0.72118009E+05	-0.39636577E+05	-0.35458265E+04	0.67051383E+03
0.18509765E+04	-0.12107795E+04	-0.85290661E+03	0.16151211E+03
0.64940103E+03	0.10522393E+03	0.81330080E+03	-0.15755282E+04
0.84735737E+03	-0.51398334E+03	0.17746050E+04	-0.15323448E+03
0.20283186E+05	0.11476672E+05	0.58140860E+04	-0.41504135E+03
-0.29904857E+04	0.95510672E+02	-0.12252649E+04	0.90949868E+03
-0.35613537E+05	-0.20819743E+05	-0.92116267E+03	0.17850871E+04
-0.31358306E+05	-0.18332189E+05	-0.86273418E+03	0.39773090E+04
0.65583747E+04	-0.20947290E+04	-0.22343039E+03	-0.18791010E+04
-0.22567532E+04	-0.10555034E+04	0.16605991E+04	-0.10210176E+04
-0.13539985E+04	0.11277924E+03	-0.49554995E+04	0.41495882E+03
0.73283634E+04	0.24101079E+03	-0.26775183E+04	0.84774463E+03
-0.22080515E+05	-0.12774839E+05	0.20702103E+04	0.37313467E+04
0.35252806E+03	0.96485357E+03	-0.13832169E+04	-0.21960748E+04
-0.58440719E+04	-0.33165615E+04	0.51092518E+04	0.15907278E+04
-0.26652054E+04	-0.10551613E+04	-0.45364957E+04	0.17914747E+04
-0.16208174E+03	-0.10441553E+04	0.20976610E+04	-0.18840941E+04
0.20170207E+04	0.15625534E+04	0.40854281E+04	-0.33742693E+04
0.26605580E+04	-0.61429434E+03	0.42728576E+03	-0.11047643E+04

Q_{RMS} (cont.)

COLUMN 13	COLUMN 14	COLUMN 15	COLUMN 16
0.15133825E+01	-0.32378475E+05	-0.13074169E+04	-0.19648788E+04
0.11767824E+01	-0.58816611E+04	0.20302772E+04	0.25843001E+04
-0.38391867E+00	0.57257529E+05	-0.67285070E+03	-0.81704179E+03
-0.92600441E+00	-0.12332910E+05	0.31563402E+03	-0.21659067E+03
0.84344081E+00	-0.42113691E+05	0.84651169E+03	0.10678876E+04
0.26222226E+01	-0.16739588E+06	0.54123216E+03	0.22062986E+04
0.77464873E-01	-0.51665287E+04	0.10673600E+04	0.29993679E+03
0.26727715E+00	-0.33703391E+04	0.68850100E+03	0.26726608E+04
0.10812865E+01	-0.72118009E+05	0.18509765E+04	0.64940103E+03
0.85323219E+00	-0.39636577E+05	-0.12107795E+04	0.10522393E+03
-0.28704662E-01	-0.35458265E+04	-0.85290661E+03	0.81330080E+03
0.10234946E+00	0.67051383E+03	0.16151211E+03	-0.15755282E+04
0.16067753E+08	0.68965963E+00	-0.17055182E-01	0.34038498E-01
0.68965963E+00	0.99921841E+06	-0.18340978E+04	0.64310169E+03
-0.17055182E-01	-0.18340978E+04	0.26326487E+08	0.12140876E+04
0.34038498E-01	0.64310169E+03	0.12140876E+04	0.80702642E+04
-0.56773481E-02	-0.32644678E+03	-0.19675054E+04	0.29364986E+03
-0.28380992E+00	0.18439265E+05	0.11295893E+04	0.78784043E+03
0.18054568E-01	-0.83393824E+03	-0.14142505E+04	0.67904528E+03
0.29994915E+00	-0.16781522E+05	0.29804464E+04	-0.32277578E+02
0.23927313E+00	-0.12787450E+05	0.99172934E+03	-0.19039027E+03
0.14242279E+00	-0.44255456E+04	-0.61915371E+03	-0.19267310E+03
0.20355781E-01	-0.50256629E+03	-0.21321428E+03	0.18563009E+03
0.14218562E-01	-0.12381570E+04	0.28763950E+03	-0.10410356E+04
0.10651009E-01	0.19331134E+04	-0.74895872E+03	0.27735932E+03
0.12351462E+00	-0.56911099E+04	-0.58119788E+03	0.96755006E+03
0.53016809E-02	-0.72636933E+03	0.13440624E+04	-0.78179518E+03
-0.47476688E-01	0.44752526E+04	-0.29021851E+03	0.16158577E+04
0.22283022E-01	-0.15241418E+04	-0.11773263E+04	-0.17868520E+02
0.16331890E-01	0.26908522E+03	0.68232013E+03	-0.62143286E+03
-0.18393382E-02	-0.83987229E+02	0.36509563E+03	0.56612541E+03
0.11653226E-01	0.10215750E+04	0.44311344E+03	-0.60204544E+03

Q_{RMS} (cont.)

COLUMN 17	COLUMN 18	COLUMN 19	COLUMN 20
-0.10924042E+04	0.33168790E+05	-0.80425386E+04	0.26973742E+05
0.18124357E+04	0.18628003E+04	-0.39023116E+04	-0.18846468E+05
-0.10061082E+04	-0.59979992E+05	0.64484834E+04	-0.13817635E+05
0.73642790E+03	0.18414489E+05	-0.19938900E+04	0.24725786E+05
0.15049361E+04	0.36464201E+05	0.16620742E+05	-0.38019844E+05
0.14253753E+03	0.56152033E+05	-0.62934175E+04	-0.76829928E+05
-0.25534632E+02	0.13138152E+05	0.10582877E+06	0.15469741E+05
0.15855482E+03	-0.15393100E+05	-0.43736730E+04	0.14296930E+05
0.84735737E+03	0.20283186E+05	-0.29904857E+04	-0.35613537E+05
-0.51398334E+03	0.11476672E+05	0.95510672E+02	-0.20819743E+05
0.17746050E+04	0.58140860E+04	-0.12252649E+04	-0.92116267E+03
-0.15323448E+03	-0.41504135E+03	0.90949868E+03	0.17850871E+04
-0.56773478E-02	-0.28380992E+00	0.18054568E-01	0.29994915E+00
-0.32644678E+03	0.18439265E+05	-0.83393824E+03	-0.16781522E+05
-0.19675054E+04	0.11295893E+04	-0.14142505E+04	0.29804464E+04
0.29364986E+03	0.78784043E+03	0.67904528E+03	-0.32277578E+02
0.35621277E+07	-0.25712598E+03	-0.50120906E+03	0.44080639E+03
-0.25712598E+03	0.10316726E+07	-0.84401510E+03	0.47124623E+04
-0.50120906E+03	-0.84401510E+03	0.37232998E+07	-0.13146381E+04
0.44080639E+03	0.47124623E+04	-0.13146381E+04	0.10304700E+07
0.12242171E+04	0.23714914E+04	-0.22447790E+04	-0.10390966E+05
-0.53922483E+03	0.44499264E+04	-0.21214763E+02	-0.33402292E+03
-0.40227247E+03	-0.43473532E+03	-0.49036251E+04	-0.15221490E+03
0.46520843E+03	0.49209054E+03	-0.41928963E+04	-0.65727563E+03
-0.25195794E+03	-0.15757691E+03	0.27595753E+04	0.32855386E+03
0.81211705E+03	-0.11485931E+04	-0.25151531E+04	-0.71580342E+04
-0.16437525E+03	0.46257303E+03	-0.35627571E+04	-0.49798831E+03
-0.10801451E+03	-0.54541836E+04	-0.19937378E+04	-0.22117591E+04
0.12808132E+03	0.61212617E+03	-0.22550865E+04	-0.21536638E+03
0.13973216E+03	-0.43604395E+03	-0.18538256E+04	0.31592629E+03
-0.77110823E+03	0.33631283E+03	-0.21698960E+04	0.11090946E+03
0.24378655E+03	-0.37028147E+03	0.44002652E+03	0.46265890E+03

Q_{RMS} (cont.)

COLUMN 21	COLUMN 22	COLUMN 23	COLUMN 24
0.28153099E+05	-0.38595127E+05	-0.84523047E+04	-0.68899534E+04
-0.13843846E+05	-0.23618456E+05	-0.57319224E+04	-0.37300713E+03
-0.29404122E+05	0.35472053E+05	0.35868363E+04	0.75533207E+04
0.26215824E+05	0.12416932E+05	0.71809721E+03	-0.54449434E+04
-0.28028571E+05	-0.38246642E+05	0.18661653E+05	0.20145246E+04
-0.64898906E+05	0.21130505E+04	-0.43907381E+04	-0.38991393E+04
0.24613692E+05	0.61871963E+03	0.42439347E+05	0.38981838E+05
0.70621300E+04	-0.83606924E+04	-0.82067041E+04	0.11047901E+05
-0.31358306E+05	0.65583747E+04	-0.22567532E+04	-0.13539985E+04
-0.18332189E+05	-0.20947290E+04	-0.10555034E+04	0.11277924E+03
-0.86273418E+03	-0.22343039E+03	0.16605991E+04	-0.49554995E+04
0.39773090E+04	-0.18791010E+04	-0.10210176E+04	0.41495882E+03
0.23927313E+00	0.14242279E+00	0.20355780E-01	0.14218562E-01
-0.12787450E+05	-0.44255456E+04	-0.50256629E+03	-0.12381570E+04
0.99172934E+03	-0.61915371E+03	-0.21321428E+03	0.28763950E+03
-0.19039027E+03	-0.19267310E+03	0.18563009E+03	-0.10410356E+04
0.12242171E+04	-0.53922483E+03	-0.40227247E+03	0.46520843E+03
0.23714914E+04	0.44499264E+04	-0.43473532E+03	0.49209054E+03
-0.22447790E+04	-0.21214763E+02	-0.49036251E+04	-0.41928963E+04
-0.10390966E+05	-0.33402292E+03	-0.15221490E+03	-0.65727563E+03
0.44644369E+08	0.65283922E+03	-0.61598256E+03	-0.76001766E+03
0.65283922E+03	0.10372341E+07	0.46859980E+02	-0.30958148E+03
-0.61598256E+03	0.46859980E+02	0.70097579E+08	-0.16709421E+04
-0.76001766E+03	-0.30958148E+03	-0.16709421E+04	0.10404222E+07
0.49727893E+03	-0.13404078E+04	0.13475934E+04	0.96204069E+03
-0.74051533E+04	0.21068440E+04	-0.93516312E+03	-0.55528984E+03
-0.55403874E+03	-0.46696431E+03	-0.13244361E+04	-0.15736160E+04
-0.34573628E+04	0.35011523E+04	-0.88704891E+03	-0.10147026E+03
-0.23288889E+03	-0.11554135E+03	-0.10525075E+04	-0.94465826E+03
0.54712620E+02	-0.10985390E+03	-0.10255205E+04	-0.54704376E+03
0.13733404E+02	-0.59541188E+03	-0.80893019E+03	-0.85392324E+03
0.39114062E+03	-0.48425790E+03	0.77958127E+02	0.23070946E+03

Q_{RMS} (cont.)

COLUMN 25	COLUMN 26	COLUMN 27	COLUMN 28
-0.97249078E+04	0.29922439E+05	-0.63792202E+04	0.31762190E+05
-0.11599333E+05	-0.88746053E+04	0.10891202E+04	-0.35730364E+04
-0.99776882E+04	-0.43646534E+05	0.63071289E+04	-0.54578073E+05
0.10297910E+05	0.25917274E+05	-0.62831538E+04	0.23315627E+05
-0.24224728E+05	-0.49684220E+04	-0.48636649E+04	0.18923882E+05
0.13049357E+05	-0.40995970E+05	-0.67345882E+03	-0.24008828E+04
-0.21925167E+05	0.26361035E+05	0.34541855E+05	0.21556630E+05
0.33990648E+04	0.89353054E+03	0.11930430E+05	-0.16367580E+04
0.73283634E+04	-0.22080515E+05	0.35252806E+03	-0.58440719E+04
0.24101079E+03	-0.12774839E+05	0.96485357E+03	-0.33165615E+04
-0.26775183E+04	0.20702103E+04	-0.13832169E+04	0.51092518E+04
0.84774463E+03	0.37313467E+04	-0.21960748E+04	0.15907278E+04
0.10651009E-01	0.12351462E+00	0.53016809E-02	-0.47476688E-01
0.19331134E+04	-0.56911099E+04	-0.72636933E+03	0.44752526E+04
-0.74895872E+03	-0.58119788E+03	0.13440624E+04	-0.29021851E+03
0.27735932E+03	0.96755006E+03	-0.78179518E+03	0.16158577E+04
-0.25195794E+03	0.81211705E+03	-0.16437525E+03	-0.10801451E+03
-0.15757691E+03	-0.11485931E+04	0.46257303E+03	-0.54541836E+04
0.27595753E+04	-0.25151531E+04	-0.35627571E+04	-0.19937378E+04
0.32855386E+03	-0.71580342E+04	-0.49798831E+03	-0.22117591E+04
0.49727893E+03	-0.74051533E+04	-0.55403874E+03	-0.34573628E+04
-0.13404078E+04	0.21068440E+04	-0.46696431E+03	0.35011523E+04
0.13475934E+04	-0.93516312E+03	-0.13244361E+04	-0.88704891E+03
0.96204069E+03	-0.55[illegible]984E+03	-0.15736160E+04	-0.10147026E+03
0.41011513E+07	0.65915011E+03	0.67572014E+03	0.50431535E+03
0.65915011E+03	0.10355788E+07	-0.31820074E+03	-0.46476468E+04
0.67572014E+03	-0.31820074E+03	0.49078001E+07	0.70493740E+02
0.50431535E+03	-0.46476468E+04	0.70493740E+02	0.10368178E+07
0.73626096E+03	-0.14936950E+03	-0.73848529E+03	0.12439416E+03
0.45222009E+03	-0.25037656E+03	-0.38313606E+03	-0.43295329E+03
0.31978510E+03	0.10298729E+03	-0.84992516E+03	0.25511736E+03
-0.44914860E+03	0.22586724E+03	0.20839052E+03	-0.24677426E+02

Q_{RMS} (cont.)

COLUMN 29	COLUMN 30	COLUMN 31	COLUMN 32
-0.73678266E+04	-0.86803842E+04	-0.58735051E+04	-0.87720668E+04
-0.19676778E+04	-0.74921923E+04	0.24010430E+04	-0.89831921E+04
0.75143206E+04	-0.26756527E+03	0.41107252E+04	-0.43152696E+04
-0.39239651E+04	0.36442780E+04	-0.64609785E+04	0.63450540E+04
0.10274277E+05	0.13005011E+05	-0.83883978E+04	0.55483557E+03
-0.61074252E+04	-0.14337242E+03	0.26520623E+04	0.50615705E+04
0.18484255E+05	0.14672135E+05	0.21670700E+05	-0.46023407E+04
0.34770222E+04	-0.67605737E+04	-0.25447058E+04	-0.24417456E+04
-0.26652054E+04	-0.16208174E+03	0.20170207E+04	0.26605580E+04
-0.10551613E+04	-0.10441553E+04	0.15625534E+04	-0.61429434E+03
-0.45364957E+04	0.20976610E+04	0.40854281E+04	0.42728576E+03
0.17914747E+04	-0.18840941E+04	-0.33742693E+04	-0.11047643E+04
0.22283022E-01	0.16331890E-01	-0.18393382E-02	0.11653226E-01
-0.15241418E+04	0.26908522E+03	-0.83987229E+02	0.10215750E+04
-0.11773263E+04	0.68232013E+03	0.36509563E+03	0.44311344E+03
-0.17868520E+02	-0.62143286E+03	0.56612541E+03	-0.60204544E+03
0.12808132E+03	0.13973216E+03	-0.77110823E+03	0.24378655E+03
0.61212617E+03	-0.43604395E+03	0.33631283E+03	-0.37028147E+03
-0.22550865E+04	-0.18538256E+04	-0.21698960E+04	0.44002652E+03
-0.21536638E+03	0.31592629E+03	0.11090946E+03	0.46265890E+03
-0.23288889E+03	0.54712620E+02	0.13733404E+02	0.39114062E+03
-0.11554135E+03	-0.10985390E+03	-0.59541188E+03	-0.48425790E+03
-0.10525075E+04	-0.10255205E+04	-0.80893019E+03	0.77958127E+02
-0.94465826E+03	-0.54704376E+03	-0.85392324E+03	0.23070946E+03
0.73626096E+03	0.45222009E+03	0.31978510E+03	-0.44914860E+03
-0.14936950E+03	-0.25037656E+03	0.10298729E+03	0.22586724E+03
-0.73848529E+03	-0.38313606E+03	-0.84992516E+03	0.20839052E+03
0.12439416E+03	-0.43295329E+03	0.25511736E+03	-0.24677426E+02
0.10590426E+09	-0.42401925E+03	-0.34753618E+03	0.10451572E+03
-0.42401925E+03	0.10416424E+07	-0.24371751E+03	-0.12203261E+03
-0.34753618E+03	-0.24371751E+03	0.15494838E+09	0.10177042E+03
0.10451572E+03	-0.12203261E+03	0.10177042E+03	0.10419420E+07

SUBJECT INDEX

AUTHOR INDEX